Homeodomain-Interacting Protein Kinase 2 (HIPK2), a Novel Kinase Regulator in the Heart

By

Yuanjun Guo

Dissertation

Submitted to the Faculty of the

Graduate School of Vanderbilt University

in partial fulfillment of the requirements

for the degree of

DOCTOR OF PHILOSOPHY

in

Pharmacology

December 14, 2019

Nashville, Tennessee

Approved:

Bjorn Christian Knollmann, M.D.

Hind Lal, Ph.D.

Joey V. Barnett, Ph.D.

Richard Gumina, M.D., Ph.D.

Scott H. Baldwin, M.D.

I dedicate this work to my amazing parents, Hong Guo and Zhen Shi, who always encourage and support

me to pursue my dreams.

Acknowledgements

was down and joys you shared together with me. I would like to thank Dr. Baldwin for all the great questions and support for the project. I would also like to acknowledge Dr. Gumina for your continuous encouragement and all the supports as our neighboring lab.

I would also like to acknowledge all the people in Force Laboratory and Lal Laboratory that I have had the pleasure to work together. This work would not be completed without the support and various collaboration within many labs and cores at Vanderbilt University and Medical Center. I especially would like to thank Dr. Young-Jae Nam and Dr. Zhentao Zhang for the AAV9 study, Dr. Kyungsoo Kim and Kaylen Kor in Knollmann Lab for the calcium study, Kevin L. Tompkins in Baldwin Lab for the embryo study. I would also like to thank Dr. Joshua Fessel and Christi Moore for the guidance and support for the Oroboro Oxygraph and Seahorse study. I would especially like to thank Dr. Zhizhang Wang and Dr. Lin Zhong for helping me complete all the echocardiographic imaging work in the project and always trying to accommodate all my needs. I would also like to thank Dr. Jenny C Schafer in the Cell Imaging Shared Resource who would always be likely to help to solve any problem regarding microscopy and image processing.

I would like to thank Dr. Robert Willette in GlaxoSmithKline to start this project and provide tremendous support during the collaboration and he also impressed me the cool part of a scientist. I would like to acknowledge Dr. Xiaoyan A. Qu, Johannes Freudenbergthe and Lea Sarov-Blat in GlaxoSmithKline for their assistance to locate and analyze the microarray data. I would also like to acknowledge the colleagues in the Center for Translational Medicine at Temple University, especially Dr. Erhe Gao for his expertise and enormous support on my work there.

I would also acknowledge the mice and rats sacrificed for this project. This work would not be possible without their participation.

I am also grateful to join the Department of Pharmacology and Cardiovascular Medicine Division, meet and work with so many amazing friends and colleagues here. I would like to thank all the labs and people working in the Cardiovascular division for all the kindness. I especially would like to thank our great neighboring lab Dr. Collins Laboratory, Dr. Moslehi Laboratory, and Dr. Brown Laboratory. I would also

Table of Contents

List of Figures

List of Abbreviations

AAV9	adeno-associated virus serotype 9
ACEI	angiotensin-converting enzyme inhibitors
Ad-HIPK2	adenovirus expressing wild-type HIPK2 construct
Ad-HIPK2-KD	adenovirus expressing HIPK2 kinase-dead (K221A) construct
Ad-LacZ	adenovirus expressing LacZ construct
Ad-scrambled	adenovirus expressing shRNA-scrambled construct
Ad-shRNA-HIPK2	adenovirus expressing shRNA-HIPK2 construct
AKT	protein kinase B
BAX	BCL2 associated X
BCL-XL	B-cell lymphoma-extra large
ChEA	ChIP enrichment analysis
CM	cardiomyocyte
COL1A2	collagen type I alpha 1 chain
Echo	echocardiography
EDD	end-diastolic dimension
EF	ejection fraction
EMMA	European Mouse Mutant Archive
ERK	extracellular signal-regulated kinase
ESD	end-systolic dimension
FB	fibroblast
FLP	B6.129S4-Gt(ROSA)26Sortm1(FLP1)Dym/RainJ mouse
FS	fractional shortening
GC	genome copies

GFP	green fluorescent protein
GSK3	glycogen synthase kinase 3
HA	hemagglutinin
Het	heterozygous
HF	heart failure
HFpEF	heart failure with preserved ejection fraction
HFrEF	heart failure with reduced ejection fraction
HIPK2	homeodomain-interacting protein kinase 2
HIPK2^{tm2a}	C57BL/6NTac-Hipk2tm2a(EUCOMM)Hmgu/Cnrm mouse
HW/TL	heart weight normalized by tibia length
IPA	Ingenuity pathway analysis
JAK/STAT	the Janus kinase/signal transducers and activators of transcription
JNK	c-Jun N-terminal kinase
KO	knockout
LVID;d	left ventricle internal dimension at end-diastole
LVID;s	left ventricle internal dimension at end-systole
LVPW	LV posterior wall thickness
LVPW;d	left ventricle posterior wall thickness at end-diastole
LVPW;s	left ventricle posterior wall thickness at end-systole
MAPK	mitogen-activated protein kinase
MI	myocardial infarction
MYH6	myosin heavy chain 6
MYH7	myosin heavy chain 7
NPPA	natriuretic peptide A
NPPB	natriuretic peptide B

NRF	nuclear respiratory factor
NRVM	neonatal rat ventricular cardiomyocyte
PE	Phenylephrine
PI3K	phosphoinositide 3-kinase
PKC	protein kinase C
PML	promyelocytic leukemia protein
PWM	position weight matrix
qRT-PCR	real-time quantitative reverse transcription polymerase chain reaction
RAAS	renin-angiotensin-aldosterone system
TAC	transaortic constriction
TAM	Tamoxifen
TF	transcription factor
TGFβ	transforming growth factor beta
TnT-MEK1-CA	Troponin T-driven constitutively active mitogen-activated protein kinase kinase 1
TTE	transthoracic echocardiography
TUNEL	terminal deoxynucleotidyl transferase dUTP nick end labeling
WT	wild-type; in reference to a native gene

Chapter 1

Introduction

1.1 Heart Failure

Epidemiology

Cardiovascular diseases are the most common cause of death in the US. Although heart failure (HF) accounts for only 9% of deaths caused by cardiovascular diseases, yet the prevalence of heart failure is rising fast. The number of HF patients increased from 5.7 million (2009-2012) to about 6.5 million (2011-2014) and is projected to be 8 million by 2030. This increased prevalence could be attributed to many reasons including evidence-based therapies, advanced management of underlying risk factors and diseases, which leads to an improved survival rate. However, the life quality of patients is greatly compromised by the associated symptoms, and the 5-year case fatality rate of HF is still as high as 42.3%, nearly 2 out of 5 patients. The management of heart failure has also become a huge burden on society. The estimated total cost was about $30.7 billion in 2012 and may reach about $69.7 billion by 2030.[1]

Definition

Heart failure, defined by Dr. Eugene Braunwald, is "a clinical syndrome caused by the inability of the heart to supply blood to the tissues commensurate to the metabolic needs of that tissue".[2] The patients may present with symptoms and signs such as fatigue, dyspnea, exercise intolerance, and jugular vein congestion. The diagnosis of heart failure is mainly based on history and physical examination, and there is no typical diagnostic test so far. Transthoracic echocardiography (TTE) is the primary non-invasive imaging test to examine cardiac anatomy and evaluate cardiac function. In this examination, a commonly used parameter to assess the cardiac function is ejection fraction (EF), a measurement of the percentage of blood ejected each contraction. Based on the value of left ventricle EF (LVEF), the HF patients can be generally classified as HF with reduced EF (HFrEF) by LVEF $\leq$ 50% and HF with preserved EF (HFpEF)

by LVEF > 50%. Considering the different pathogenesis of HFpEF and the limitation of the text, in this paper, we will mainly focus on the HFrEF which represents about half of HF cases and it is also the disease model we studied.

Etiology

As is defined, any disease or risk factor damaging the cardiac structure or function will eventually cause heart failure and systemic disorders. A majority of diseases can lead to heart failure, including ischemic cardiomyopathy, dilated cardiomyopathy, primary valvular heart diseases, hypertension, myocarditis, etc. The risk factors for heart failure include smoking, sedentary lifestyle, metabolic syndrome diabetes, and obesity.

Current management of heart failure

Based on the etiology and pathology of heart failure, the management mainly focuses on two aspects: 1) manage the risk factors and underlying diseases 2) control the symptoms and maintain the heart function.[3] The most widely used management approach is pharmacological therapies, including 1) medications targeting the renin-angiotensin-aldosterone system (RAAS) such as angiotensin-converting enzyme inhibitors (ACEI), angiotensin II receptor blockers, aldosterone antagonists, 2) medications targeting sympathetic nervous system such as β-blockers, 3) diuretics, 4) hydralazine and nitrate, 5) digoxin, etc. Most of these medications function by targeting RAAS or β receptors to decrease pathologic sympathetic activation, fluid retention, and pathologic remodeling. Other approaches to manage HF such as device therapy, are more limited to certain indications rather than widely used methods. Unlike the management of various cancers that novel targeted therapies come out rapidly, very few new drugs or therapies for HF have arisen over the last decades. Therefore, to improve clinical outcomes and avoid hemodynamic liabilities, new therapies to target intrinsic cardiac mechanisms are urgently needed.

1.2 Pathological, Cellular and Molecular Events in Cardiac Remodeling

The heart is the power source of the entire circulatory system. It has a remarkable capability to accommodate both the physiological and pathological stimuli and maintain the flow to circulate the whole body.[4] "Remodeling" is a commonly used term to describe this compensated change of the heart. According to a consensus in the cardiac field, cardiac remodeling is defined as "genome expression, molecular, cellular and interstitial changes that are manifested clinically as changes in size, shape, and function of the heart after cardiac injury."[5] As mentioned above, HF emphasizes more as a clinical symptom, whereas, cardiac remodeling depicts the change of heart precedes heart failure.[6]

Hypertrophy is the main adaptation process in the cardiomyocyte during remodeling. Based on the types and outcomes of the stimuli, it can be classified as physiological and pathological hypertrophy. Physiological hypertrophy usually occurs in exercise and pregnancy. In physiological hypertrophy, CMs enlarge in both width and length without LV mass change. However, pathological hypertrophy occurs after some cardiovascular diseases (ischemic cardiomyopathy, valvular disease, genetic cardiomyopathy, etc.) or with persistent excessive workload. In pathological hypertrophy, CMs grow either longer in series or wider in parallel, which exhibits at the organ level with increased LV mass and concentric or eccentric hypertrophy (Figure 1.1).[7] This remodeling change can help to maintain the stroke volume and reduce wall stress based on LaPlace law at first, but eventually it makes HF worse.
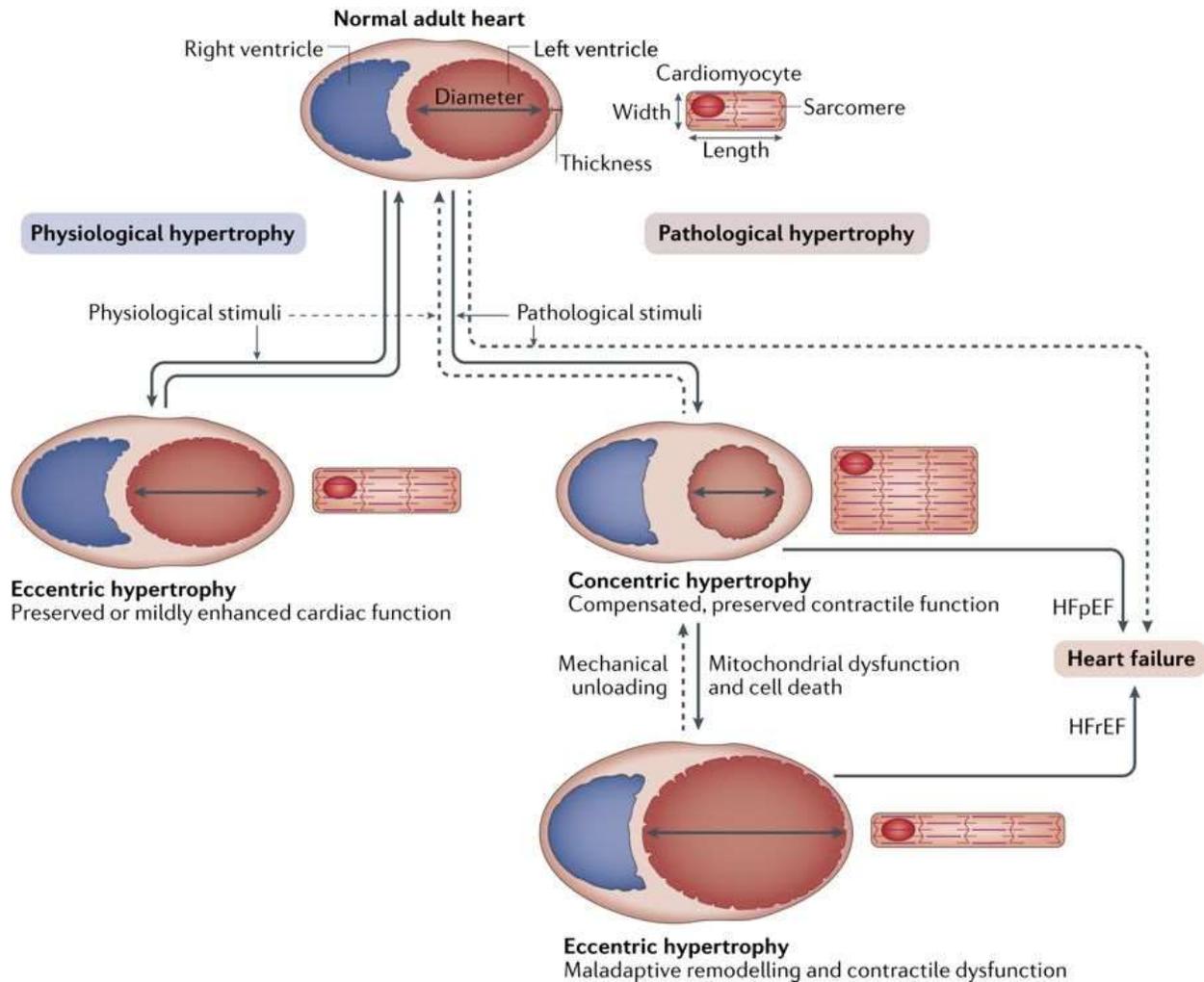
Figure 1.1 Physiological and pathological cardiac hypertrophy. The heart would undergo hypertrophy for adaptation. There are two types of hypertrophy, physiological and pathological hypertrophy. In physiological hypertrophy, CMs enlarge in both width and length without LV mass change. In pathological hypertrophy, CMs grow either longer in series or wider in parallel, which exhibits at the organ level with increased LV mass and concentric or eccentric hypertrophy respectively. Adapted from Nakamura M et al, 2018.[7]

Accompanied with pathological hypertrophy, other cellular processes also occur in remodeling, including fibrosis, enhanced cell death, metabolic dysfunction, inflammation, electrophysiological interruption, etc.[5,8] These processes are mediated not only by CMs, but also cardiac fibroblasts, endothelial cells, and possibly some circulating cells. Intriguingly, many recent studies indicated that CM dysfunction is not the sole driver of heart failure. Mutation or dysfunction in these non-CM cell types, for example, the cardiac fibroblast activation can also drive the disease progression.[9] This notion also brings the attention to the function of non-cardiomyocytes and their interaction with the cardiomyocytes. At the molecular level, multiple signaling pathways, as well as related gene expression changes conduct these cellular processes. The understanding of the molecular mechanism not only elucidate the pathology but also provide potential targets for treatment. However, what we know about the molecular mechanism of HF is still the tip of the iceberg.

1.3 Kinases and Cardiac Kinome

Protein kinases are enzymes catalyzing the translocation of a phosphate group from a nucleoside triphosphate to the substrate. They serve as important components in the signal transduction by phosphorylating their substrates. Based on the specificity of the substrate amino acids, kinases can be divided into 3 groups: serine/threonine kinase, tyrosine kinase or dual-specificity kinases which can phosphorylate both serine/threonine or tyrosine residue.[10] The mapping of the protein kinase complement of the human genome, "kinome", was accomplished in 2002.[11] Among 22,300 human protein-coding genes, only 518 of them encode kinases. In 2004, the full kinome of the mouse genome was determined by the same group. They predicted 540 protein kinases in the mouse with 510 human orthologs.[12]

Beyond biological functions, kinases are also tractable drug targets with a special conserved kinase pocket in the structure. A classic example is the first kinase inhibitor Imatinib (Gleevec) approved in 2001, which is used for the treatment of chronic myeloid leukemia. Imatinib exerts its biological effects by specifically inhibiting the BCR/ABL tyrosine kinase (the Philadelphia Chromosome). In fact, the kinases are the second-largest drug target group after G-protein-coupled receptors.

Cardiac kinases possess the basic kinase function and also play essential roles in cardiac remodeling by directly regulating cardiac hypertrophy, contractility, and cardiomyocyte death.[13,14] The cardiac kinome was described in 2015 by the Fuller and Clerk group. They not only catalogued 402 transcripts of cardiac kinases but also identified the kinase expression profile in normal versus failing human hearts.[15] Previous studies about cardiac kinases are limited to few kinase families, such as Rho kinase, PKC, GSK3β, PI3K, MAPKs, CaMKIIδ,[16] GRK2,[17] etc. Unfortunately, none of these kinase inhibitors have been approved for HF treatment so far. This is limited by both the specificity and efficacy of the inhibitors and a thorough understanding of their functions. On the other hand, the majority of those aberrant kinases and highly expressed cardiac kinases have never been studied. Therefore, it is essential to understand the role of those less studied cardiac kinases involved in HF to better understand the pathogenesis as well as for therapeutic purposes.

1.4 HIPKs and HIPK2

Homeodomain-interacting protein kinase family was discovered by Young Ho Kim et al in 1998 and named for containing a characteristic homeoprotein interacting domain and a conserved kinase domain.[18] HIPK1-3, sharing a highly homologous kinase domain, were discovered first, and HIPK4, with about 50% similarities in the kinase domain but smaller in structure (616 amino acids), was cloned later in 2007.[19]

Gene and Protein Structure

Human HIPK2 is located on chromosome 7q34, encoding 1198 amino acids, while the mouse HIPK2 is on chromosome 6. HIPK2 is conserved among species. The structure of HIPK2 from N-terminal to C-terminal includes kinase domain, homeoprotein interacting domain, and the autoinhibitory domain. It also contains multiple functional and modification sites such as the speckle-retention signal (SRS), a

sumoylation site (K25) and a ubiquitination site (K1182) as well as several caspase cleavage sites (Figure 1.2).[20]

Figure 1.2 Schematic representation of murine HIPK2. From N-terminal to C-terminal, it contains the kinase domain, homeoproteins interacting domain (HID), speckle-retention signal (SRS) and the autoinhibitory domain (AID). Sites regulated by phosphorylation, ubiquitination and caspase cleavage are also shown. Modified from Puca et al, 2010.[20]

Tissue Expression and Cellular Localization

HIPK2 expresses in multiple tissues including brain, kidney, heart, muscle, adipose tissue, etc. In the cells, HIPK2 mainly localizes in the nuclear speckle regulated by the SRS region.[18,21] In a certain context, it can also relocate to the cytoplasm.[22] The kinase function of HIPK2 is also important for the HIPK2 nuclear localization, yet the underlying mechanism is still unknown.[23]

Regulation of HIPK2

HIPK2 is constantly degraded and maintains at a low level in proliferating cells.[23] In normal conditions, HIPK2 is constantly ubiquitinated by several ubiquitin E3 ligases including Siah1, WSB-1 and Fbx3.[23–25] In response to lethal DNA damage, HIPK2 is released from E3 ligase and stabilized. HIPK2 then phosphorylates p53 at Ser46, which initiates the programmed cell death.[26,27] In sublethal DNA damage, however, HIPK2 does not phosphorylate p53 at Ser46 and is degraded by MDM2, which directs cells into cell cycle arrest for recovery. Besides severe DNA damage, the level of HIPK2 is also upregulated in response to many stress and pathological conditions such as ultraviolet (UV), ionizing radiation, genotoxic chemo-therapy, zinc in hypoxia environment, and extracts from some traditional Chinese medicine (saponin and Verbascoside). In the contrast, it is inhibited by cytoplasmic localization, hypoxia, gene mutation, LOH, and HPV23 E6.[28] As a protein, HIPK2 can also be dynamically regulated by multiple post-translational

modifications, including ubiquitination, phosphorylation, acetylation, and sumoylation. Since the change of HIPK2 level is highly related to its function, it is critical to understand the stimuli and upstream regulators of HIPK2 in different tissues.

1.5 Biological Functions of HIPK2

The role of HIPK2 in development

As how HIPKs family was named, the primary function of HIPK2 is interacting with homeodomain proteins, which is encoded by the homeobox sequence of 180bp discovered in *Drosophila melanogaster*. The homeodomain is a highly conserved DNA-binding domain and is extremely important during development.[29] This also implicates a crucial role of HIPK2 in development. Indeed, loss of both HIPK1 and HIPK2 is embryonic lethal in the mouse. The double knockout (KO) mice died between 9.5-12.5 days postcoitus due to neural tube defects.[30] Some other defects were also observed in the double KO mice including hematopoiesis, vasculogenesis, angiogenesis, and lens formation.[31–33] Of note, deletion of only HIPK1 or HIPK2 in mice does not affect the survival but is still sufficient to cause dysfunction. These findings indicate not only the importance of HIPKs in the development but also the partial overlapping role of HIPK1 and HIPK2. This redundancy may be a reassurance for the essential stage in development.

The role of HIPK2 in the nervous system

HIPK2 is highly expressed in the central and peripheral nervous system. It plays an essential role in not only neural development but also critical to maintaining the neuron function and survival. Remarkably, HIPK2 KO mice exhibited severe psychomotor behavioral abnormalities characterized by dystonia, retardation and impaired coordination.[34,35] This phenotype is mainly caused by HIPK2-mediated cell survival in different types of neurons. J.Zhang et al showed that the dysfunction was mainly due to increased apoptosis of midbrain dopamine neurons mediated by the TGFβ-SMAD-HIPK2 signaling pathway.[35] This TGFβ-HIPK2 mediated survival of dopamine neurons was also observed in the gastrointestinal nervous system. Loss of enteric dopaminergic neurons in HIPK2 KO mice results in

gastrointestinal motility dysfunction, which eventually leads to about 40% death rate before weaning.[36] In addition, Anzilotti et al found activation of apoptosis in HIPK2 deficient Purkinje cells by impaired protein degradation also attributes to the cerebellar dysfunction and ataxia-like phenotype in KO mice.[34]

Intriguingly, HIPK2 can also affect some types of neurons by enhancing apoptosis. Wiggins et al showed that deletion of HIPK2 decreased apoptosis in sensory neurons by interacting Brn3a and regulating Brn3a-mediated gene expression.[37] Enhanced apoptosis by HIPK2 overexpression was also observed in sensory and sympathetic neurons with neutrophin.[38] However, the mechanistic basis of this differential regulation of cell death in different types of neurons by HIPK2 is still unknown.

The role of HIPK2 is also recognized in neurodegenerative diseases and neural injury models. In amyotrophic lateral sclerosis, HIPK2 is required for ER-stress induced cell death via the ASK1/HIPK2/JNK pathway. Loss of HIPK2 attenuates the SOD1 mutation mediated ALS phenotype.[39] In Alzheimer disease patients, the misfolded p53 protein in fibroblasts is found to be associated with HIPK2 inhibition.[40]

The Role of HIPK2 in Other Tissues

HIPK2 KO mice also exhibited defects in other organ systems. Increased apoptosis and decreased proliferation of erythroid progenitor cells were reported in terminal erythroid proliferation and differentiation.[41] HIPK2 KO mice also have lower body weight and white fat tissue, which result from the suppression of the white fat differentiation due to HIPK2 deficiency. However, loss of HIPK2 increased insulin sensitivity and resistance to the high-fat diet-induced weight gain.[42]

The Role of HIPK2 in Tumorigenesis

HIPK2 is recognized as an important tumor suppressor due to its role in apoptosis. As mentioned above, HIPK2 determines cell fate in response to DNA damage by phosphorylating p53. Besides direct phosphorylation, HIPK2 interacts with p53 in multiple ways to control cell apoptosis. HIPK2 is recruited by promyelocytic leukemia protein (PML) IV isoform with p53 and CBP to PML nuclear bodies, where is known for p53 modification occurs.[43] HIPK2 also regulates several cofactors of p53 Ser46 phosphorylation,

including Axin, Daxx, PML. Furthermore, to prevent p53 degradation and induce cell apoptosis, HIPK2 can phosphorylate MDM2 which degrades p53 in unstressed cells.[44] On the other hand, p53 can also promote HIPK2 activity through cleavage of HIPK2 auto-inhibitory domain by caspase 6, a known p53 regulated genes.[45] The truncated HIPK2 has an increased activity to induce cell apoptosis. HIPK2 can also regulate apoptosis through a p53-independent pathway. In hepatoma cells, HIPK2 regulates TGFβ-induced apoptosis through JNK signaling pathway.[46] HIPK2 can also phosphorylate CtBP[47] and ΔNp63α[48] to promote degradation of these HIPK2 targets in apoptosis.

Decreased level of HIPK2 is found in several cancer types, such as bladder cancer and esophageal squamous cell carcinoma.[49–51] In a skin tumor model induced by two-stage carcinogenesis protocol, HIPK2 KO and heterozygous mice are more susceptible to tumor formation. This indicates not only the tumor suppressor function of HIPK2 in the skin but also the haploinsufficiency of this function.[24,52] Beyond directly regulating tumorigenesis, HIPK2 is also a key mediator in hypoxia-induced chemoresistance. HIPK2 expression is suppressed in response to hypoxia, which relieved its suppression on HIF1α and eventually can promote angiogenesis and tumor progression. Hypoxia can also increase resistance to chemotherapy by upregulating MDM2 expression to decrease apoptosis facilitated by HIPK2 mediated p53 phosphorylation. In addition, Zinc can reverse the dysfunctional HIPK2 as well as p53 inhibition in the hypoxic tumor cells.[53,54] These studies reveal the important role of HIPK2 in tumorigenesis and emphasizes its potential in cancer treatment.

Surprisingly, HIPK2 can also function as an oncogene in certain conditions. The elevation of HIPK2 at both mRNA and protein levels was observed in cervical cancer.[55] In familial adenomatous polyposis, HIPK2 mRNA level was found higher than normal, which may promote tumorigenesis by suppressing PGE2 generation.[56] Furthermore, multiple-platform genomic analyses also showed increased mRNA as well as protein levels of HIPK2 in pilocytic astrocytoma.[57]

Overall, HIPK2 is an essential regulator of cell death in both proliferating cells and non-proliferating cells. However, most of the cancer studies were performed in tumor cell lines rather than tumor in situ studies which compromised the cause-and-consequence effect of HIPK2 mediated regulation of cell

death.[58] More in vivo studies are needed to validate the associated mechanism and the translational application of targeting HIPK2. In addition, the underlying mechanism of the contradictory role of HIPK2 on cell death is still unclear. This could be related to the temporal or spatial role of HIPK2 in different diseases context, stimulation or derivation of the cells. Thus, on one hand, it is essential to elucidate the relationship of the HIPK2 level on the biological effect to exclude the potential false-positive findings. On the other hand, it would be crucial to elucidate the mechanism of HIPK2 regulation and function in cell death in different cell types. Even so, HIPK2 is still a promising hit for targeted therapy, and the recent discovery of the crustal structure of HIPK2[59] will largely accelerate the development of HIPK2-targeted therapies.

HIPK2 in other proliferative diseases

The role of HIPK2 is also recognized in other diseases related to cell proliferation. Jin et al used a systemic computational bioinformatics approach to identify the role of HIPK2 as a potential regulator in kidney fibrosis.[60] They reported that HIPK2 KO animals demonstrated a significantly decreased fibrosis in multiple renal fibrosis models. Analysis of human idiopathic pulmonary fibrosis samples revealed that HIPK2 dysfunction may play a role in pulmonary fibroblasts behavior and pathogenesis.[61] BT173, a small inhibitor of HIPK2 was identified as a potential hit for the antifibrotic therapy.[62]

1.6 Objectives

Using a novel bioinformatics approach to identify kinase targets in heart failure, we predicted HIPK2 as a potential regulator of cardiac remodeling. The main goal of this project is to examine the role of HIPK2 in cardiac biology.

Aim 1 Determine the role of cardiomyocyte HIPK2 in cardiac biology.

Since this is the first study to determine the role of HIPK2 in cardiac biology, I first examined the heart function in the global KO mouse model. However, this model was compromised by the multiple

defects caused by global gene ablation **(Chapter III)**. Therefore, I generated cardiomyocyte-specific HIPK2 KO mice (driven by αMHC-Cre, CM-KO), heterozygous null mice (CM-Het) **(Chapter IV)** and tamoxifen-induced conditional CM-specific KO mice (driven by αMHC-MerCreMer, cKO) **(Chapter V)** to elucidate the role of HIPK2 in the heart. Besides these mouse models, I also used adenoviruses carried expressing wildtype (WT) HIPK2 or shRNA-HIPK2 as the gain-of-function or loss-of-function approaches in the in vitro model of neonatal rat ventricular cardiomyocytes (NRVMs) **(Chapter IV)**. To examine the clinical relevance of HIPK2 in heart failure, we also examined the HIPK2 expression level in human and mouse failing hearts **(Chapter II)**.

Aim 2 Determine the underlying mechanism of how HIPK2 regulates cardiac function.

In Aim 1, using three different genetic mouse models, we established that the deletion of cardiomyocyte HIPK2 leads to cardiac dysfunction. In this aim, our goal is to delineate how the deletion of HIPK2 leads to heart failure. To identify the dysregulated pathways in HIPK2 deficient hearts, I examined the major pathways and cellular processes involved in cardiac remodeling. Moreover, I used in vitro models and AAV9 rescue experiments to further validate my mechanistic findings from the in vivo models. Eventually, I found that cardiac dysfunction in HIPK2 deficient hearts is mainly due to dysregulated ERK signaling mediated cardiomyocyte apoptosis **(Chapter IV)**.

Aim 3 Identify the role of HIPK2 in cardiac fibroblasts and fibrosis.

Recent studies have demonstrated that fibroblast (FB)-specific genetic manipulation can lead to robust cardiac phenotype.[9] HIPK2 is also known as a pro-fibrotic factor in kidney fibrosis. Thus, the main goal of this aim is to specifically identify the role of HIPK2 in cardiac fibroblasts and fibrosis. I examined the change of the TGFβ1-SMAD3 pathway in cardiac fibroblasts, which is the key signaling pathway in fibroblasts and fibrosis. We also generated cardiac fibroblast-specific HIPK2 KO mice and examined the cardiac function after myocardial infarction (MI) **(Chapter VI)**.

Chapter 2

Identification of HIPK2

Part of this work was accepted to publish in *Circulation*.[63]

2.1 Introduction

Protein kinases are essential regulators of cardiac function and also highly tractable and precedented drug targets. Thus, it is important to expand our understanding of the cardiac kinome as a means of exploring potential therapeutic opportunities for heart failure treatment. To identify novel cardiac kinases potentially involved in heart failure development, we used an integrated transcriptome and bioinformatics approach (Expression2Kinases)[64] by using control and failing mouse hearts. Unlike conventional transcriptome screenings, this approach links upstream kinases with the global pattern of observed gene expression via transcription factors to predict potential key regulators of disease progression and potential therapeutic targets.[60] By using this approach, we identified an unexplored cardiac kinase in the context of cardiac function and dysfunction—HIPK2.

2.2 Methods and Materials

Human heart samples

The human specimens used in this study were obtained from the Vanderbilt Main Heart Biorepository (VMHB). The study protocol was approved by the Vanderbilt University Medical Center, Institutional Review Board, and written informed consent was obtained from the heart tissue donors. Left ventricle (LV) from 9 subjects with ischemic heart failure was identified from the VMHB, and 5 of unmatched donor hearts were also obtained from the VMHB.

Microarray gene expression assay

Adult C57BJ6 male mice were subjected to transaortic constriction (TAC) or sham surgery. RNA samples from the 6-week post-TAC or sham mice were subjected to Affymetrix microarray analysis (sham: n=5, TAC: n=4; GEO accession: GSE136308). The differentially expressed genes were identified in TAC versus sham hearts using one-way ANOVA. Adjusted p-value was corrected using Benjamini–Hochberg false discovery rate with a threshold of 0.01.

RNA isolation and Real Time-PCR

RNA was isolated from cells or tissue using the RNeasy Mini Kit (Qiagen #74104) following the manufacturer's instructions. The RNA concentration was measured and equal amounts of RNA were used to synthesize cDNA using the iScript cDNA Synthesis Kit (BioRad #1708891) according to the manufacturer's instructions. Quantitative Real Time-PCR (qRT-PCR) was performed using TaqMan Gene Expression Master Mix (Applied Biosystems #4369016) as well as the TaqMan Gene Expression Assay primers (Thermo Fisher Scientific) according to the manufacturer's instructions. Eukaryotic 18srRNA is used as the control gene in all experiments. Fold change is calculated using Delta delta Ct methods. Primers used are listed as follows: *HIPK2* (mouse) (Assay ID: Mm00439329_m1), *HIPK2* (human) (Assay ID: Hs00179759_m1), *Nppa* (mouse) (Assay ID: Mm01255747_g1), *Nppa* (rat) (Assay ID: Rn00664637_g1), *Nppb* (mouse) (Assay ID: Mm01255770_g1), eukaryotic 18S rRNA (4319413E). The fold change is calculated using ΔΔCt method.

Statistics

Differences between data groups were evaluated for significance with the use of the nonparametric Mann-Whitney test or Student t test for comparison between 2 groups, and ANOVA or mixed-effects analysis with Turkey post hoc test for comparison among >2 groups (GraphPad Prism Software Inc). Data are presented as mean±SEM unless noted otherwise. For all tests, a *P* value of <0.05 was considered to denote statistical significance.

2.3 Results

Identification and Characterization of HIPK2 in Failing Hearts

Considering the essential role of cardiac kinases in disease progression and their general tractability as drug targets, we used a novel bioinformatics approach (Expression2Kinase)[64] to identify kinase regulators involved in heart failure progression (Figure 2.1A). C57BL/6 male mice were subjected to transaortic constriction (TAC) to induce heart failure or sham surgery. At 6 weeks after TAC, RNA samples from the left ventricle were subjected to microarray analysis. We first identified the differentially expressed genes (fold change≥1.5, adjusted P<0.01) in TAC versus sham hearts. Second, we postulated transcription factors (TFs) of those differentially expressed genes using 3 algorithms: Ingenuity Pathway Analysis (IPA, Qiagen), Position Weight Matrix (PWM), and ChIP Enrichment Analysis (ChEA).[64] With the IPA approach, a total of 40 associated transcription factors were identified. These TFs were responsible for 27 upregulated genes, and 13 downregulated genes (Figure 2.1B). We also predicted responsible TFs for the observed gene expression changes by using 2 additional approaches: (1) ChEA, based on chromatin-protein binding, and (2) TransFac and Jasper analysis, based on specific promotor binding (PWM) (Figure 2.1C). Thus, these 3 approaches to predict the responsible TFs generated 3 distinct lists of TFs for further analysis. Third, we linked these TFs with potential upstream kinase regulators by constructing a protein-protein interaction network.[65] We then performed a Kinase Enrichment Analysis[66] on those proteins interacting with predicted TFs and identified the top 25 extrapolated kinase regulators of each TF prediction approach (Figure 2.1A). Even though predicted by distinct approaches, 52% kinase targets (in red) were common in 3 kinase lists, and 70% (in blue) were common in 2 lists. Furthermore, these 3 lists were highly dominated by commonly described kinases known for their indispensable role in cardiac biology (eg, AKT, GSK3, and MAPKs). The identification of these positive-control kinases was also a validation of this analytical approach. Among those candidates, we identified a potential modulator of heart failure, HIPK2, a kinase whose role in cardiac biology has never been studied before.
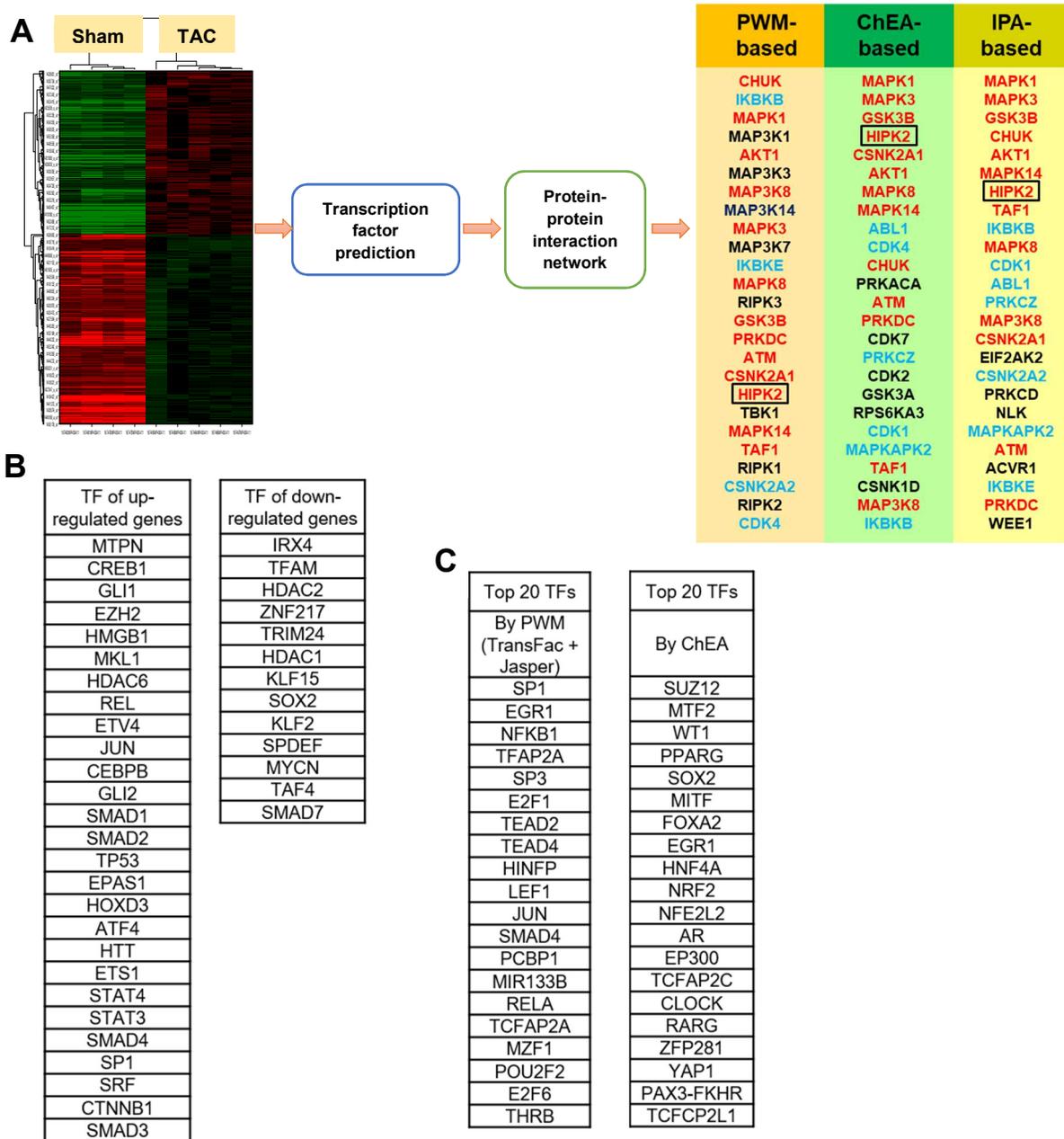
Figure 2.1 Identification of HIPK2 as a potential regulator of heart failure. A. Adult C57BJ6 male mice were subjected to transaortic constriction (TAC) or sham surgery. RNA samples from the 6-week post-TAC or sham mice were subjected to microarray analysis. Transcriptomic analysis was performed to identify differentially expressed genes between TAC versus the sham group. Hierarchical clustering by these differentially expressed genes was performed with results as depicted in the heat map (green denotes downregulated genes; red denotes upregulated genes). Transcription factors (TFs) were predicted based on these gene expression changes by using 3 approaches based on Ingenuity Pathway Analysis (IPA), Position Weight Matrix (PWM), and ChIP Enrichment Analysis (ChEA) algorithms, and then upstream kinases of those TFs were identified using Kinase Enrichment Analysis. Top kinase targets are represented in 3 columns for respective TF prediction methods used. Red indicates kinases identified by all 3 approaches; Blue, kinases identified by 2 approaches; Black, kinase identified by one approach. **B.** TFs of differentially expressed genes identified by IPA. 27 transcription factors of upregulated genes and 13 transcription factors of downregulated genes are listed. **C.** Top 20 transcription factors of differentially expressed genes identified by PWM, and ChEA algorithms, respectively.

16

HIPK2 Expression in Heart Failure Models

      To determine the role of HIPK2 in failing human hearts, we examined the expression of HIPK2 in heart tissue from patients with end-stage ischemic cardiomyopathy. The expression of HIPK2 was dramatically decreased in the failing hearts in comparison with normal human hearts (Figure 2.2A). Consistently, ischemic mouse failing hearts after MI were also associated with significantly decreased HIPK2 expression (Figure 2.2B). Overall, these data indicate that HIPK2 may be involved in cardiac pathogenesis.
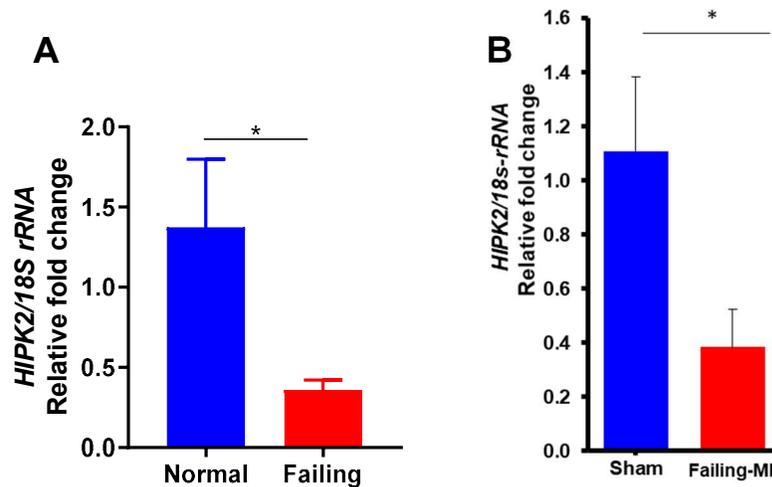
Figure 2.2 Expression of HIPK2 in failing hearts. A. Quantification of HIPK2 mRNA expression in human normal hearts versus failing hearts. Normal hearts: n=5, failing hearts: n=9. **B.** C57BL6 male mice were subjected to left anterior coronary artery ligation or sham surgery. The heart was harvested 4 weeks after the surgery. RNA was isolated from the left ventricle for qRT-PCR. Quantification of HIPK2 mRNA expression in MI-induced failing hearts versus sham hearts. Sham: n=4, failing hearts: n=4. *$P<0.05$, Mann-Whitney test. All bar graphs are represented by mean±SEM.

2.4 Discussion

      Alarming statistics of human experience with heart failure and the resultant economic impact necessitate the investigation of new efficient molecular targets to improve preventive and therapeutic strategies. Cardiac kinases are essential molecules in the cardiac pathogenesis, and the tractable targets for treatment, as well. In the current study, we used the Expression2Kinase approach to screen kinase targets in a heart failure model and identified a previously unexplored cardiac kinase HIPK2.

Expression2Kinase approach was developed by Ma'ayan's group in 2012 and applied in multiple disease models.[60,67] The conventional microarray data analysis mainly focuses on the gene expression changes for the predictions of pathways and cellular processes based on known connections in the literature. The Expression2Kinase deeply digs the screening data by connecting the change of transcripts with the regulation of transcription factors. And the last step in this pipeline using Kinase Enrichment Analysis is more than exploring the protein interaction, but "functional kinase" phosphorylating targets.[66] This algorithm is more likely to identify key regulators leading to the global gene expression pattern changes in the disease context. Overall, this Expression2Kinase is a reliable approach to analyze the transcriptome data to predict novel targets at multiple levels.

Besides the identification of new targets, we also found that HIPK2 expression was consistently downregulated in human and mouse ischemic failing hearts. The change of HIPK2 expression in failing hearts indicates that HIPK2 may be involved in the disease progression. Since HIPK2 expression is suppressed by hypoxia, this could partially explain the decreased expression. However, what triggers this decrease and how this decrease affects heart function needs further investigation.

Chapter 3

Characterization of HIPK2 Global Knockout Mice

Part of this work was accepted to publish in *Circulation*.

3.1 Introduction

HIPK2 is a conserved serine-threonine kinase and regulates transcription of multiple genes and various cellular processes. We identified in Chapter II that HIPK2 may be involved in heart failure progression. However, the role of HIPK2 in cardiac biology has never been studied. The essential role of HIPK2 in development has been identified in several systems. HIPK2 is also known for its function as a tumor suppressor and pro-fibrotic molecule in kidney fibrosis models. Based on these findings in the literature, we hypothesized that deletion of HIPK2 may be protective to the heart function.

3.2 Methods

HIPK2 global KO mice

The HIPK2 global KO mice were a generous gift from Dr. Eric Huang, University of California, San Francisco.[37] The global KO mice were maintained in 129 and B6 mixed background. The WT littermates were used as controls in the study of HIPK2 global KO mice. The Institutional Animal Care and Use Committee of Vanderbilt University Medical Center approved all animal procedures and treatments. All animals were housed in a temperature-controlled room with a 12:12h light-dark cycle and received humane care.

Echocardiography

Transthoracic 2-dimensional echocardiography was performed with a 12-MHz probe (VisualSonics 2100) on mice anesthetized by isoflurane inhalation (1%-1.5%) in the HIPK2 global KO study. For the rest of the study, echocardiography was performed without anesthesia. M-mode interrogation was performed in the parasternal short-axis view at the level of the greatest LV end-diastolic dimension (EDD). EDD, LV end-systolic dimension (ESD), and LV posterior wall thickness (LVPW) were measured and used to calculate the percentage of fractional shortening (FS) and ejection fraction (EF). FS and EF values were exported from the echo program Vevo Lab 2.2.0.

Histological Analysis

LV tissue was fixed with 10% formaldehyde for 24 hours, dehydrated through increasing concentrations of ethanol, and then embedded in paraffin. LV sections (5µm) were stained with Masson trichrome (Sigma-Aldrich #HT-15) per manufacturer instructions. A Nikon AZ100 and NIS Elements software were used to record and analyze images.

Fibrosis quantification

Images were acquired using a Nikon AZ100 at 10X magnification of the whole LV ventricles. The fibrosis area was selected manually by color threshold method as described earlier.

Body composition measurement

Body composition was measured using Nuclear Magnetic Resonance analyzer (Minispec Model mq7.5, Bruker Instruments) following the manufacturer's instructions.

Neonatal rat ventricular cardiomyocyte isolation

Primary cultures of neonatal rat ventricular cardiomyocytes (NRVMs) were prepared from 1-3 day-old Sprague-Dawley rats as previously described.[68] Cells were plated on the Primaria cell culture dishes

(BD) and cultured in Ham's F-10 medium with 5% horse serum, 5% Fetal Bovine Serum, and 1% antibiotics. Following desired treatments, the cells were lysed for immunoblotting as described above.

Primary myocyte isolation and Calcium handling measurement

Adult cardiomyocytes were isolated from mice in Knollmann's Lab using the method as previously described.[69] Myocytes were loaded with Fura-2 acetoxymethyl ester, Fura-2 AM (Molecular Probes Inc., Eugene, OR). Briefly, myocytes were incubated with 2 μM Fura 2 AM for 8 min at room temperature to load the indicator in the cytosol. Myocytes were washed twice for 10 min with Tyrode's solution containing 250 μM probenecid to retain the indicator in the cytosol. A minimum of 30 min were allowed for de-esterification before imaging the cells. Fura 2-AM loaded myocyte Ca transients recorded during 0.5 Hz field stimulation in 2 mM Ca Tyrode's solution for 20 s at room temperature. Then stimulation was switched off followed by the application of caffeine 10 mM for 5 s to estimate SR Ca content. A subset of cells were exposed to 0Ca0Na Tyrode's solution for 10 s then caffeine 10 mM applied for 30 s to estimate non-NCX Ca extrusion. For each cell and each experimental condition, tau (τ), amplitude and baseline values were averaged from 3 consecutive Ca transients. Ca transients were recorded and analyzed using commercially available data analysis software (IonOptix, IonWizardTM Milton, MA). All experiments were conducted at room temperature.[69,70]

3.3 Results

Global KO of HIPK2 Leads to Decreased Cardiac Function

To evaluate the cardiac function of HIPK2, we first examined HIPK2 global KO mice[37] by TTE. At 2 months of age, heart function of wildtype (WT) and KO was comparable (Figure 3.1A-F). However, HIPK2 KO mice developed cardiac dysfunction at ≈5 months of age, reflected by significantly decreased Ejection Fraction (EF) and Fractional Shortening (FS) (Figure 3.2A-B). There was no significant change in left ventricle dimension and posterior wall thickness (Figure 3.2C-F). We also examined the contractility and calcium handling in single isolated adult CMs at the same age. It is surprising that there was no

significant change in the KO versus WT at basal as well as the isoproterenol-stimulated condition (Figure 3.3, 3.4). The intact contractility and calcium handling in HIPK2 deficient cardiomyocytes suggest a minimal to no role of these processes in observed detrimental phenotype in KO hearts. The heart weight of KOs, and the heart weight normalized by the tibia length, as well, was significantly decreased in comparison to WT (Figure 3.5A-B). It is important to note that the body weight of KOs was significantly less than that of the littermate controls (Figure 3.5C-D). Further examination of the body mass composition using the nuclear magnetic resonance analyzer revealed that the decreased body weight was mainly attributable to a lower percentage of fat mass in KOs (Figure 3.5E), which is consistent with previous findings.[42]
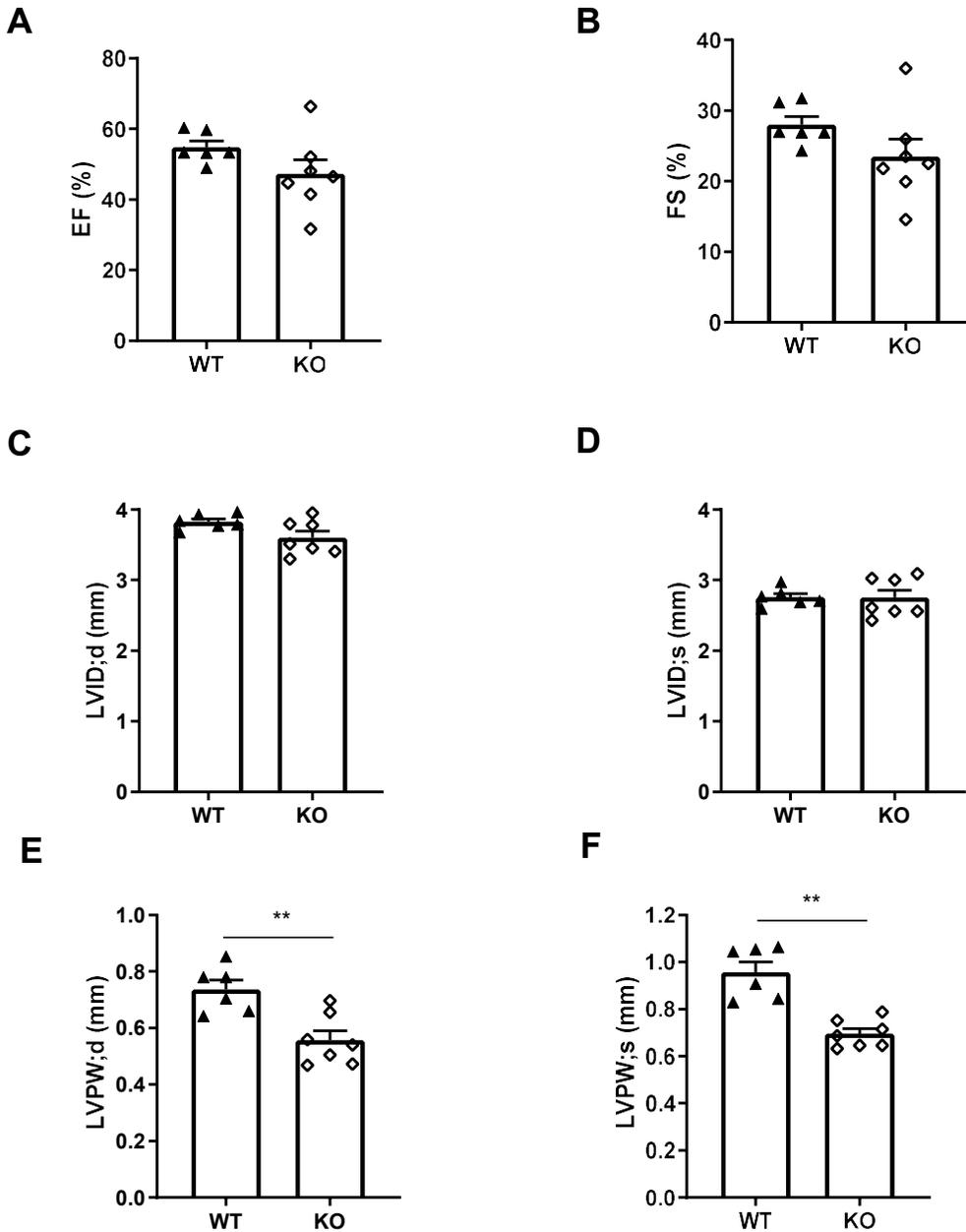
Figure 3.1 Echocardiographic assessment of HIPK2 global KO mice at 2 months of age. 2-month-old KO and WT mice were examined by transthoracic echocardiogram. **A.** Ejection fraction (EF). **B.** Fractional shortening (FS). **C.** Left ventricle internal dimension at end-diastole (LVID; d). **D.** Left ventricle internal dimension at end-systole (LVID; s). **E.** Left ventricle posterior wall thickness at end-diastole (LVPW; d). **F.** Left ventricle posterior wall thickness at end-systole (LVPW; s). n=5-7 per group. ** p<0.01, Mann-Whitney test.
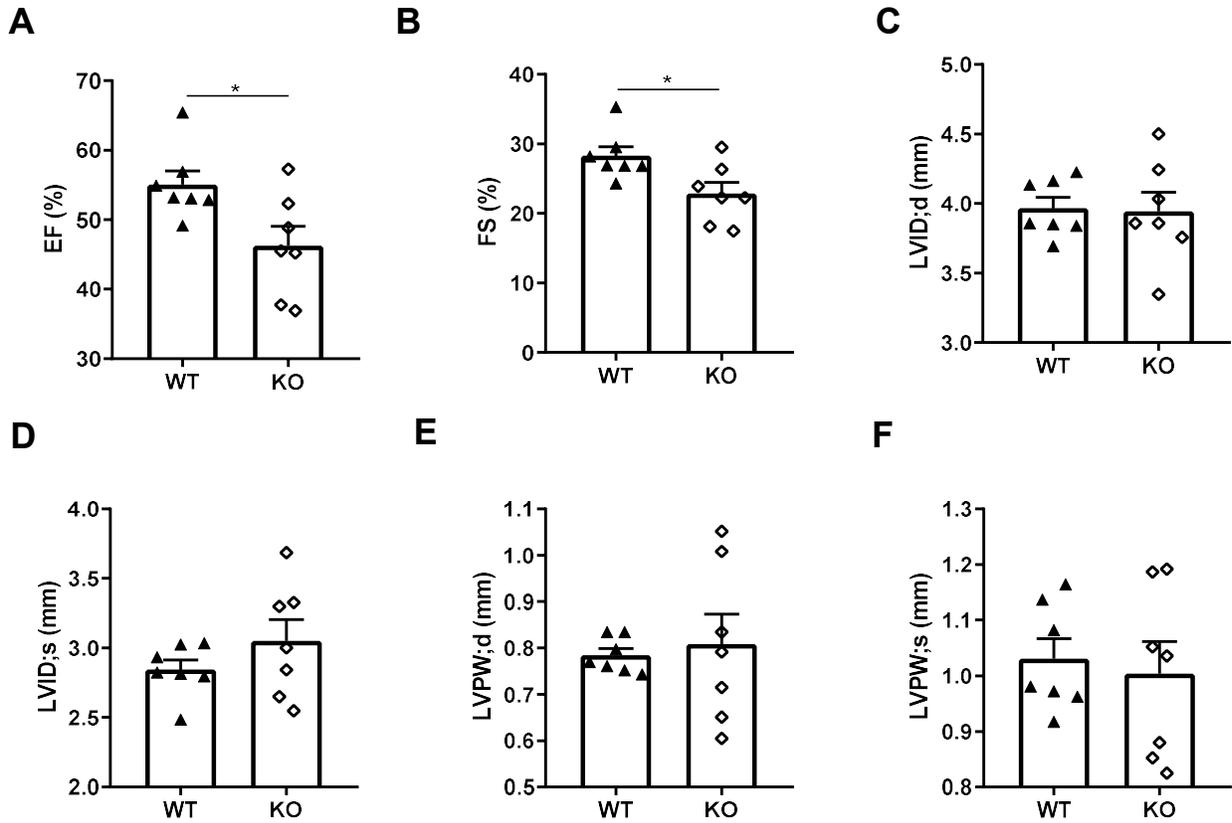
Figure 3.2 Echocardiographic assessment of HIPK2 global KO mice at 5 months of age. 5-month-old KO and WT mice were examined by transthoracic echocardiogram. **A.** Ejection fraction (EF). **B.** Fractional shortening (FS). **C.** Left ventricle internal dimension at end-diastole (LVID; d). **D.** Left ventricle internal dimension at end-systole (LVID; s). **E.** Left ventricle posterior wall thickness at end-diastole (LVPW; d). **F.** Left ventricle posterior wall thickness at end-systole (LVPW; s). n=4-7 per group. * p<0.05, Mann-Whitney test.
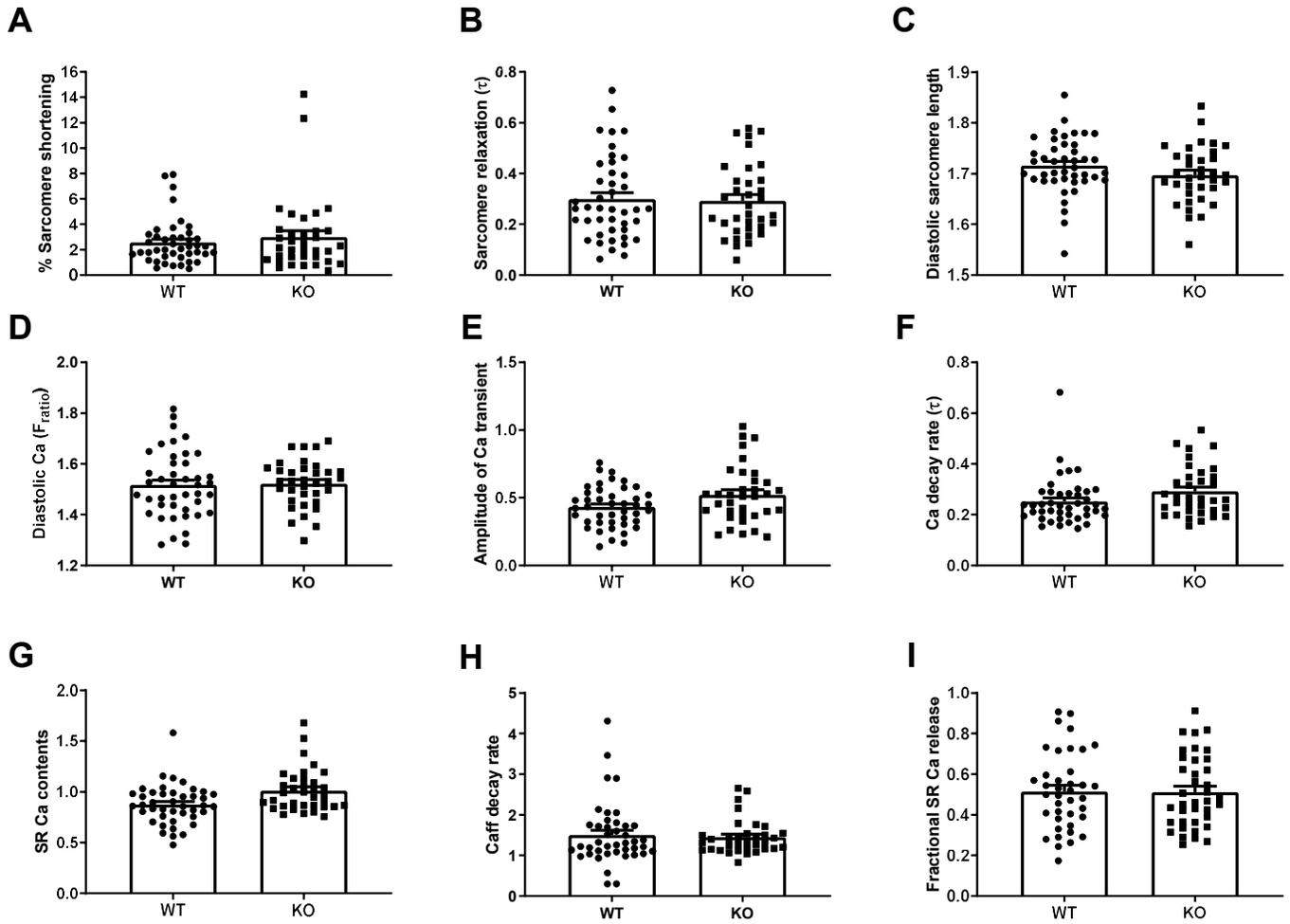
Figure 3.3 Measurement of contractility and calcium handling in isolated adult CMs from HIPK2 KO and WT mice at basal condition. Adult CMs were isolated from 5-month-old KO and WT mouse hearts. CMs were stained with 2μM Fura 2-AM and paced at 1 Hz for 20 seconds for contractility and Calcium (Ca) handling measurement. Caffeine (Caff, 10mM, 5s) was applied after pacing transient to estimate sarcoplasmic reticulum (SR) Ca content. CMs were examined in 2 mM Ca Tyrode's solution. **A.** Sarcomere peak shortening normalized to resting sarcomere length (% Sarcomere shortening). **B.** Sarcomere relaxation (τ). **C.** Diastolic sarcomere length. **D.** Diastolic Ca (F_{ratio}). **E.** Amplitude of Ca transient. **F.** Calcium decay rate (τ). **G.** SR Ca contents. **H.** Caff decay rate. **I.** Fractional SR Ca release. WT: n=43 from 3 mice, KO: n=35 from 3 mice. Student t-test.
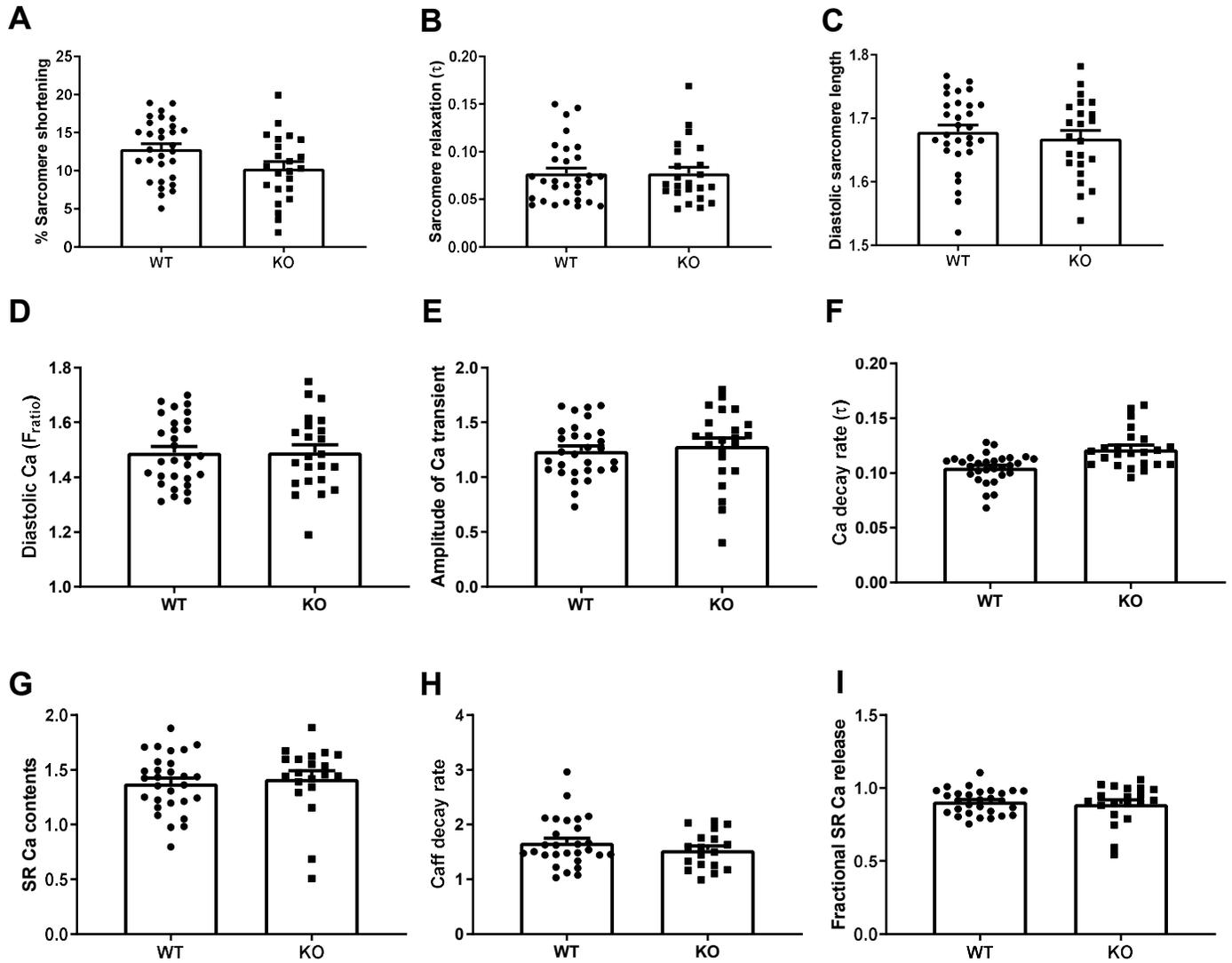
Figure 3.4 Measurement of contractility and calcium handling in isolated adult CMs from HIPK2 KO and WT mice at isoproterenol-stimulated condition. Adult CMs were isolated from 5-month-old KO and WT mouse hearts. CMs were stained with 2μM Fura 2-AM and paced at 1 Hz for 20 seconds for contractility and Calcium (Ca) handling measurement. Caffeine (Caff, 10mM, 5s) was applied after pacing transient to estimate sarcoplasmic reticulum (SR) Ca content. **A-I:** CMs were examined with Isoproterenol (ISO, 1 μM) stimulation in 2 mM Ca Tyrode's solution. **A.** Sarcomere peak shortening normalized to resting sarcomere length (% Sarcomere shortening). **B.** Sarcomere relaxation (τ). **C.** Diastolic sarcomere length. **D.** Diastolic Ca (F_{ratio}). **E.** Amplitude of Ca transient. **F.** Calcium decay rate (τ). **G.** SR Ca contents. **H.** Caff decay rate. **I.** Fractional SR Ca release. WT: n=29 from 3 mice, KO: n=20 from 3 mice. Student t-test.

26
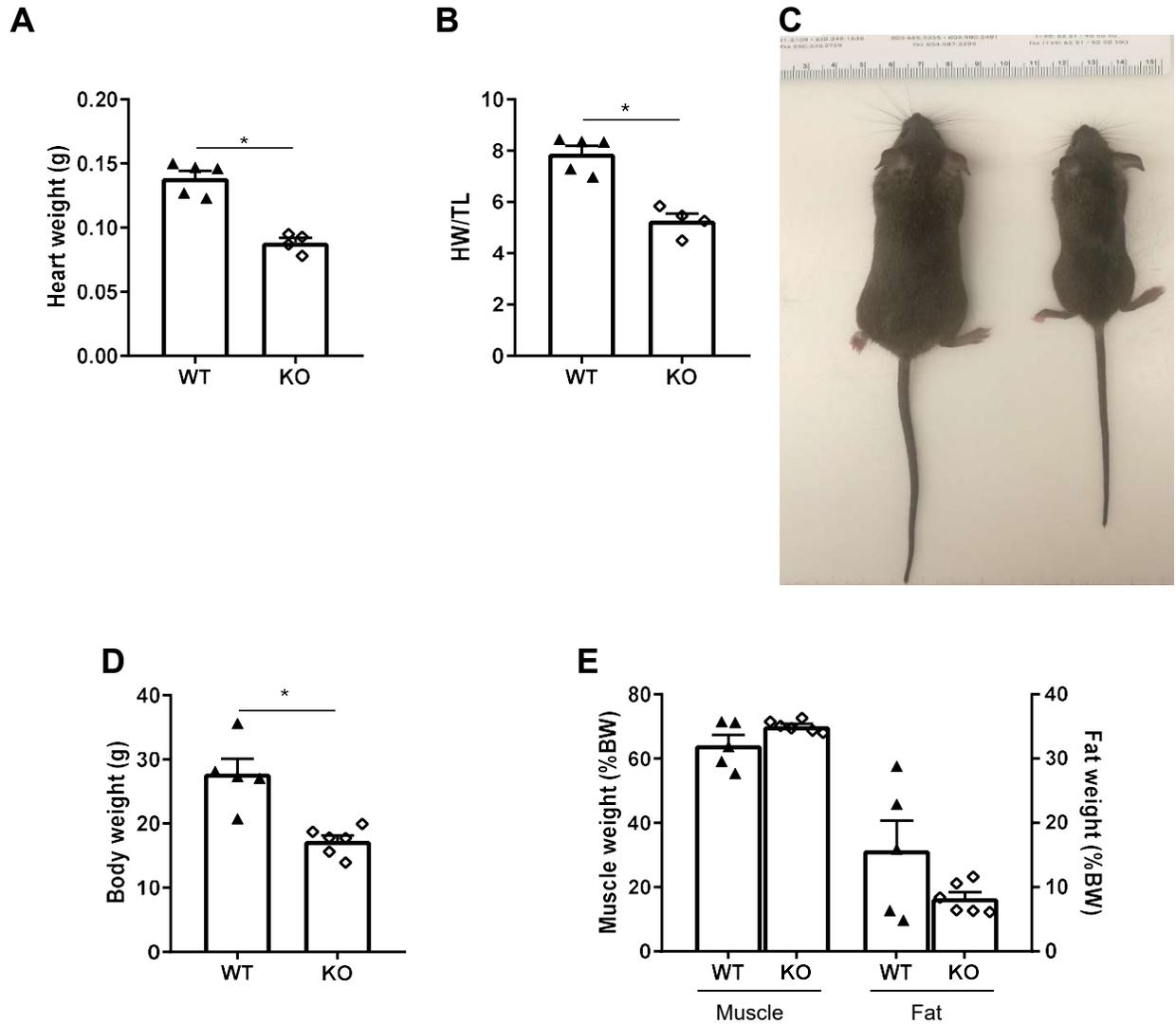
Figure 3.5 Morphologic characterization of HIPK2 global KO mice. A. Heart weight. **B.** Heart weight normalized by tibia length (HW/TL). **C.** Representative image of the HIPK2 global KO mouse and the littermate WT mouse. **D.** Body weight (BW). **E.** Body composition: muscle weight and fat weight was measured by NMR machine. The percentage of muscle weight and fat weight was then calculated by dividing the muscle or fat weight by body weight. * $p < 0.05$, Mann-Whitney test.

Right Ventricle Function in the HIPK2 Global KO Mice

The loss-of-haploinsufficiency of HIPK2 was identified in the human idiopathic pulmonary fibrosis.[61] Pulmonary dysfunction can lead to right heart dysfunction which can eventually drive the whole heart dysfunction. Therefore, we investigated if pulmonary hypertension could be a cause of heart failure in the HIPK2 global KO mice. We examined the right heart function using TTE and compared right ventricle (RV) stroke volume and cardiac output. There was no significant difference between the WT and KO in RV stroke volume and cardiac output (Figure 3.6A-B). To directly measure the pressure of right ventricle, we did hemodynamic analysis which showed that the RV systolic pressure (Figure 3.6C) was comparable between the WT and KO. RV hypertrophy was assessed by Fulton index, weight ratio of RV/(LV+ septum), showing no significant change of KO RV (Figure 3.6D). Taken together, these data indicated that deletion of HIPK2 does not significantly affect RV function and right-sided heart failure is not a driver of cardiac dysfunction in the HIPK2 global KO mouse.
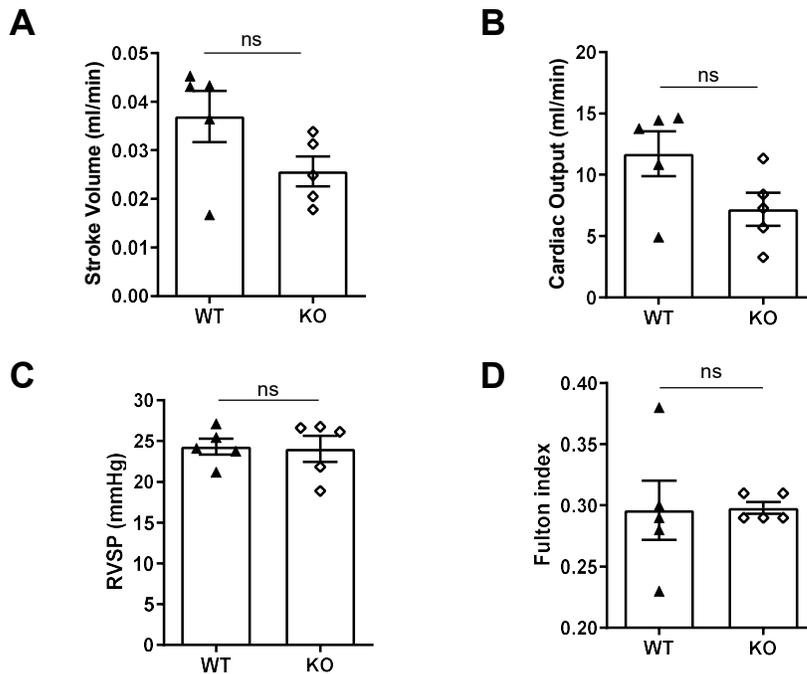
Figure 3.6 Characterization of right heart function in HIPK2 global KO mice. 5-month-old HIPK2 global KO and WT mice were examined by transthoracic echocardiographic and hemodynamic examination. **A.** RV stoke volume. **B.** RV cardiac output. **C.** RV systolic pressure (RVSP). The heart was harvest and the weight of RV, LV and septum was measured to calculate Fulton index, the weight ratio of RV/(LV+septum). **D.** Fulton index. n=5 per group. Mann-Whitney test.

3.4 Discussion

Our data suggest that HIPK2 global KO mice spontaneously developed cardiac dysfunction at 5 months of age, which indicates that HIPK2 may be essential in maintaining normal cardiac function. Specifically, the cardiac dysfunction developed gradually in adulthood although the deletion was from the embryonic stage. These findings suggest that the role or the expression of HIPK2 vary with the age: developmental vs adulthood. Evaluation of the level of HIPK2 expression at different stages will be reasonable to elucidate this.

The underlying mechanism of observed cardiac dysfunction in HIPK2 KO animals is completely unknown. At this end, we examined the contractility and calcium handling in isolated adult cardiomyocytes. However, none of these processes were significantly changed, which in turn suggests that they do not drive the cardiac dysfunction. Furthermore, analysis of RV function revealed a comparable RV function of HIPK2 KOs and littermate WT controls. Therefore, more studies are needed to elucidate the underlying mechanism of cardiac dysfunction in HIPK2 KO.

As described above, we established a cardiac dysfunction phenotype in global HIPK2 KO animals. However, this finding is compromised by the difference in body weight between the WT and KO mouse. HIPK2 global KO mice are known to have a defective fat development phenotype that accounts for a significantly reduced body weight of KOs in comparison to littermate controls. Of note, body weight is a prominent confounding factor of cardiac function. Furthermore, global gene deletion can lead to compensatory effects that may further complicate the interpretation of phenotypes. Indeed, the HIPK2 global KO mouse displays several defects in various systems.[32,35,36,41,42] All these factors limit the use of this global KO mouse model to further study the role of HIPK2 in the heart. Thus, a cardiomyocyte-specific KO mice model is critical to study the role of HIPK2 in the heart.

Chapter 4

Characterization of the Role of HIPK2 in Cardiomyocytes

Part of this work was accepted to publish in *Circulation*.[63]

4.1 Introduction

As discussed in the previous chapter, HIPK2 global KO mice developed cardiac dysfunction spontaneously at 5 months of age. However, this model is compromised by various defects due to the global deletion of the gene. To better elucidate the role of HIPK2 in cardiac biology, we generated cardiomyocyte-specific HIPK2 KO mice.

4.2 Methods

Cardiomyocyte-specific deletion of HIPK2 KO and Het mice

C57BL/6NTac-Hipk2^tm2a(EUCOMM)Hmgu/Cnrm mice (EM:05113) were purchased from the European Mouse Mutant Archive (EMMA). B6.129S4-*Gt(ROSA)26Sor*^*tm1(FLP1)Dym*/RainJ (stock# 009086)[71] and B6.FVB-Tg(Myh6-cre)2182Mds/J mice (stock# 011038)[72] were purchased from the Jackson Laboratory. Generation of the cardiomyocyte-specific HIPK2 KO mice is described in the results. The Institutional Animal Care and Use Committee of Vanderbilt University Medical Center approved all animal procedures and treatments (protocol # M1700133-00). All animals were housed in a temperature-controlled room with a 12:12 hour light-dark cycle and received humane care.

Adenovirus infection

The Ad-LacZ virus was a generous gift from Dr. David E. Dostal, Texas A&M University. The Ad-HIPK2 virus was purchased from Vector Biolabs (#1484). Ad-scrambled-shRNA and Ad-shRNA-

HIPK2 were purchased from SignaGen Laboratories. For each adenovirus employed, the viral multiplicity of infection (MOI) was determined by dilution assay in HEK293 cells using the protocol from the Untergasser Lab ("Titration of Adenoviral Vectors" http://www.untergasser.de/lab/protocols/adeno_vectors_titration_v1_0.htm). For adenoviral infection of NRVMs, levels of expressed proteins were determined by Western blot or qRT-PCR analysis. NRVMs were treated with viruses at 0, 5, 10, 25, and 50 MOI to maximize protein expression while limiting viral toxicity. Corresponding MOIs of adenoviruses expressing LacZ or scrambled-shRNA were used as viral controls. At 24 hrs after plating, NRVMs were starved overnight with serum-free medium following adenoviral infection for another 24 hrs. The medium was then replaced with virus-free SFM.

Adeno-Associated Virus Serotype 9 Virus Construction and Administration

pMCL-HA-MAPKK1-R4F [delta(31-51)/S218E/S222D](MEK1-CA) plasmid was a gift from Natalie Ahn (Addgene plasmid No. 40810; http://n2t.net/addgene:40810 ; RRID:Addgene_40810). MEK1-CA plasmid was cloned into a premade adeno-associated virus serotype 9 (AAV9) generating plasmid with troponin (TnT) promoter (VectorBuilder #VB180411-1135acz) to make the TnT-MEK1-CA plasmid (troponin T-driven constitutively active mitogen-activated protein kinase kinase 1). The TnT-MEK1-CA plasmid was then packaged into AAV9 virus (Vigene Biosciences, Inc). AAV9 virus was delivered by tail vein injection or jugular vein injection.[73] In brief, mice were anesthetized by xylazine/ketamine. A 1-cm cut was made above the right clavicle, and then the jugular vein was exposed. The virus was diluted by 0.9% saline to 250 μL and slowly delivered into the jugular vein.

4.3 Results

Generation and Characterization of CM-Specific HIPK2 KO Mice

To generate CM-specific HIPK2 KO mice, we obtained the C57BL/6NTac-Hipk2[tm2a(EUCOMM)Hmgu]/Cnrm mouse (HIPK2[tm2a]) from the European Mouse Mutant Archive (EMMA)[74] and crossed it with B6.129S4-*Gt(ROSA)26Sor*[tm1(FLP1)Dym]/RainJ[71] (FLP) mice to generate mice with the *HIPK2*

flox allele. Thereafter, *HIPK2 flox* mice were mated with mice expressing αMHC promoter-driven Cre to achieve the CM-specific HIPK2 KO mice (HIPK2$^{flox/floxCre+/}$, CM-KO), heterozygous mice (HIPK2$^{flox/Cre+/}$, CM-Het), and littermate controls (HIPK2$^{flox/flox}$, Control) (Figure 4.1). αMHC-Cre expression led to ≈87% reduction of HIPK2 expression in CM-KO hearts (Figure 4.2A). As expected, heterozygous hearts demonstrated ≈50% reduction of HIPK2 in comparison with control hearts (Figure 4.2B). It is important to note that the body weights of CM-KO and Control mice were comparable (Figure 4.2C).
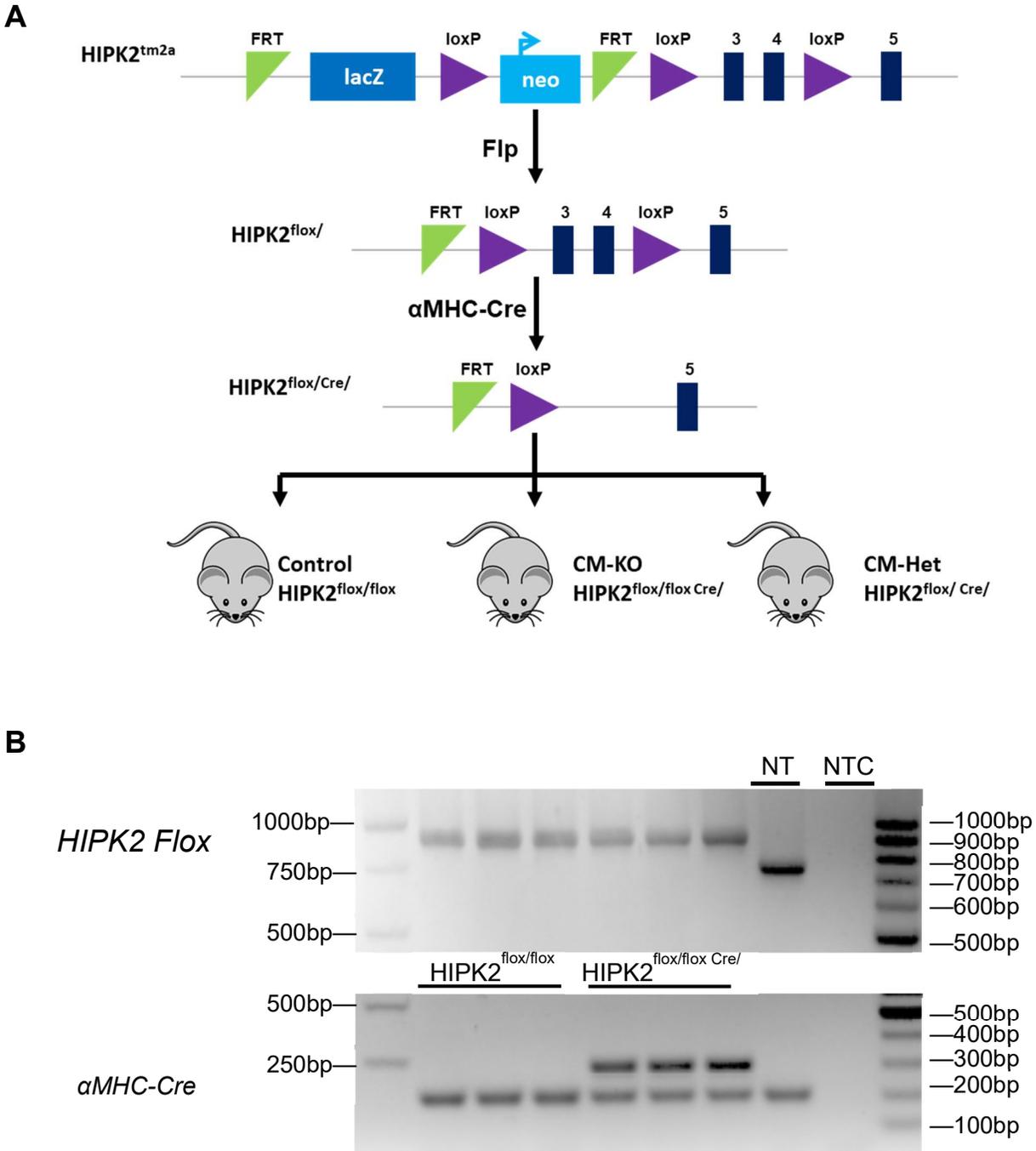
Figure 4.1 Generation of cardiomyocyte-specific HIPK2 KO mice. A. Scheme of CM-specific HIPK2 KO and Het mice generation. HIPK2[tm2a] mice from the European Mouse Mutant Archive (EMMA) were crossed with FLP mice to obtain mice with *HIPK2 flox* allele. Then, HIPK2[flox/flox] mice were crossed with αMHC-Cre mice to achieve CM-specific HIPK2 KO (HIPK2[flox/flox Cre/], CM-KO) or CM-specific HIPK2 Het (HIPK2[flox/ Cre/], CM-Het) or littermate controls (HIPK2[flox/flox], Control). CM, cardiomyocyte. **B.** PCR genotyping results show the HIPK2 flox and Cre expression. NT: non-transgenic, NTC: no template control.
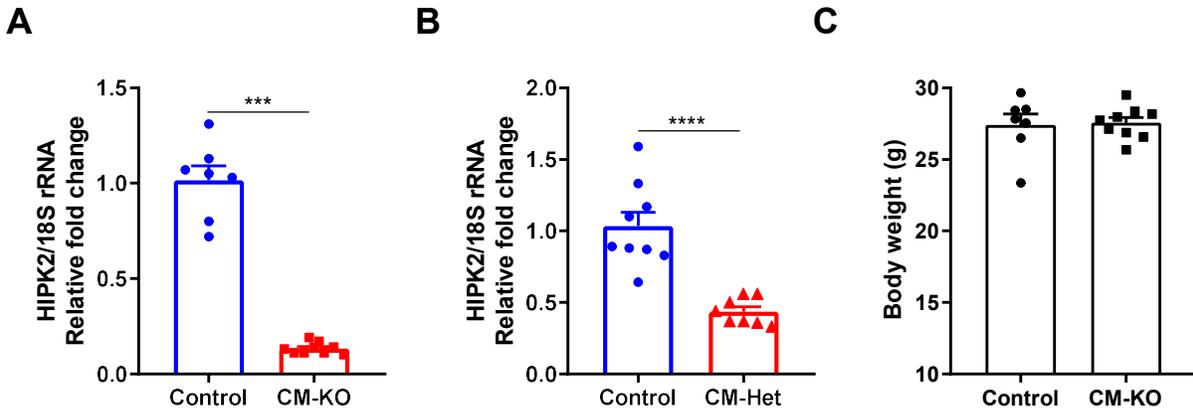
Figure 4.2 Gene deletion efficiency of HIPK2 in CM-KO and CM-Het mice. A. Quantification of *HIPK2* mRNA expression in the Control and CM-KO mouse left ventricle. n=7-9 per group. **B.** Quantification of HIPK2 mRNA expression in the Control and CM-Het mouse left ventricle. n=8-9 per group. **C.** Body weight of CM-KO and Control mice. Control: n=7, CM-KO: n=9. *** *P<0.005*, **** *P<0.0001*, Mann-Whitney test.

The Genotype of αMHC-Cre HIPK2 does not Follow the Mendelian Frequency.

Interestingly, we found that the mice acquired by crossing HIPK2$^{flox/flox}$ and HIPK2$^{flox/ Cre/}$ did not follow the Mendelian frequency. There was an extremely low ratio of HIPK2$^{flox/}$ and HIPK2$^{flox/flox Cre/}$ genotype. To examine if this unusual ratio is due to the embryonic death. We harvested embryos at E8, E9.5, and E12.5. However, there was no HIPK2$^{flox/flox Cre/}$ found in the examined embryos. As listed in the table below, the ratio for each genotype is consistent as observed in adult mice. The demise found was not HIPK2$^{flox/flox Cre/}$.

Genotype	*flox/flox*	*flox/ Cre/*	*flox/*	*flox/flox Cre/*	**Total**
mice #	23	2	22	0	47
%	49%	4%	47%	0%	100%

Genotype / Age	flox/flox	flox/ Cre/	flox/	flox/flox Cre/	Total number of embryos
E8	2	5	1	0	8
E9.5	7	4	0	0	11
E12.5	2	2	0	0	4
Sum	11	11	1	0	23
%	48%	48%	4%	0%	100%

CM-Specific Deletion of HIPK2 Leads to Cardiac Dysfunction

To determine the cardiac phenotype of CM-KO mice, CM-KO and Control mice were examined by echocardiography. At 2 months of age, CM-KOs and Controls had comparable heart function (Figure 4.3A-B), suggesting the absence of any developmental cardiac defects. It is intriguing that, at 3 months of age, the EF and FS of CM-KO mice were significantly decreased in comparison with their littermate controls (Figure 4.3A-B). Consistent with deteriorating cardiac function, the internal dimension of KO hearts had a trend of dilation, yet not significantly different from the control at this age (Figure 4.3C-F). The mRNA expression of heart failure markers *NPPA* and *NPPB* was significantly elevated, as was the *MYH7* and the *MYH6/MYH7* ratio, which all indicate LV failure (Figure 4.3G). There was no significant change in heart weight normalized by tibia length (Figure 4.4A) and CMs cross-sectional area (Figure 4.4B-C) in CM-KO mice in comparison with Controls. To further assess the change in cell growth, we isolated adult CMs from CM-KOs and Controls at 3 months of age and measured cell volume by using Imaris.[70] The cell volume and the length/width ratio were consistently comparable between CM-KO and Control mice (Figure 4.4D-F). Taken together, these findings exclude the development of hypertrophic remodeling in CM-KO mice at both the organ and cellular levels. Because HIPK2 is known for its function in regulating fibrosis and fibroblasts,[24] we evaluated the mRNA expression of profibrotic genes *COL1A1* and *COL1A2*. Surprisingly, the gene expression was comparable between the CM-KO and Control (Figure 4.4G). We also did not observe significant fibrosis deposition in Masson trichrome-stained CM-KO heart sections (Figure 4.4B). This suggests that CM HIPK2 is not a key regulator of myocardial fibrosis, and thus, this excludes

the driving role of fibrosis in the pathogenesis of heart failure in CM-KO hearts. Because calcium handling is key to the LV function, we further examined the contractility and calcium handling in the isolated adult CMs. It is surprising that all parameters of contractility and calcium handling were comparable between CM-KOs and Controls at both basal (Figure 4.5) and isoproterenol-stimulated conditions (Figure 4.6). This indicates that loss of HIPK2 does not affect single-cell contractility and calcium handling, eliminating these factors as contributors to the cardiac dysfunction in CM-KOs.
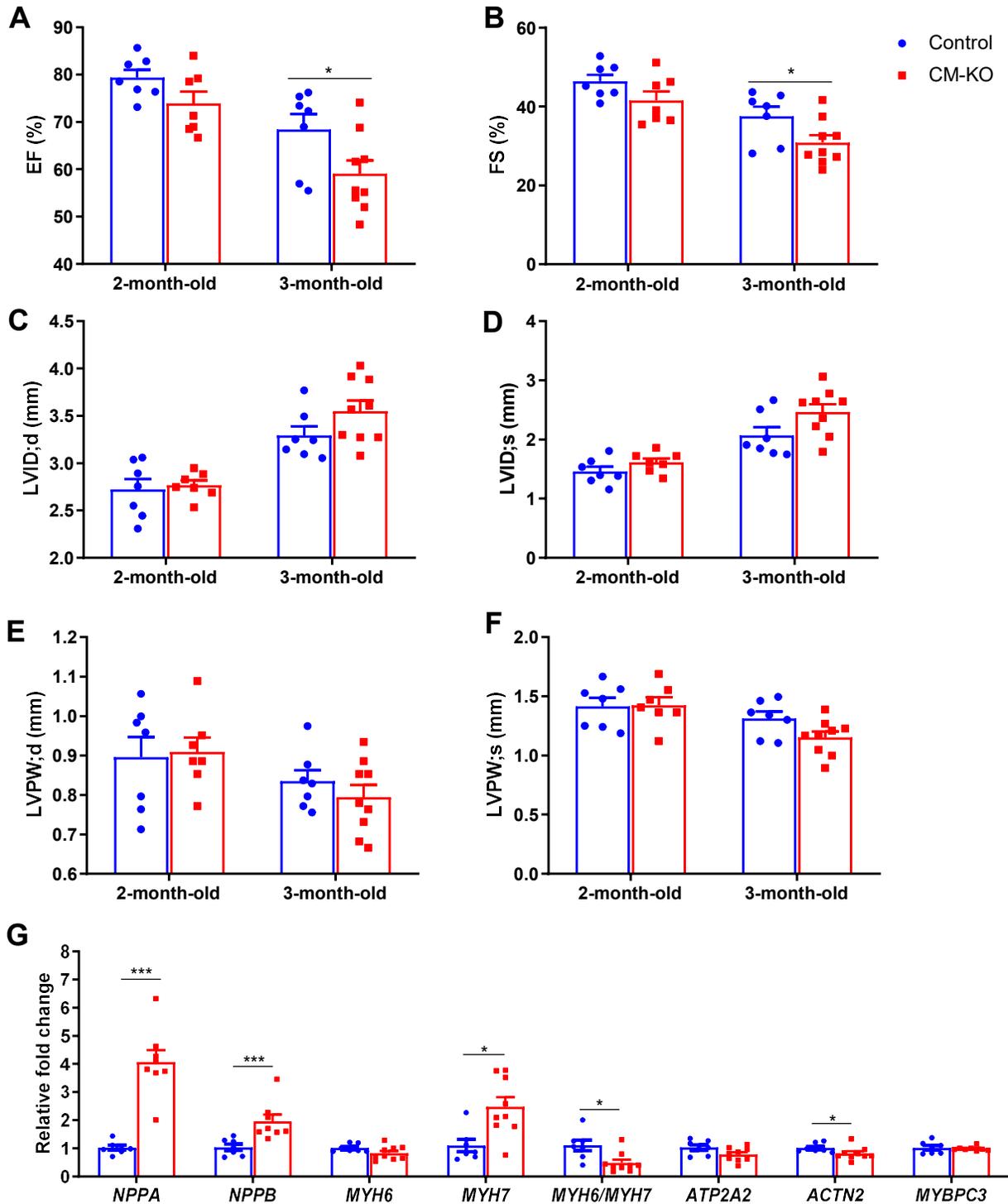
Figure 4.3 Measurement of cardiac function and heart failure markers in CM-KO mice at 3 months of age.
A-F: Heart function of CM-KO and littermate controls was measured by transthoracic echocardiogram at 2 months and 3 months of age. **A.** Ejection fraction. **B.** Fractional shortening. **C.** Left ventricle internal dimension at end-diastole (LVID; d). **D.** Left ventricle internal dimension at end-systole (LVID; s). **E.** Left ventricle posterior wall thickness at end-diastole (LVPW; d). **F.** Left ventricle posterior wall thickness at end-systole (LVPW; s). n=7-9 per group. **G.** Quantification of mRNA expression of heart failure markers and sarcomere genes. * $p < 0.05$, *** $p < 0.005$, Mann-Whitney test.
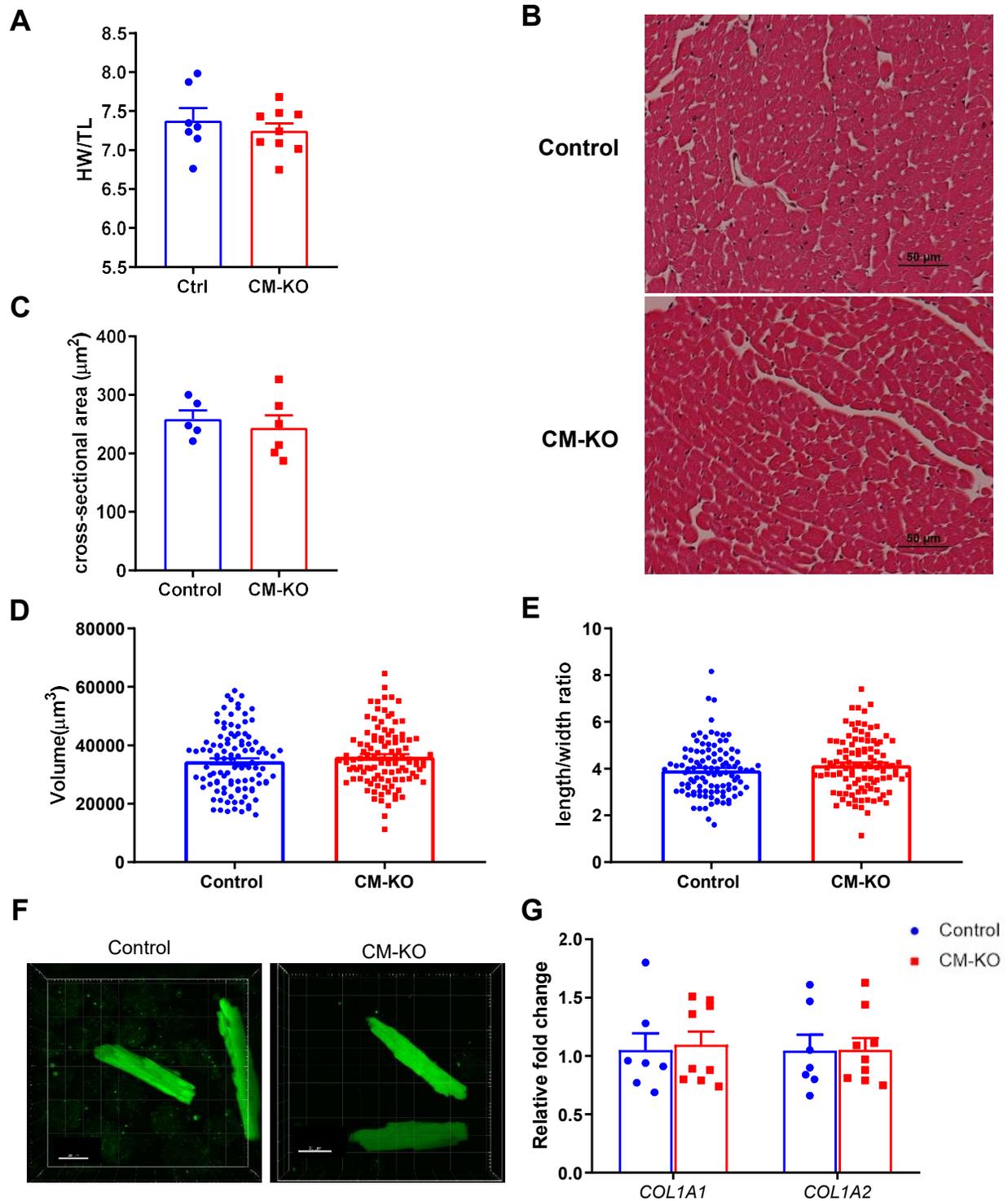
Figure 4.4 Remodeling changes in CM-KO mice. A. Heart weight normalized by tibia length (HW/TL). **B.** Representative images of Masson's Trichrome stained heart sections. **C.** Quantification of CM cross-sectional area. **D-F:** Cell volume and length/width ratio of isolated adult CMs from 3-month-old CM-KO or Control male mice. Control: n=106 from 4 mice, CM-KO: n=108 from 4 mice. **D.** Quantification of CM cell volume. **E.** Quantification of isolated CM length/width ratio. **F.** Representative images of three-dimensional reconstruction of CMs. **G.** Quantification of mRNA expression of *COL1A1* and *COL1A2*. Mann-Whitney test.
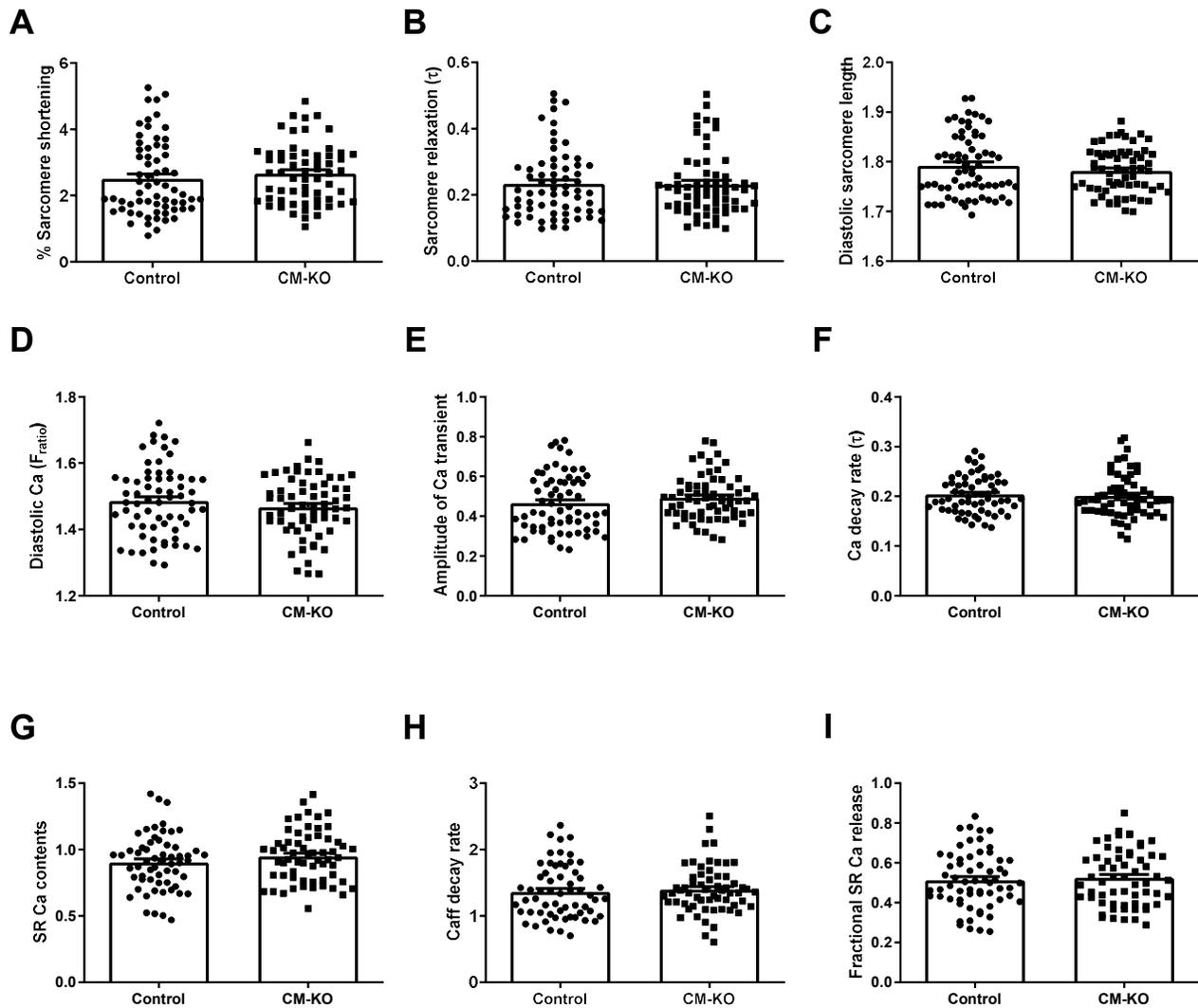
Figure 4.5 Measurement of contractility and calcium handling in isolated adult CMs from CM-HIPK2 and Control mice at basal condition. Adult CMs were isolated from 3-month-old CM-KO and Control mouse hearts. CMs were stained with 2μM Fura 2-AM and paced at 1 Hz for 20 seconds for contractility and Calcium (Ca) handling measurement. Caffeine (Caff, 10mM, 5s) was applied after pacing transient to estimate SR Ca content. CMs were examined in 2 mM Ca Tyrode's solution. **A.** Sarcomere peak shortening normalized to resting sarcomere length (%Sarcomere shortening). **B.** Sarcomere relaxation (τ). **C.** Diastolic sarcomere length. **D.** Diastolic Ca (F$_{ratio}$). **E.** Amplitude of Ca transient. **F.** Calcium decay rate (τ). **G.** SR Ca contents. **H.** Caff decay rate. **I.** Fractional SR Ca release. WT: n=66 from 4 mice, KO: n=64 from 4 mice. Student t-test.
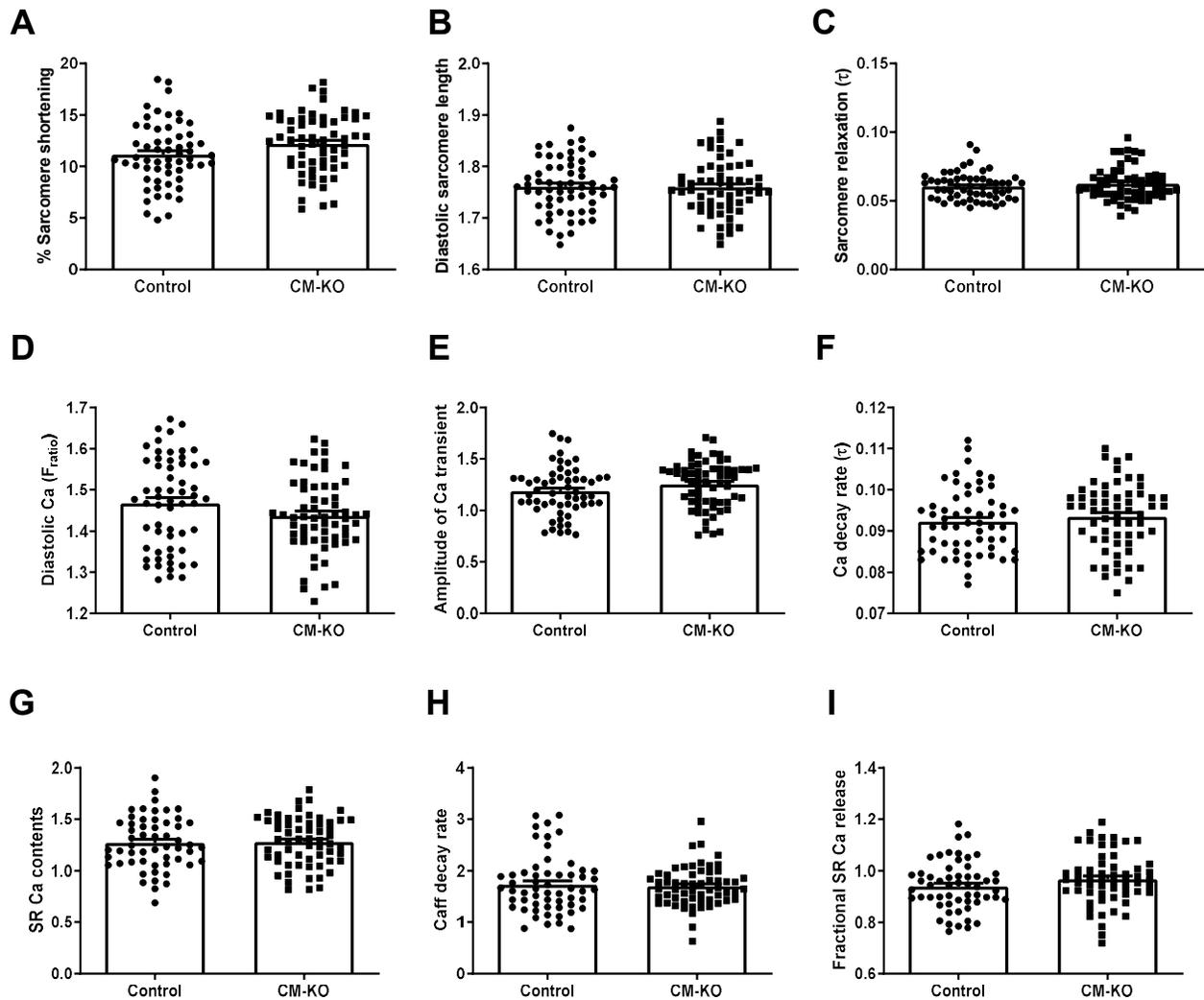
Figure 4.6 Measurement of contractility and calcium handling in isolated adult CMs from CM-HIPK2 and Control mice at isoproterenol stimulation. Adult CMs were isolated from 3-month-old CM-KO and Control mouse hearts. CMs were stained with 2μM Fura 2-AM and paced at 1 Hz for 20 seconds for contractility and Calcium (Ca) handling measurement. Caffeine (Caff, 10mM, 5s) was applied after pacing transient to estimate SR Ca content. CMs were examined with Isoproterenol (ISO, 1 μM) stimulation in 2 mM Ca Tyrode's solution. **A.** Sarcomere peak shortening normalized to resting sarcomere length (%Sarcomere shortening). **B.** Sarcomere relaxation (τ). **C.** Diastolic sarcomere length. **D.** Diastolic Ca (F_{ratio}). **E.** Amplitude of Ca transient. **F.** Calcium decay rate (τ). **G.** SR Ca contents. **H.** Caff decay rate. **I.** Fractional SR Ca release. WT: n=60 from 4 mice, KO: n=62 from 4 mice. Student t-test.

At 8 months of age, the heart failure much worsened with the disease progression as reflected by a dramatic decrease in EF and FS (Figure 4.7A-B). Consistently, the CM-KO heart also gradually developed dilatative remodeling with significantly enlarged LV internal diameter, thinner posterior wall, increased heart weight, cell surface area and fibrosis deposition (Figure 4.7C-J).

To further delineate the role of HIPK2 in the CM, we used a cell culture model of neonatal rat ventricular cardiomyocytes (NRVMs). NRVMs were infected with adenovirus carrying shRNA-HIPK2 (Ad-shRNA-HIPK2) or shRNA-scrambled (Ad-scrambled) for 48 hours, and reactivation of the fetal gene program was examined. The suppression of HIPK2 in NRVMs resulted in significant elevation of *NPPA* (Figure 4.8A), which is consistent with the phenotype in CM-KOs. As a gain-of-function approach, we infected NRVMs with adenovirus-expressing WT HIPK2 (Ad-HIPK2) or LacZ (Ad-LacZ). Adenovirus-mediated overexpression of HIPK2 suppressed the *NPPA* and *NPPB* expression at the basal condition (Figure 4.8B-C). Strikingly, the phenylephrine-induced elevation of *NPPA* and *NPPB* was completely abolished by overexpression of HIPK2 (Figure 4.8B-C). Overexpression or knockdown of HIPK2 does not alter the CM cell surface area (Figure 4.8D-E). This finding is consistent with the phenotype we observed in vivo and with the literature, as well.[75] Overall, these in vitro results are consistent with the detrimental phenotype of HIPK2 CM-KO hearts and also suggest a cardioprotective role of HIPK2.
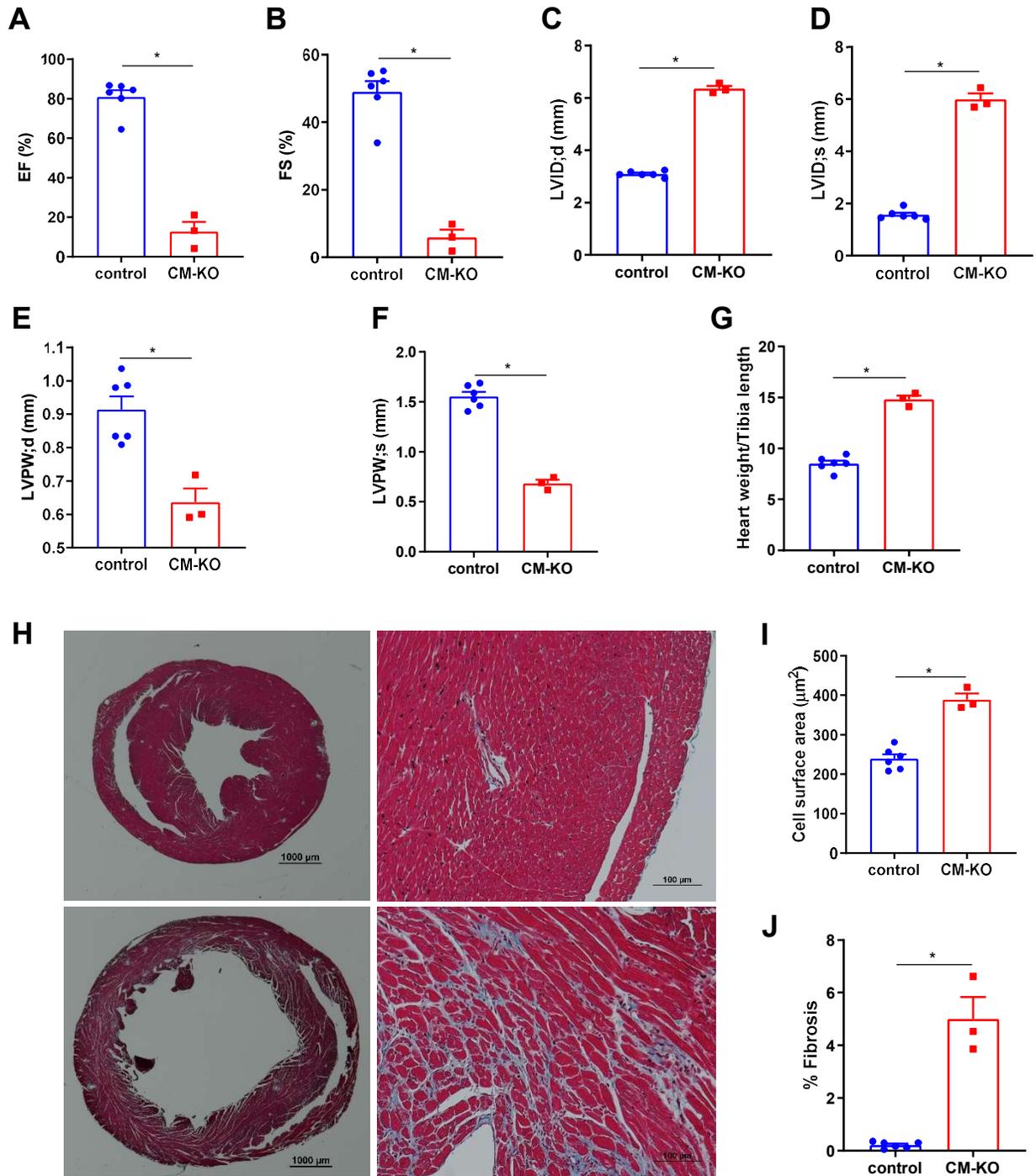
Figure 4.7 Measurement of cardiac function and heart failure markers in CM-KO mice at 8 months of age. 8-month-old male CM-KO and control mice were examined by transthoracic echocardiogram. **A.** Ejection fraction (EF). **B.** Fractional shortening (FS). **C.** Left ventricle internal dimension at end-diastole (LVID; d). **D.** Left ventricle internal dimension at end-systole (LVID; s). **E.** Left ventricle posterior wall thickness at end-diastole (LVPW; d). **F.** Left ventricle posterior wall thickness at end-systole (LVPW; s). **G.** Heart weight normalized by tibia length (HW/TL). **H.** Representative images of Masson's Trichrome stained heart sections. **I.** Quantification of CM cross-sectional area. **J.** Quantification of fibrosis deposition. The control group contained 2 age-matched HIPK2[flox/flox] mice and 4 C57BJ6 mice. * p<0.05, Mann-Whitney test.
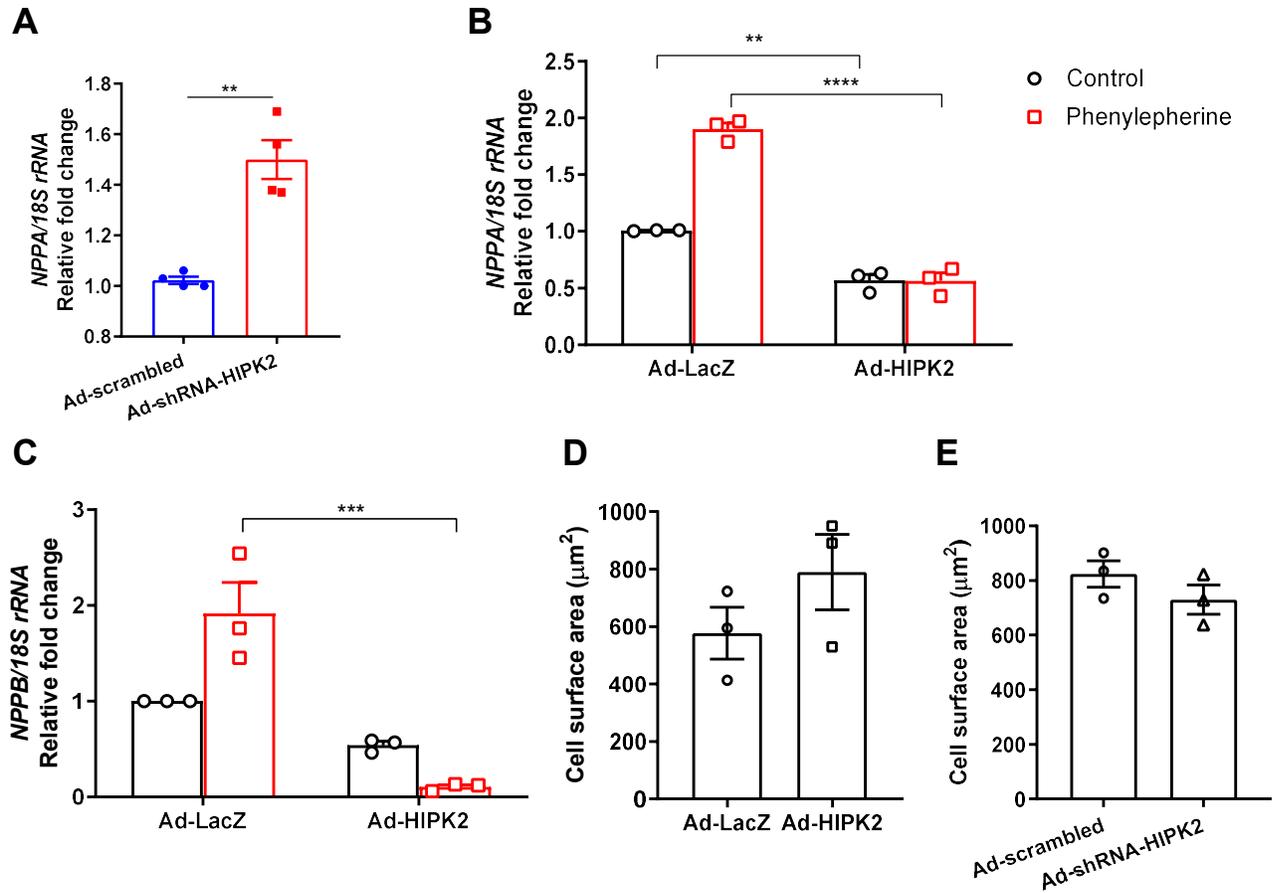
Figure 4.8 The effects of HIPK2 in cardiomyocytes. A. NRVMs were infected with adenovirus expressing scrambled shRNA (Ad-scrambled) or shRNA-HIPK2 (Ad-shRNA-HIPK2) for 48 hours. qRT-PCR was performed to examine the mRNA expression of *NPPA*. n=4 independent replicates. ** p<0.01, unpaired t-test. **B-C:** NRVMs were infected with adenovirus expressing LacZ (Ad-LacZ), or HIPK2 (Ad-HIPK2) for 24 hours. Thereafter, cells were treated with phenylephrine (PE, 100μM) for 48 hours. qRT-PCR was performed to examine the mRNA expression of *NPPA* and *NPPB*. **B.** Quantification of mRNA expression of *NPPA*. **C.** Quantification of mRNA expression of *NPPB*. n=3 independent replicates. * p<0.05, **p<0.01, *** p<0.005, two-way ANOVA with Turkey's post hoc test. **D-E.** NRVMs were infected with adenovirus, and then cells were fixed and stained with α-actinin and DAPI. Immunofluorescent images were taken using Nikon TIRF microscope and cell surface area was measured with Nikon NIS Elements. **D.** Quantification of cell surface area of NRVMs infected with Ad-LacZ or Ad-HIPK2. **E.** Quantification of cell surface area of NRVMs infected with Ad-scrambled or Ad-shRNA-HIPK2. n=3 independent replicates. Unpaired t-test.

CM-Specific HIPK2 Haploinsufficiency is Sufficient to Induce an Adverse Cardiac Phenotype

To determine if the level of HIPK2 gene expression in the heart directly corresponds to function, we compared CM-Het with the littermate control. Cardiac function was comparable between the CM-Het and Control up to 3 months of age. However, the heart function of CM-Hets gradually decreased after 3 months and was significantly reduced at 6 months of age as reflected by significantly decreased EF and FS (Figure 4.9A-B). As discussed above, the CM-KO demonstrated marked cardiac dysfunction much earlier, at 3 months of age. Thus, these findings indicate a direct relationship between the level of cardiomyocyte HIPK2 expression and cardiac function. CM-Het mice also exhibited left ventricular dilation and thinning of the left ventricular wall (Figure 4.9C-F). Consistent with the finding in CM-KOs, the heart weight/tibia length did not change significantly (Figure 4.10A). CM cross-sectional area was comparable between the CM-Het and Control (Figure 4.10B-C). At the molecular level, the expression of the heart failure marker *NPPA* was elevated by ≈10-fold in the Het heart (Figure 4.10D). Comparable fibrosis in CM-Het and Control hearts indicated that CM-specific dysfunction preceded the development of fibrosis in the HIPK2-deficient hearts (Figure 4.10C).

HIPK2 Facilitates its Cardioprotective Effects through ERK Signaling

We next explored the potential molecular mechanism of the development of cardiac dysfunction in HIPK2-deficient hearts. It is well accepted that analysis of heterozygote animals is a more physiologically relevant strategy than that of homozygous KOs. Considering this, we used 6-month-old Het null heart tissue for the molecular mechanistic studies. Because there is no literature regarding HIPK2 and cardiac function, we chose to examine major pathways implicated in myocardial function and dysfunction[13] in the setting of HIPK2 deficiency. Many of these cardiac pathways were either not significantly changed or the nature of the change was not consistent with the observed phenotype (Figure 4.11). It is important to note, however, that we discovered that ERK1/2 phosphorylation was significantly decreased in the CM-Het mouse heart (Figure 4.12). It is well established that ERK is essential to maintain cardiac function because mice with cardiac-specific deletion of ERK1/2 progress to spontaneous cardiac dysfunction and heart failure.[76]

Figure 4.9 Cardiac function of CM-Het mice. Heart function of CM-Het and Controls was measured by transthoracic echocardiogram at 3 months and 6 months of age. **A.** Ejection fraction (EF). **B.** Fractional shortening (FS). **C.** Left ventricle internal dimension at end-diastole (LVID; d). **D.** Left ventricle internal dimension at end-systole (LVID; s). **E.** Left ventricle posterior wall thickness at end-diastole (LVPW; d). **F.** Left ventricle posterior wall thickness at end-systole (LVPW; s). n=7-10 per group. * p<0.05, *** p<0.005, Mann-Whitney test.

Figure 4.10 Characterization of remodeling in CM-Het and Control mice hearts. A. Heart weight normalized by tibia length. **B.** Representative images of Trichrome stained heart sections. **C.** Quantification of CM cross-sectional area. **D.** Quantification of *NPPA* gene expression in CM-Het and Control left ventricle. * p<0.05, *** p<0.005, Mann-Whitney test.
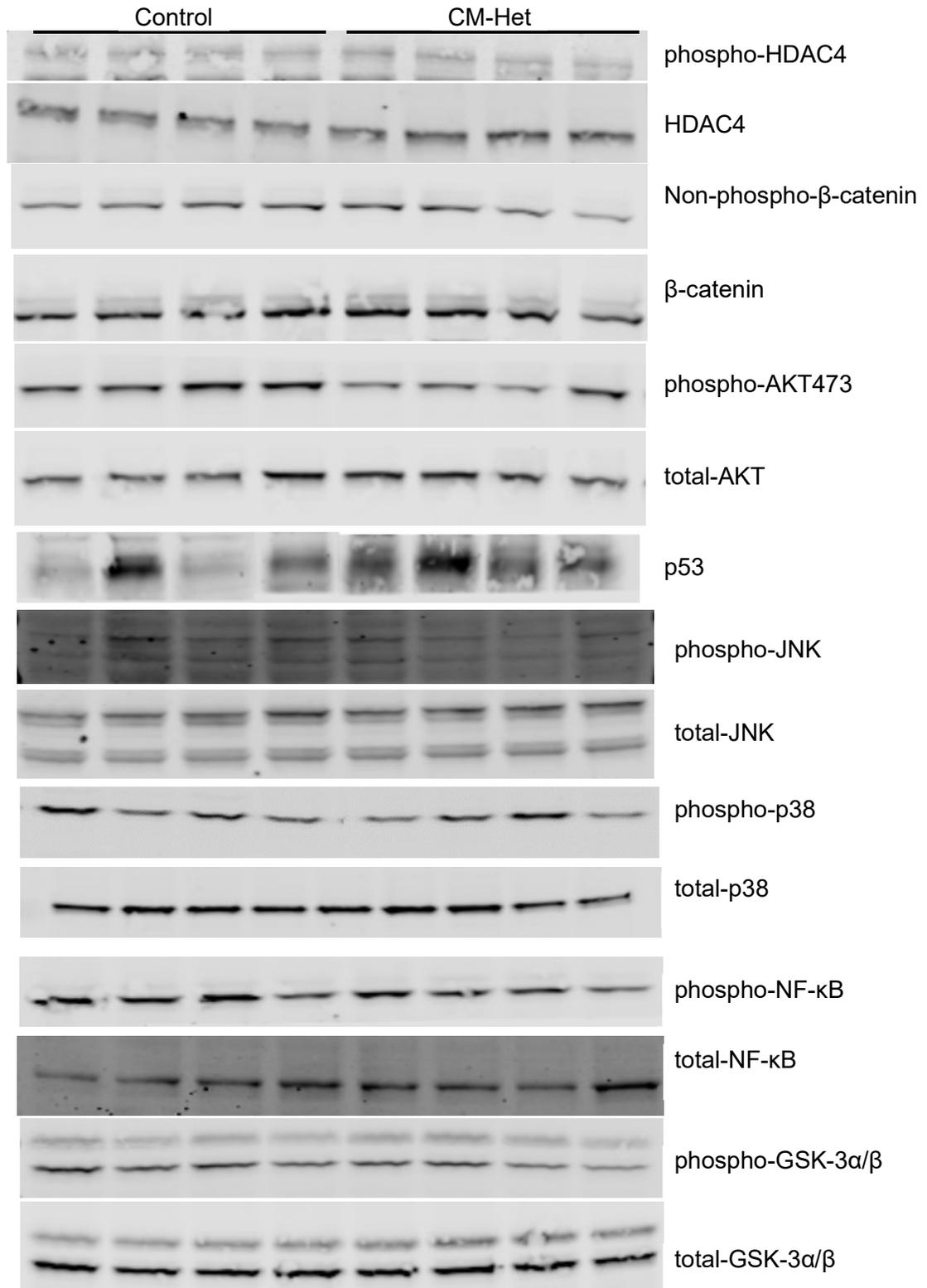
Figure 4.11 Characterization of major cardiac signaling pathways in CM-Het null mice. Representative immunoblots showing expression of phosphorylation and total expression of HDAC4, β-catenin, AKT, p53, JNK, p38, NF-κB and GSK-3α/β in the left ventricle of CM-Hets versus littermate Controls.
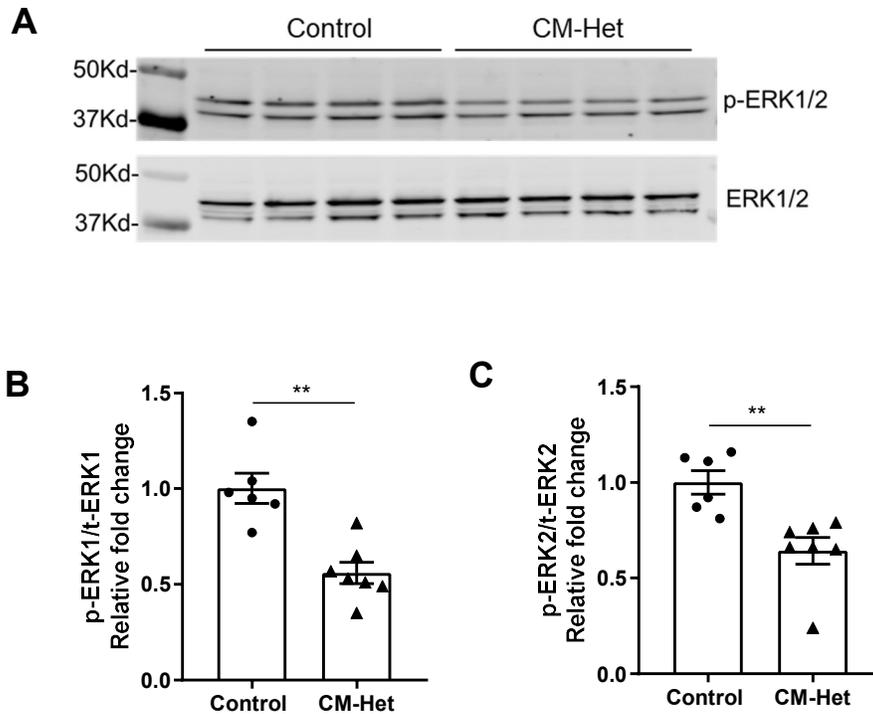
Figure 4.12 The effects of HIPK2 on ERK signaling in the heart. A. Representative immunoblot showing significantly decreased ERK1 and ERK2 phosphorylation in the left ventricle of CM-Hets versus littermate Controls. **B-C.** Quantification of ERK1 and ERK2 phosphorylation in the left ventricle of CM-Het versus Controls. n=6-7 per group. * $p<0.05$, ** $p<0.01$, Mann-Whitney test.

Further mechanistic studies to examine HIPK2 regulation of ERK were performed in vitro using NRVMs. For the loss-of-function approach, NRVMs were infected with Ad-shRNA-HIPK2 or Ad-scrambled, and cell lysates were analyzed for the phosphorylation of ERK. As expected, knockdown of HIPK2 significantly decreased both ERK1 and ERK2 phosphorylation (Figure 4.13A-C). As a gain-of-function strategy, NRVMs were infected with Ad-HIPK2 or Ad-LacZ and cell lysates were analyzed to examine the ERK phosphorylation (Figure 4.13D-F). In contrast to the loss-of-function approach, overexpression of HIPK2 leads to a significant elevation of ERK1/2 phosphorylation. Because the function of HIPK2 could be dependent on its kinase domain or protein-protein interaction with other domains,[18,43] to examine the requirement of HIPK2 kinase function in ERK phosphorylation, we infected NRVMs with HIPK2 kinase-dead (K221A) adenovirus (Ad-HIPK2-KD). It is interesting to note that Ad-HIPK2-KD did not affect ERK phosphorylation, which indicates that the regulation of ERK by HIPK2 is kinase-dependent

(Figure 4.13G). Furthermore, in contrast to HIPK2 overexpression, kinase-dead mutation of HIPK2 failed to display any cardioprotective effect (Figure 4.13H). This indicates that the regulation of ERK and cardiac function by HIPK2 is kinase-dependent. Taken together, these findings suggest that HIPK2 is critical to myocardial ERK signaling which, in turn, is vital to the maintenance of basal cardiac function.

Loss of HIPK2 in CMs Promotes Apoptosis

It is well established that ERK signaling protects the heart from stress-induced apoptosis,[77] a key driver of cardiac remodeling and heart failure.[8] HIPK2 is also known as a key regulator of apoptosis,[28] although its function in this process is complex and context-dependent. Therefore, we investigated the extent of CM death and the underlying mechanism in our model. We first assessed the pro-apoptotic and anti-apoptotic pathway modulators—BAX and BCL-XL by Western blot analysis in 3-month-old LV tissue. The expression of pro-apoptotic molecule BAX was significantly elevated in the CM-KO, as was the BAX/BCL-XL ratio (Figure 4.14A-D). We confirmed the activation of apoptosis by terminal deoxynucleotidyl transferase dUTP nick end-labeling (TUNEL) assay. There was a significant elevation of TUNEL-positive CM nuclei in CM-KO (Figure 4.14E-F). The apoptotic events became more remarkable with the disease progression at 8 months of age (Figure 4.15A-F). Because cell apoptosis is highly regulated by mitochondria, we further examined whether mitochondrial dysfunction or energetic dysregulation was altered. To examine the mitochondrial function, we measured the tissue O_2 flux with Orobros Oxygraphy, but there was no significant change in the CM-KO LV tissue on the addition of different substrates (Figure 4.16A). We further assessed the cell O_2 consumption rate by Seahorse in NRVMs with HIPK2 overexpression or knockdown. Consistent with the in vivo findings, HIPK2 does not affect mitochondrial function and O_2 consumption (Figure 4.16B-C). Therefore, metabolic dysfunction of cardiomyocytes is not a driver of the cardiac phenotype seen in CM-KOs. Overall, our data clearly implicate impaired ERK signaling, leading to the loss of functional CMs, as a primary driver of cardiac dysfunction in CM-KOs.

49
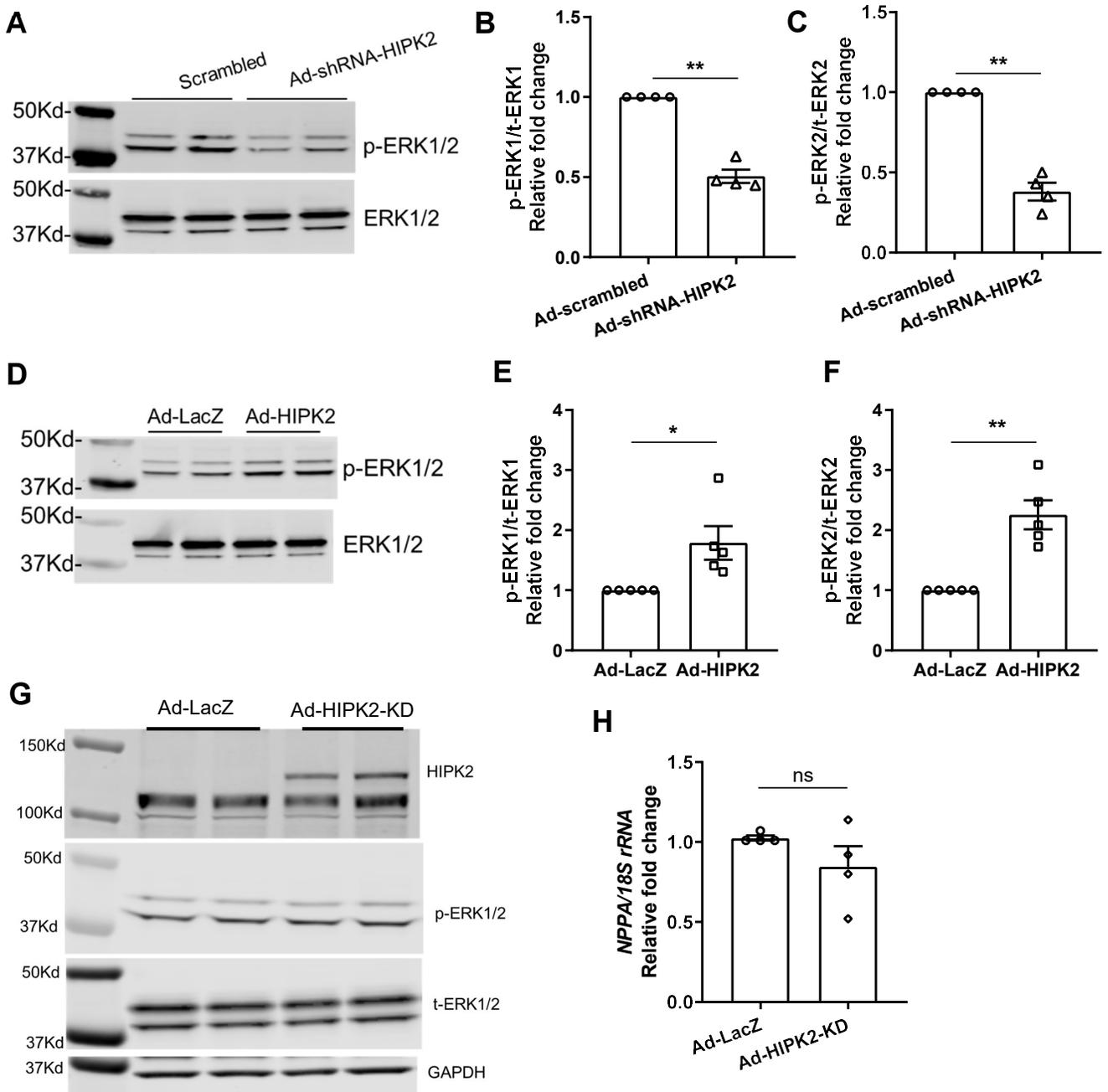
Figure 4.13 The effects of HIPK2 on ERK signaling in cardiomyocytes. NRVMs were infected with adenovirus expressing scrambled shRNA (Scrambled), HIPK2 shRNA (Ad-shRNA-HIPK2), LacZ (Ad-LacZ), HIPK2 (Ad-HIPK2), or HIPK2 kinase-dead (Ad-HIPK2-KD) virus. Western blot analysis was performed to determine the phosphorylation of ERK1 and ERK2. **A.** Representative immunoblot showing significantly decreased phosphorylation of ERK1 and ERK2 in HIPK2 knockdown group. **B-C.** Quantification of ERK1 and ERK2 phosphorylation in Ad-shRNA-HIPK2 group versus scrambled group. n=5 independent replicates. **D.** Representative immunoblot showing significantly increased phosphorylation of ERK1 and ERK2 in HIPK2 overexpression group. **E-F.** Quantification of ERK1 and ERK2 phosphorylation in Ad-HIPK2 group versus Ad-LacZ group. n=4 independent replicates. **G.** Representative immunoblot showing no change of phosphorylation of ERK1 and ERK2 in kinase-dead group. **H.** Quantification of mRNA expression of *NPPA* in NRVMs overexpressed with Ad-HIPK2-KD or Ad-LacZ. n=4 independent replicates. * p<0.05, ** p<0.01, unpaired t-test.

50
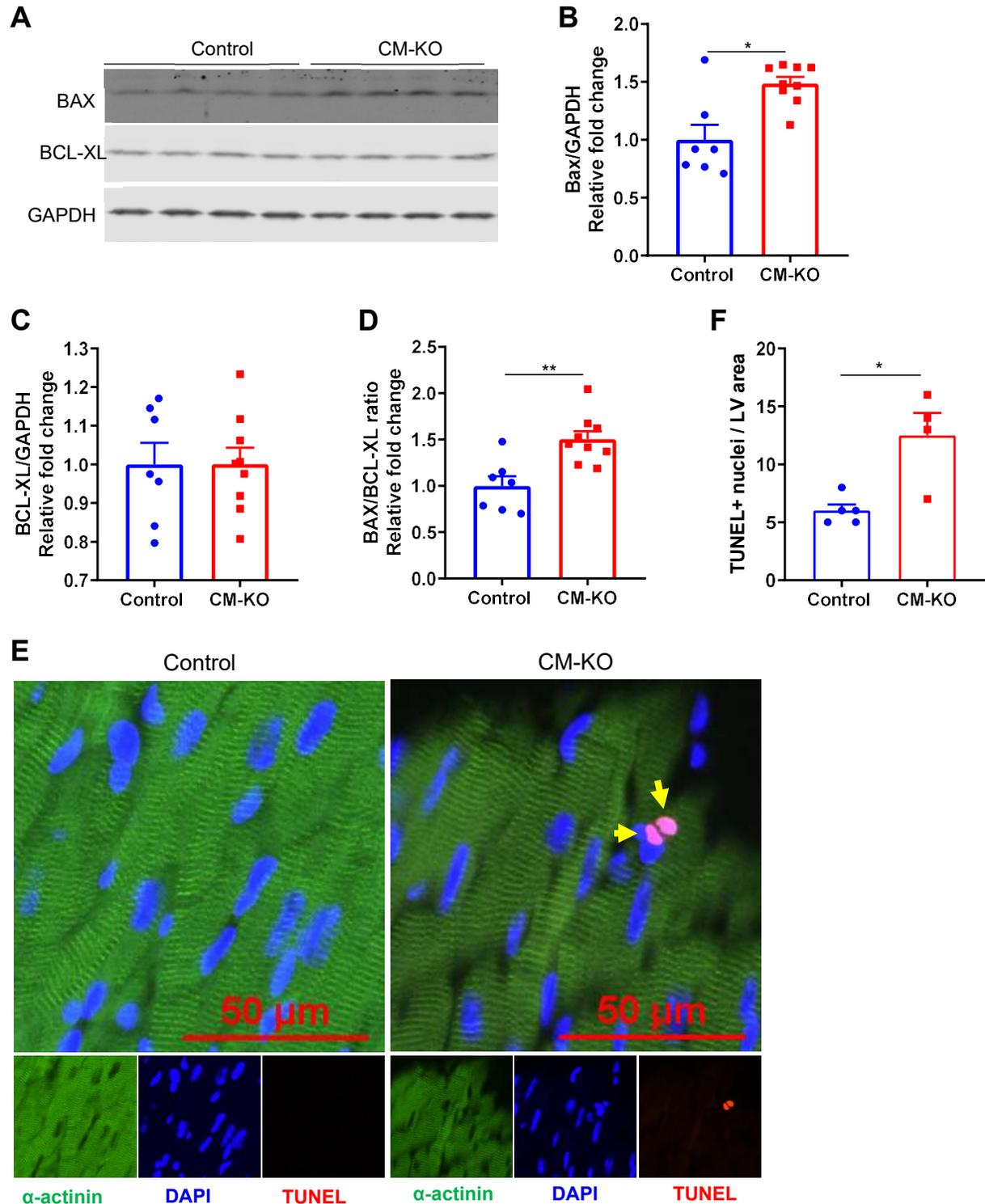
Figure 4.14 Enhanced apoptosis in CM-KO hearts at 3 months of age. A-D. Protein expression of regulators of apoptotic pathway were measured with Western blot. **A.** Representative immunoblot showing expression of BCL-XL and BAX. **B-D.** Quantification of BAX, BCL-XL expression, and BAX/BCL-XL ratio in the CM-KO and Control LV. Control: n=7, CM-KO: n=9. **E.** Representative images of TUNEL positive CMs nuclei in the CM-KO and Control LV section. **F.** Quantification of TUNEL positive CM nuclei in the CM-KO and Control LV section. Control: n=5, CM-KO: n=4. * $p<0.05$, ** $p<0.01$, Mann-Whitney test.

51
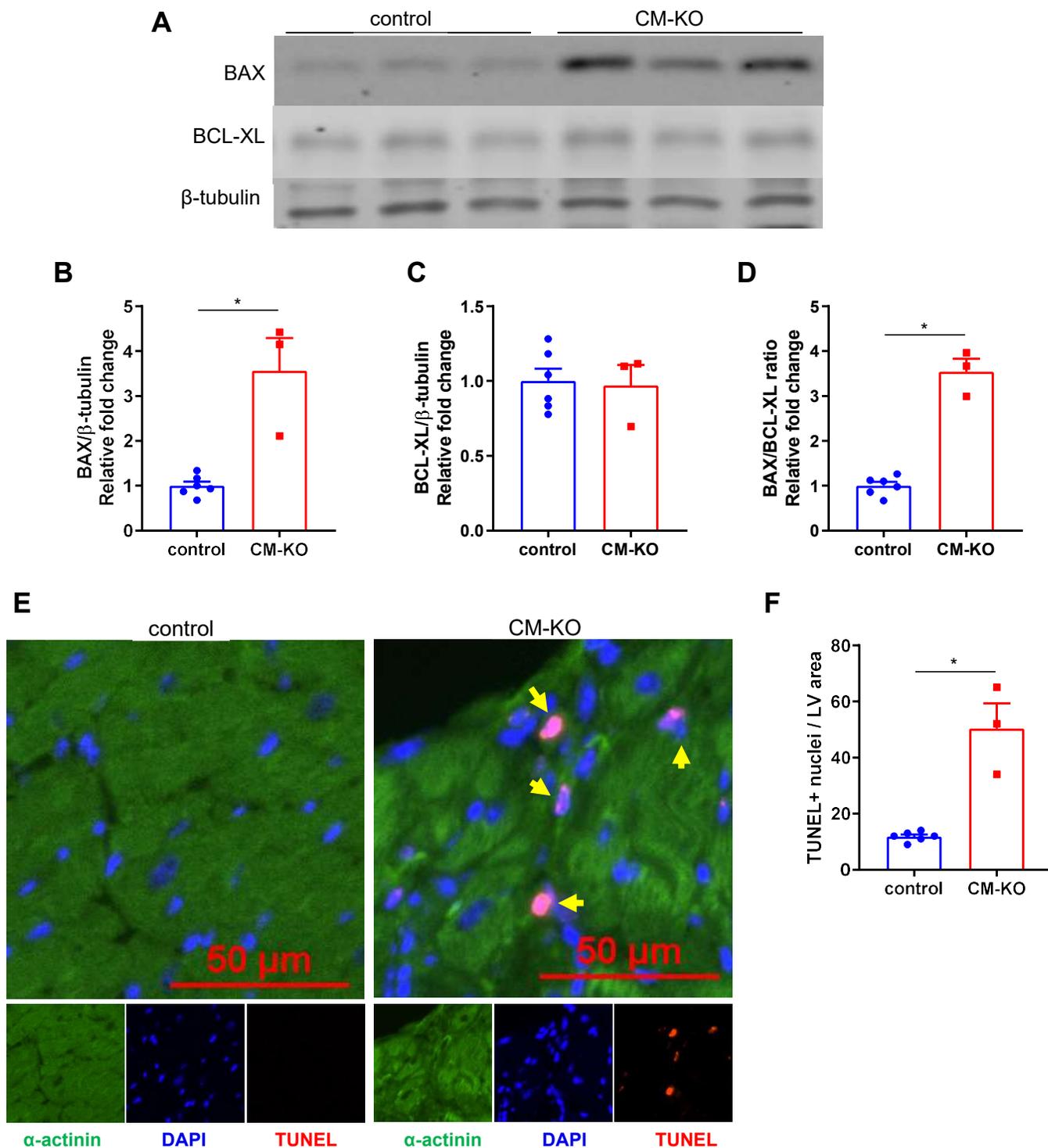
Figure 4.15 Enhanced apoptosis in CM-KO hearts at 8 months of age. A-D. Protein expression of regulators of apoptotic pathway were measured with Western blot in 8-month-old CM-KO and control mice. **A.** Representative immunoblot showing expression of BCL-XL and BAX. **B-D.** Quantification of BAX, BCL-XL expression, and BAX/BCL-XL ratio in the 8-month-old CM-KO and Control LV. **E.** Representative images of TUNEL positive CMs nuclei in the CM-KO and Control LV section. **F.** Quantification of TUNEL positive CM nuclei in the CM-KO and Control LV section. control: n=6, CM-KO: n=3. The control group contained age-matched 2 HIPK2flox/flox mice and 4 C57BJ6. * $p<0.05$, Mann-Whitney test.
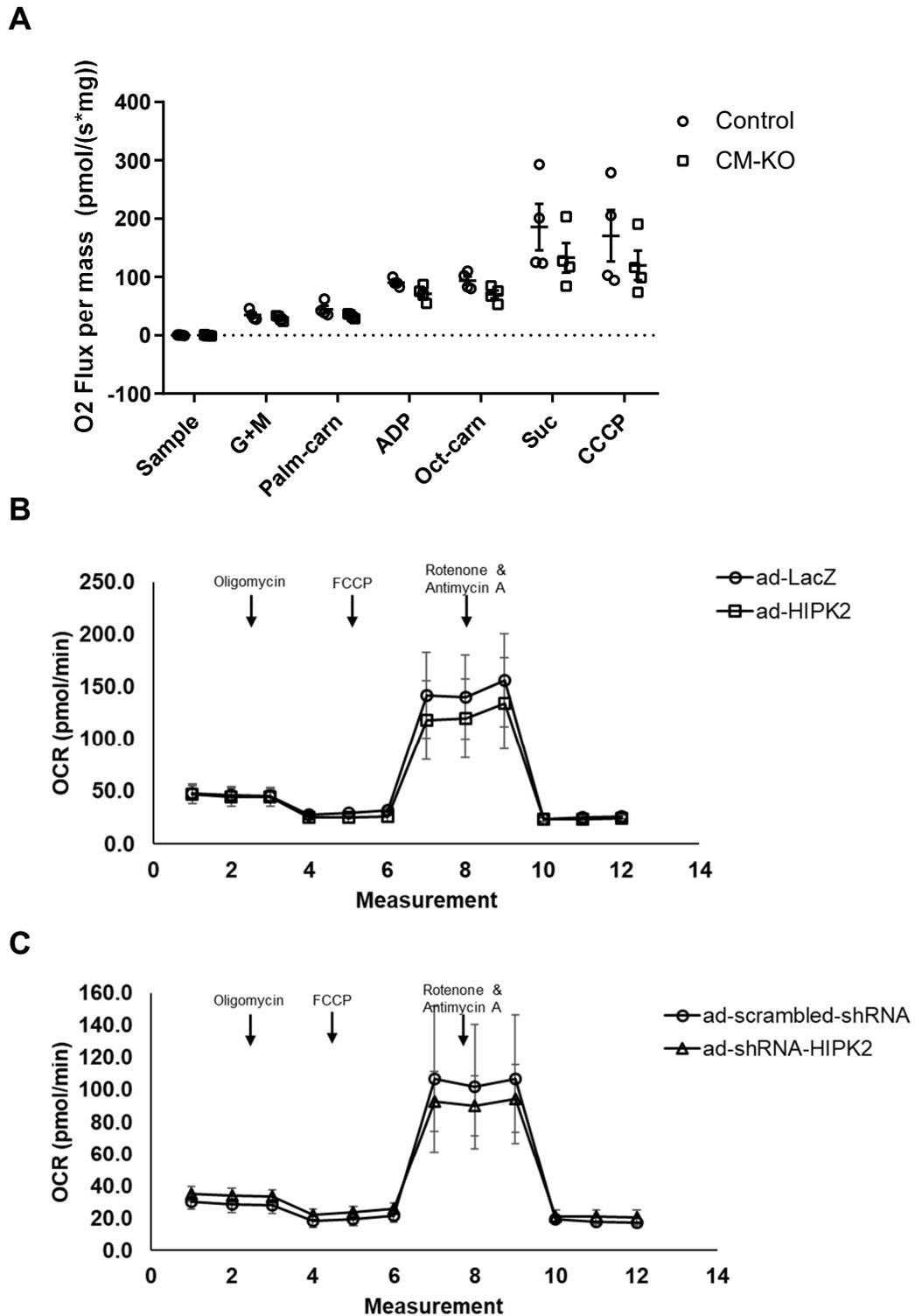
Figure 4.16 The effects of HIPK2 on Mitochondrial function in CM-KO hearts and NRVMs. A. LV from CM-KO and control mice were processed and Oxygen flux was measured with different substrates as indicated in Methods. n=4 per group. Mann-Whitney test. **B-C.** NRVMs were infected with Ad-LacZ, Ad-HIPK2, Ad-scrambled shRNA or Ad-shRNA-HIPK2, and oxygen consumption rate (OCR) was measured with different stimulation using Seahorse Analyzer as indicated in Methods. n=4 independent replicates. Student t-test.

AAV9 TnT-MEK1-CA Rescues the Cardiac Dysfunction of CM-KO Mice

Finally, we aimed to determine the molecular mechanism of the observed detrimental phenotype in CM-KO mice, with our hypothesis being that impaired ERK signaling in CM-KO hearts is the primary driver of the observed cardiac dysfunction. To test this hypothesis, we performed an in vivo rescue experiment with the AAV9-mediated gene therapy system to restore ERK signaling. We used Troponin (TnT)-driven constitutively active MEK1 (MEK1-CA), upstream of ERK, to see whether AAV9 TnT-MEK1-CA can rescue the HIPK2-deficient phenotype by restoring ERK phosphorylation. To generate the AAV9 TnT-MEK1-CA, MEK1-CA plasmid with hemagglutinin (HA) tag[78] was cloned into a premade AAV9 TnT plasmid construct, thereafter packaged to AAV9 (Figure 4.17). First, we performed a pilot experiment using AAV9 TnT-GFP to test the feasibility of CM-specific gene expression delivered by AAV9 and optimize the appropriate viral dose and route of delivery. To ensure the reliability of AAV9 delivery in C57BJ6 background mice, we compared the jugular vein delivery to the tail vein injection.[73] The dose-dependent expression of GFP in the LV clearly indicated the jugular vein as a comparatively more efficient route for reliable and consistent viral delivery (Figure 4.18). Thereafter, we delivered 5×10^{11} genome copies (GC) of AAV9 TnT-MEK1-CA or AAV9 TnT-GFP to 1-month-old CM-KO or Control mice via the jugular vein and heart function was monitored by serial echocardiography. The infection efficiency was confirmed by Western blot analysis of GFP and HA (Figure 4.19A). As expected, the ERK phosphorylation was restored in the CM-KO mice with AAV9 TnT-MEK1-CA administration (Figure 4.19). Indeed, AAV9 TnT-MEK1-CA significantly improved the EF and FS of CM-KO so that the cardiac function of CM-KO with MEK1-CA was no longer significantly different from the Control (Figure 4.20). There was no significant change in the normalized heart weight among groups (Figure 4.21A). Histological analysis of heart sections showed a comparable CM cross-sectional area and fibrosis deposition (Figure 4.21B-C) in the AAV9 groups, consistent with prior observations in CM-KO hearts. The increased proapoptotic pathway—BAX expression and BAX/BCL-XL were also significantly rescued by MEK1-CA injection (Figure 4.22A-D). TUNEL staining also consistently showed decreased positive CM nuclei in the rescue group (Figure 4.22E-F). Thus, restoring ERK signaling in KOs with MEK1-CA efficiently rescued

the aberrant activation of proapoptotic signaling, attenuated the ongoing CM death, and thus preserved the cardiac function. These findings strongly validate the hypothesis that impaired ERK signaling is a key mechanism of cardiac dysfunction in HIPK2 CM-KOs.
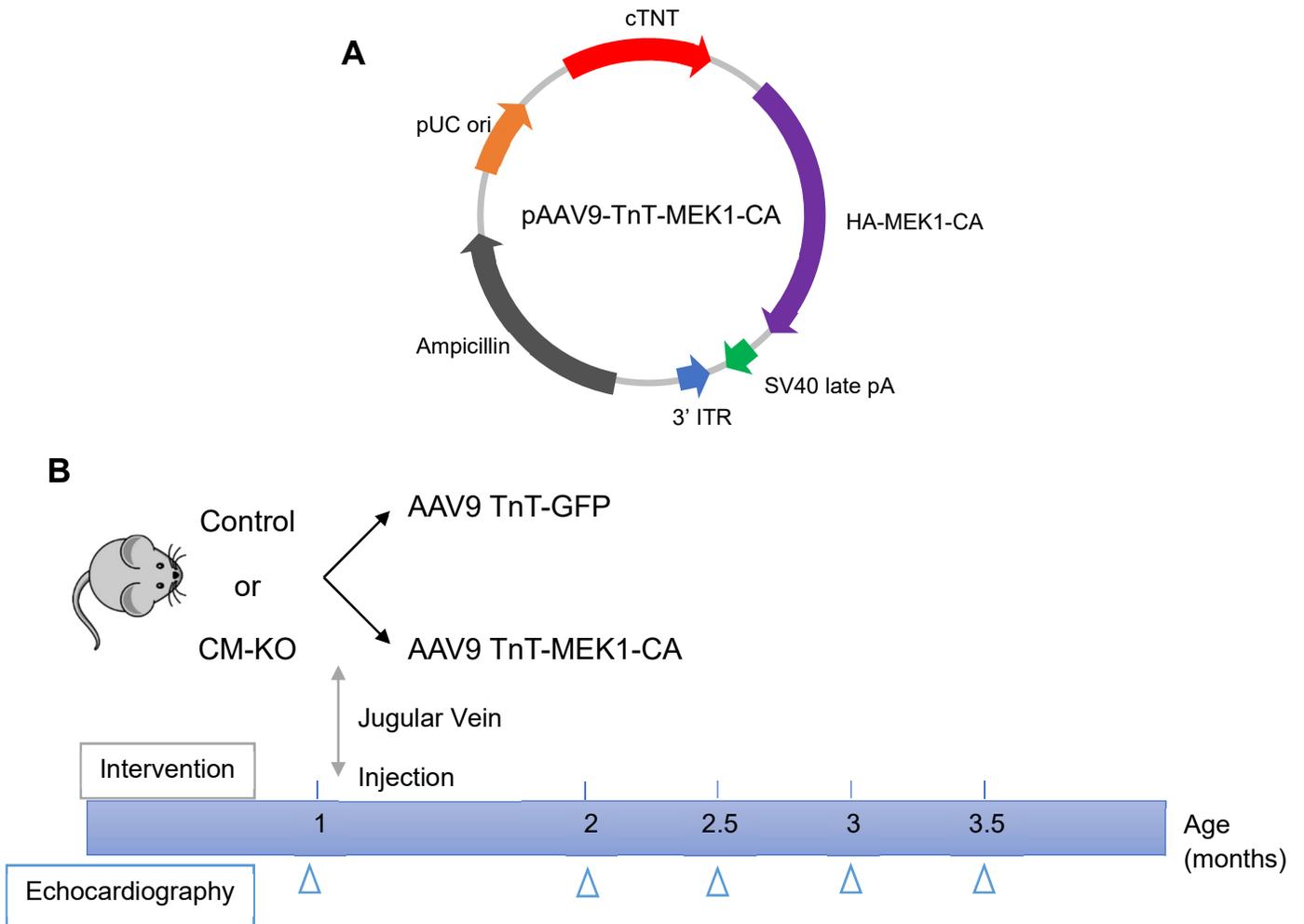
Figure 4.17 Experimental design of AAV9 rescue experiment. A. The Map of the TnT-MEK1-CA plasmid used in our experiments for AAV9 packaging. **B.** Design of AAV9 rescue experiment. 1-month-old CM-KO or Control male mice were injected with either AAV9 TnT-GFP or AAV9 TnT-MEK1-CA via jugular vein. Echocardiography was performed before and after the injection at indicated time points to assess heart function.
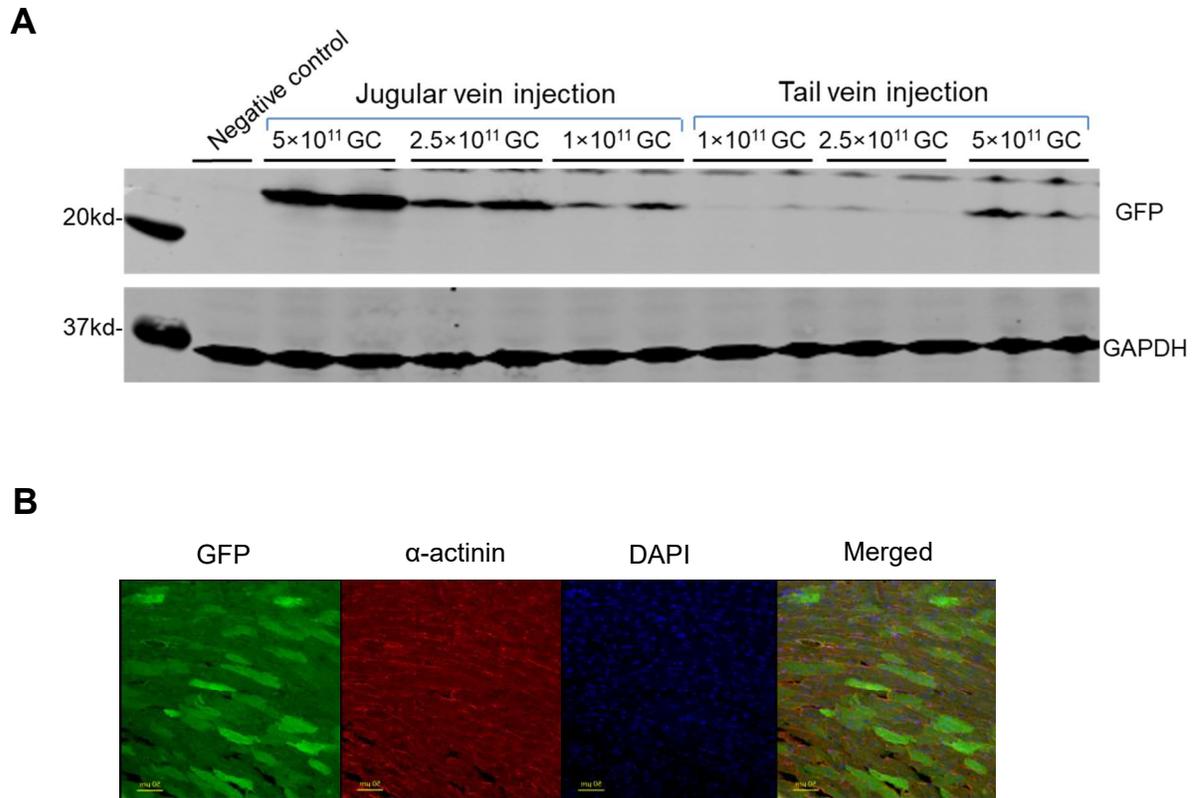
Figure 4.18 Pilot study of AAV9 gene delivery and infection efficiency in the heart. 1.5-month-old C57BL/6J male mice were injected with AAV9 TnT-GFP via jugular vein or tail vein with the indicated dose. Two weeks after injection, the heart was harvested and processed for protein lysates or froze for staining. **A.** Representative immunoblot of protein expression of GFP in the heart. **B.** Representative immunofluorescent images of ventricles from mice injected with 5×10^{11} GC via jugular vein, 20X.
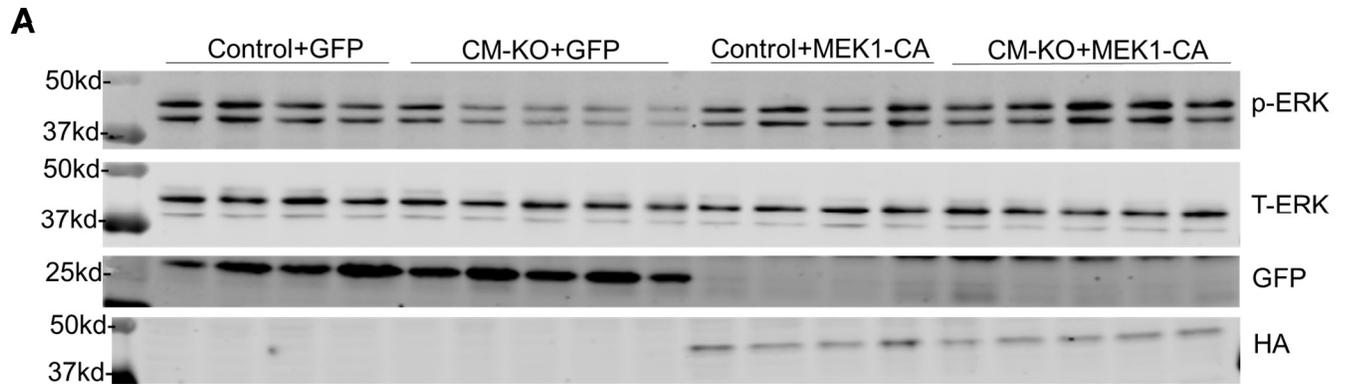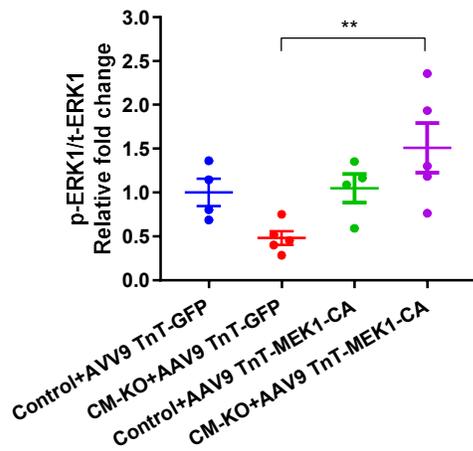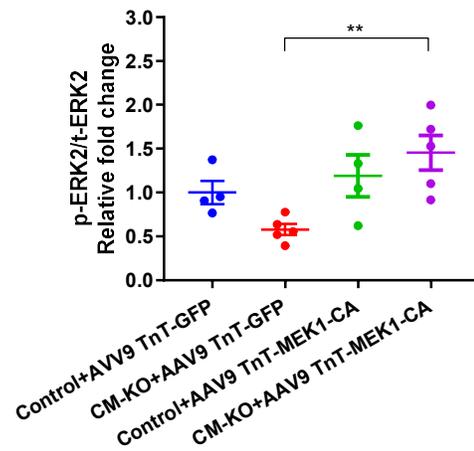
Figure 4.19 ERK signaling change in AAV9 rescue experiment. Protein expression of ERK phosphorylation, GFP and HA in LV by Western blot. **A.** Representative immunoblot showing expression of p-ERK, t-ERK, GFP and HA. **B-C.** Quantification of ERK1 and ERK2 phosphorylation. Control+AAV9 TnT-GFP: n=4, CM-KO+AAV9 TnT-GFP: n=5, Control+AAV9 TnT-MEK1-CA: n=4, CM-KO+AAV9 TnT-MEK1-CA: n=5. **p<0.01, *** p<0.005, one-way ANOVA with Turkey's post hoc test.
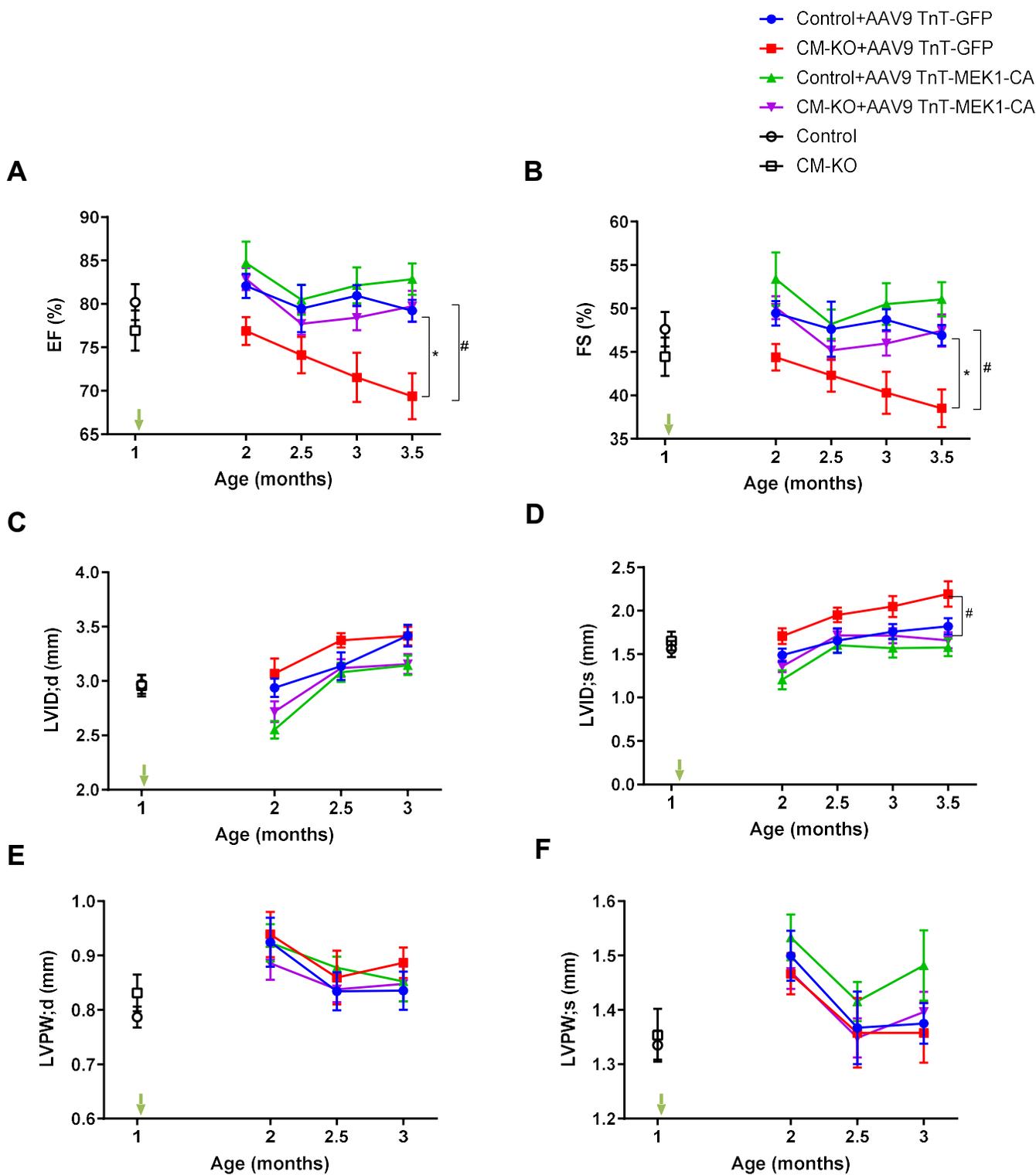
Figure 4.20 Echocardiographic assessment of heart function in AAV9 rescue experiment. A. Ejection fraction (EF). **B.** Fractional shortening (FS). **C.** Left ventricle internal dimension at end-diastole (LVID; d). **D.** Left ventricle internal dimension at end-systole (LVID; s). **E.** Left ventricle posterior wall thickness at end-diastole (LVPW; d). **F.** Left ventricle posterior wall thickness at end-systole (LVPW; s). Control+AAV9 TnT-GFP: n=7, CM-KO+AAV9 TnT-GFP: n=8, Control+AAV9 TnT-MEK1-CA: n=11-12, CM-KO+AAV9 TnT-MEK1-CA: n=9-10. *p<0.05 versus Control+AAV9 TnT-GFP, #p<0.05 versus CM-KO+AAV9 TnT-MEK1-CA, Mixed-effects analysis with Turkey's test.
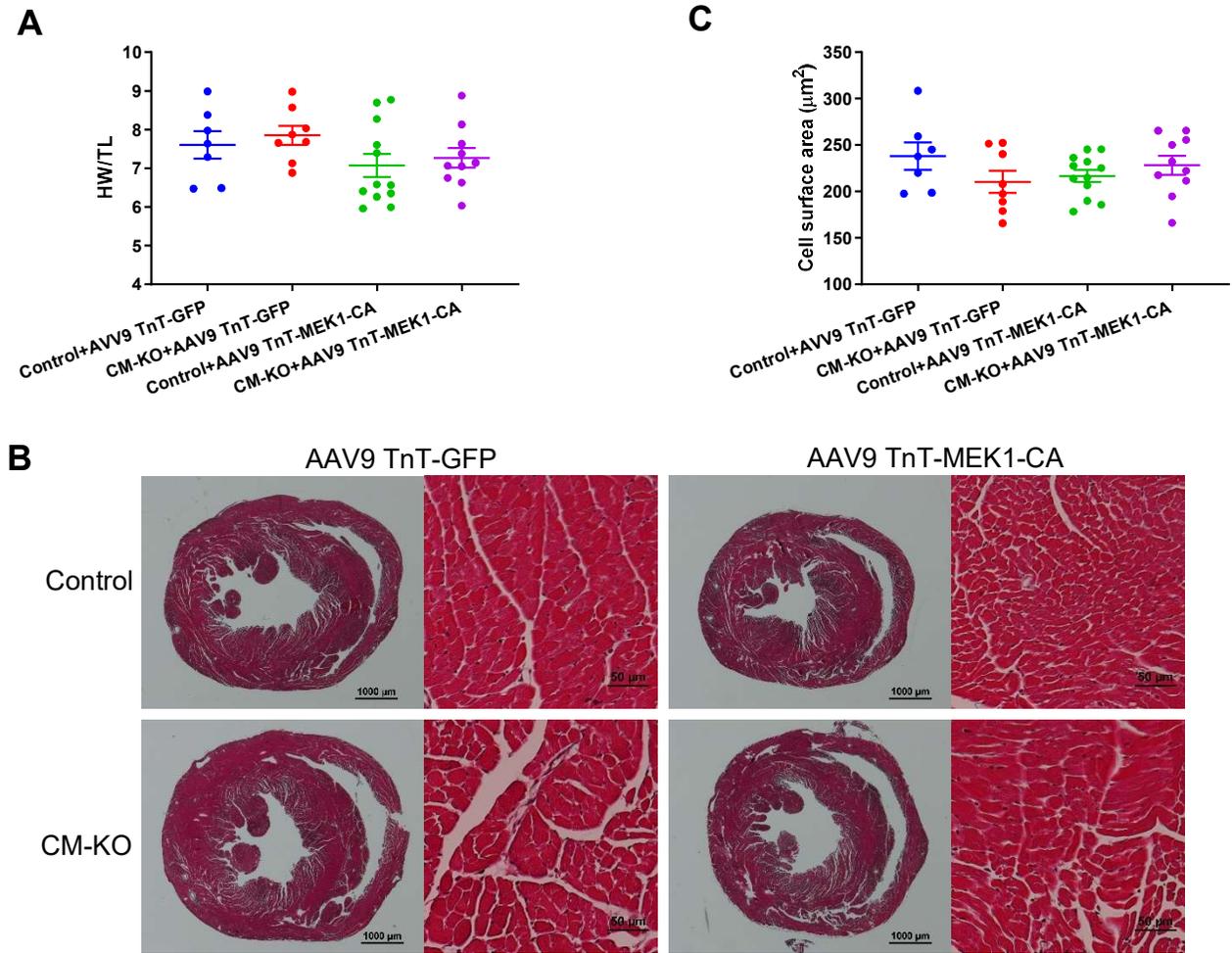
Figure 4.21 Characterization of remodeling in AAV9 rescue experiment. A. Heart weight normalized by tibia length. **B.** Representative images of Trichome staining heart sections. **C.** Quantification of CM cross-sectional area. Control+AAV9 TnT-GFP: n=7, CM-KO+AAV9 TnT-GFP: n=8, Control+AAV9 TnT-MEK1-CA: n=11-12, CM-KO+AAV9 TnT-MEK1-CA: n=9-10.

Figure 4.22 Apoptotic events in AAV9 rescue experiment. Protein expression of regulators in apoptotic pathway were measured with Western blot. **A.** Representative immunoblot showing expression of BCL-XL and BAX. **B-D.** Quantification of BAX, BCL-XL expression, and BAX/BCL-XL ratio in the CM-KO and Control LV. **E.** Representative images of TUNEL positive CM nuclei from all groups. **F.** Quantification of TUNEL positive CM nuclei in the LV section. Control+AAV9 TnT-GFP: n=4, CM-KO+AAV9 TnT-GFP: n=5, Control+AAV9 TnT-MEK1-CA: n=4, CM-KO+AAV9 TnT-MEK1-CA: n=5. **p<0.01, *** p<0.005, one-way ANOVA with Turkey's post hoc test.

60

HIPK2 and Cardiotoxicity

MEK inhibitor Trametinib (brand name Mekinist, GlaxoSmithKline Pharmaceuticals) was approved by the FDA in 2013 and by the European Union in 2014 for the treatment of metastatic melanoma with BRAF (V600E or V600K) mutations. Adverse cardiovascular effects of Trametinib is a serious concern.[79] The mechanistic studies and AAV9 rescue experiment strongly indicated that HIPK2 exerts its protection in cardiomyocytes partially through ERK signaling. Therefore, we hypothesized that overexpression of HIPK2 can protect cardiomyocytes from injury induced by ERK or MEK1 inhibitors. At basal condition, we found that neither overexpression or knockdown of HIPK2 in NRVMs affect NRVMs cell viability (Figure 4.23A). We then pre-conditioned NRVMs with overexpression or knockdown of HIPK2 by Ad-LacZ, Ad-HIPK2, Ad-scrambled or Ad-shRNA-HIPK2 infection. Then, we treated cells with MEK inhibitor U0126 for 24 hours and measured the cell viability. Strikingly, overexpression of HIPK2 significantly preserved the cell viability compared with NRVMs infected with ad-LacZ (Figure 4.23B). Conversely, knockdown of HIPK2 resulted in decreased cell viability with MEK1 inhibition (Figure 4.23C). This indicates that overexpression of HIPK2 makes the cardiomyocyte resistant to MEK1 inhibition. Consistently, knockdown of HIPK2 makes NRVMs susceptible to MEK1 inhibition.

Meanwhile, we asked if this protection to the cardiotoxicity drugs is specifically through ERK signaling. We stressed the NRVMs overexpressing HIPK2 or LacZ with Doxorubicin for 48 hrs. We observed comparable cell viability between the overexpression and control group (Figure 4.23D), suggesting that HIPK2 was unable to protect against doxorubicin-induced cardiotoxicity.
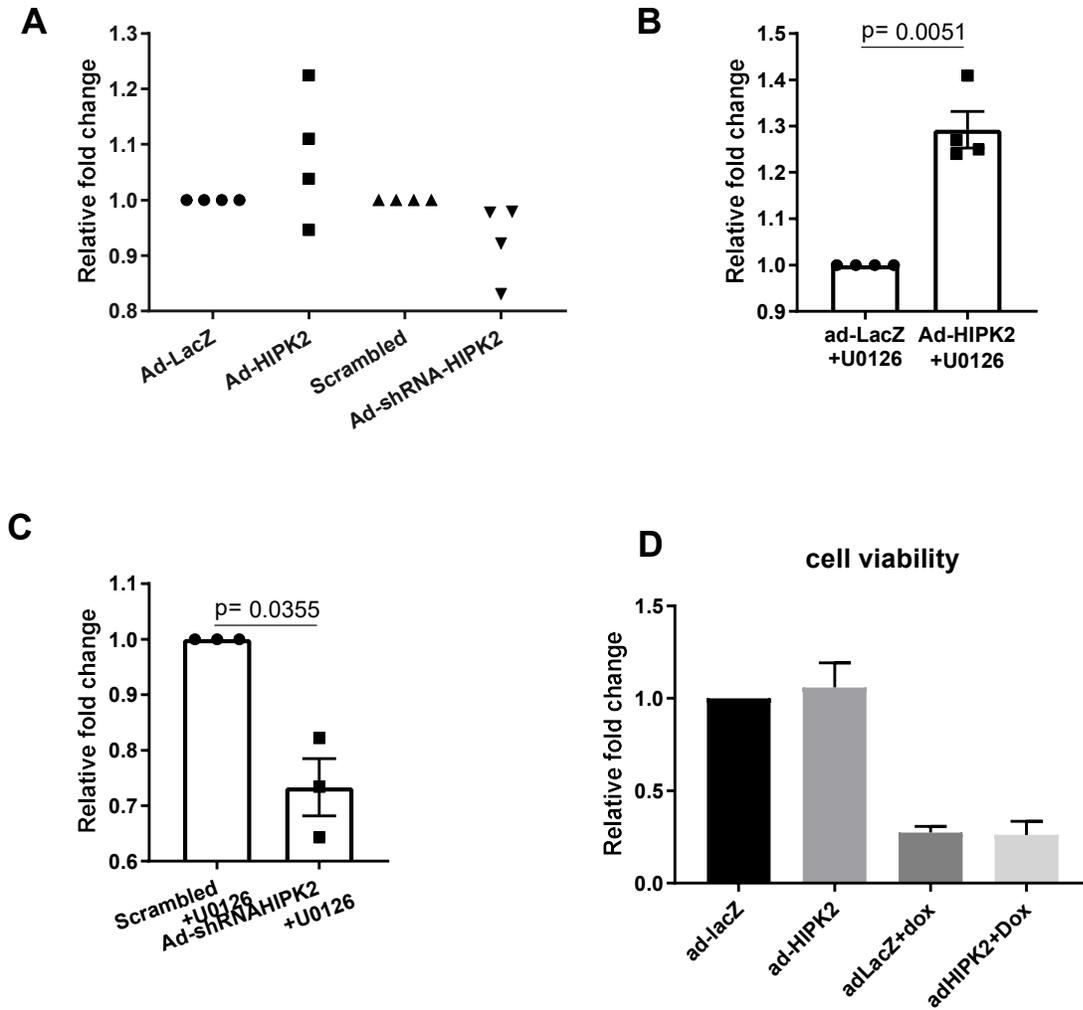
Figure 4.23 The effect of HIPK2 in cardiotoxicity. NRVMs were infected with ad-HIPK2, ad-LacZ, ad-scrambled, or ad-shRNA-HIPK2, and then treated with different drugs and cell viability was measured using Cell-Tilter Glo Assay. **A.** Cell viability with HIPK2 overexpression or knockdown. **B-C.** Cell viability with HIPK2 overexpression or knockdown in response to 24hr U0126 treatment. **D.** Cell viability with HIPK2 overexpression or knockdown in response to 48hr doxorubicin treatment. n= 3 biological replicates. Student t-test.

Heart Function of αMHC-Cre Control Mice

The αMHC-Cre mouse has been reported to develop heart failure spontaneously by age.[80,81] Therefore, we created αMHC-Cre control mice (αMHC-Cre$^{+/-}$) by crossing αMHC-Cre with C57BJ6 mice and examined their heart function at the corresponding time point as in CM-Het and CM-KO studies. The echo data showed no significant change of EF between αMHC-Cre$^{+/-}$ and C57BJ6 mice at 3 months of age. The αMHC-Cre$^{+/-}$ mice developed significantly decreased heart function at 6 months of age compared with age-matched C57BJ6 mice (Figure 4.24). Compared to αMHC-Cre$^{+/-}$ group, the heart function (EF and FS) of HIPK2 αMHC-Cre Het was still significantly decreased, which indicated cardiac dysfunction in CM-Het is indeed due to loss of HIPK2.
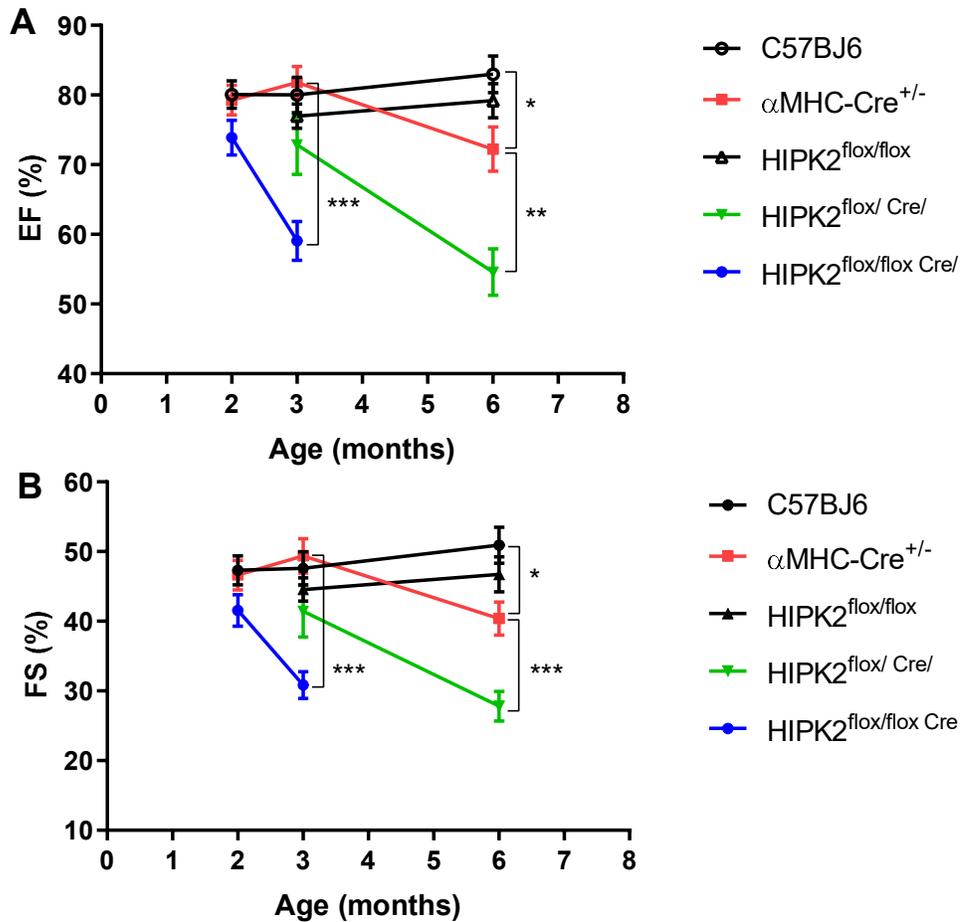
Figure 4.24 Echocardiographic examination of heart function in αMHC-Cre controls. A. EF. **B.** FS. n=7 in C57BJ6 and αMHC-Cre$^{+/-}$ group. *P<0.05, **P<0.01, ***P<0.005, Mann-Whitney test.

4.4 Discussion

This is the first study to fully describe the role of HIPK2 in the heart. By using CM-specific KO mice in conjunction with a series of in vitro studies, we showed that loss of HIPK2 is detrimental to heart function. In addition, we clearly established a dose-dependent effect of the gene level of HIPK2 on cardiac function, because ≈50% knockdown of HIPK2 (CM-Het mice) slowed down the progression of heart failure in comparison to an almost complete loss of HIPK2 (CM-KO mice). This precise dose-dependent effect of the HIPK2 level on cardiac function further indicates the functional relevance of HIPK2 in cardiac pathology.

Previous studies indicate that HIPK2 is critical to development and differentiation, such as in neural development,[30,37,38] angiogenesis,[32] and hematopoiesis.[41,82] Our findings indicate that HIPK2 is essential to cardiac function in adults rather than to cardiac development or maturation. The cardiac function of global KO and cardiac-specific KO mice were comparable to their respective controls up to 2 months of age. However, the heart function of KOs quickly deteriorates in adults suggesting the necessity of HIPK2 to maintain adult heart homeostasis. This line of reasoning is further supported by the literature that HIPK2 expression is significantly increased in mature hearts.[15] Taking into account the protection with HIPK2 overexpression in NRVMs and reduced HIPK2 expression in failing human hearts, we predict that cardiac-specific restoration of HIPK2 in failing hearts may slow down the disease progression. Further studies with cardiac-specific HIPK2 transgenic mice will be required to test this hypothesis.

Mechanistically, we characterized the main cellular processes and signaling pathways involved in cardiac remodeling thoroughly and identified that HIPK2 exerts its cardiac effect primarily through ERK-regulated apoptosis. It is important to note that this is the first study to identify ERK as a downstream target of HIPK2. Using both gain- and loss-of-function approaches, we clearly demonstrate that HIPK2 is required for cardiac ERK signaling. Furthermore, our studies suggest that impaired ERK signaling in CM-KO is the primary mechanism leading to cardiac dysfunction. This conclusion is strongly supported by our rescue experiment with AAV9-mediated gene therapy to restore ERK signaling, which significantly improved heart function in CM-KOs. Indeed, numerous studies have suggested the essential role of ERK signaling in

myocardial pathophysiology.[76,77] Mice with cardiac-specific deletion of ERK1/2 showed spontaneous cardiac dysfunction and chamber dilation leading to severe heart failure and death.[76] Conversely, transgenic mice with cardiac-specific activation of ERK1/2 signaling (via MEK1 expression) augmented cardiac function. Cardiac-specific MEK1 transgenic mice were partially resistant to stress-induced heart failure.[77] It is intriguing that Trametinib, a MEK inhibitor used for the treatment of metastatic melanoma, is also found to decrease heart function.[79] These pieces of evidence suggest that an intact ERK signaling is critical to maintain cardiac homeostasis in humans. Our AAV9 rescue experiment also supports the concept that impaired ERK signaling exerts its detrimental cardiac effects by activating the apoptotic signaling and CM death. The continuous loss of functional CMs in KO hearts could also explain the disagreement that KOs maintained the normal contractility and calcium handling at the cellular level, whereas the contractile function decreased at the organ level.[83,84] Although it is well established that ERK signaling can protect CMs from apoptosis, the targets and underlying mechanism are still unclear and certainly warrants future investigation. Considering the direct regulation of HIPK2 on cell death, it will also be interesting to determine if HIPK2 also regulates cardiomyocytes apoptosis in an ERK-independent manner.

With both overexpression and knockdown tools, we demonstrated that HIPK2 can protect the cardiomyocyte from MEK inhibitor mediated toxicity but not from doxorubicin. This study further demonstrated that HIPK2 exerts its protective effect in the cardiomyocyte mainly through ERK signaling. One limitation of these studies is that the cell viability assay we employed here is based on the total ATP content, which is not a specific parameter to indicate a change in certain cellular processes. The change of ATP content is very dynamic and can be affected by many factors such as proliferation, cell death, and/or ATP generation process. Therefore, more specific assays are needed to determine the underlying mechanisms. The HIPK2/ERK mediated cell death might be one of the underlying mechanisms. It would be informative to study if other potential ERK regulated cellular processes especially the ATP production[85] and utilization process are dysregulated. In the doxorubicin study, since doxorubicin dysregulated many cellular processes via multiple signaling pathways, it would not be surprising to see that reserving ERK signaling only is not sufficient to rescue cardiomyocytes.

Previous studies indicated that αMHC-Cre mice from Dr. Schneider's laboratory may develop cardiomyopathy with age. Pugach et al[80] indicated that the heart function (EF) of the αMHC-Cre^{+/-} male mice was significantly increased together with an increase of heart rate at 3 months of age, however, these parameters were significantly decreased at 6 months of age. The authors interpreted the early increase of EF and HR (at 3 months) as a compensatory response to developing pathology. Davis and Molkentin group reported that this αMHC-Cre line developed by Schneider laboratory started to display cardiac dysfunction by 8 to 12 months of age.[81] Our results are almost consistent with Pugach's finding that we observed significant cardiac dysfunction by 6 months of age. Of note, compared to the αMHC-Cre^{+/-} mice, the heart function of CM-Het mice was still significantly decreased. Furthermore, at a much younger age, while there is no significant change in heart function of αMHC-Cre^{+/-} mice, the CM-KO mice also exhibited strikingly decreased heart function compared to either αMHC-Cre control or *flox/flox* littermate controls. Taken together, these findings suggest that the dysfunction in the cardiomyocyte-specific HIPK2 Het null and KO mice are mainly driven by HIPK2 deficiency.

Overall, this study identifies HIPK2 as a critical regulator of cardiac homeostasis. Cardiac-specific deletion of HIPK2 leads to impaired ERK signaling and cardiac dysfunction. This pathway is central to the pathology because a rescue experiment to restore ERK signaling abolished the cardiac dysfunction phenotype in CM-KOs. We also identified that HIPK2 is downregulated in the myocardium of patients with heart failure (Chapter II). From a translational perspective, our results suggest HIPK2 as a target for cardioprotective therapy. Clinically, the inhibition of HIPK2 has been proposed as a therapeutic approach for the management of renal fibrosis and certain cancers.[82,86] Our current data provide a cautionary note for the potential cardiac side effects of systemic HIPK2 inhibition.

Chapter 5

Characterization of Heart Function in Cardiomyocyte-Specific HIPK2 Conditional Knockout Mice

5.1 Introduction

HIPK2 is known for its role in development. However, our data in Chapter III and Chapter IV showed development of the cardiac dysfunction in adult stage despite the deletion during embryogenesis. We hypothesized that HIPK2 may be indispensable in maintaining the adult heart function. To further investigate its role in the fully mature heart, we generated cardiomyocyte-specific HIPK2 conditional KO (inducible) mice driven by αMHC-MerCreMer.

5.2 Methods

Generation of αMHC-MerCreMer driven conditional HIPK2 KO mice

The αMHC-MerCreMer mice B6.FVB(129)-*A1cf*$^{Tg(Myh6-cre/Esr1*)1Jmk}$/J[15] (JAX Stock #005657) and C57BL/6J mice (JAX Stock #000664) were purchased from the Jackson Laboratory. The conditional KO mice and littermate control mice were generated by crossing HIPK2$^{flox/flox}$ mice and αMHC-MerCreMer mice. The primers used for HIPK2$^{flox/flox}$ mice genotyping are:

Forward: CAGAGACATTAGCTCCTACAACC; Reverse: CCCAGACCTACCTGATCATACT.

Step #	Temp °C	Time	Note
1	94	3 min	-
2	94	30 sec	-
3	61	45s	-
4	72	1 min	repeat steps 2-4 for 35 cycles
5	72	5 min	-
6	10	-	hold

5.3 Results

Generation of the Cardiomyocyte-Specific HIPK2 Conditional KO Mice

To generate the CM-specific HIPK2 conditional KO mice, HIPK2$^{flox/flox}$ mice mentioned in Chapter III were crossed with mice expressing αMHC promoter-driven MerCreMer. HIPK2$^{flox/flox}$ MerCreMer$^{+/}$ represented the cardiomyocyte-specific HIPK2 conditional KO mice (cKO), whereas HIPK2$^{flox/flox/}$ represented the littermate control (Control). To induce deletion, at 2 months of age, both Control and cKO mice were fed with Tamoxifen chow (Tam) for 2 weeks, and then the Tam chow was switched back to normal chow for another 2 weeks for Tamoxifen washout (to allow the clearance of tamoxifen and any associated effects) (Figure 5.1A).
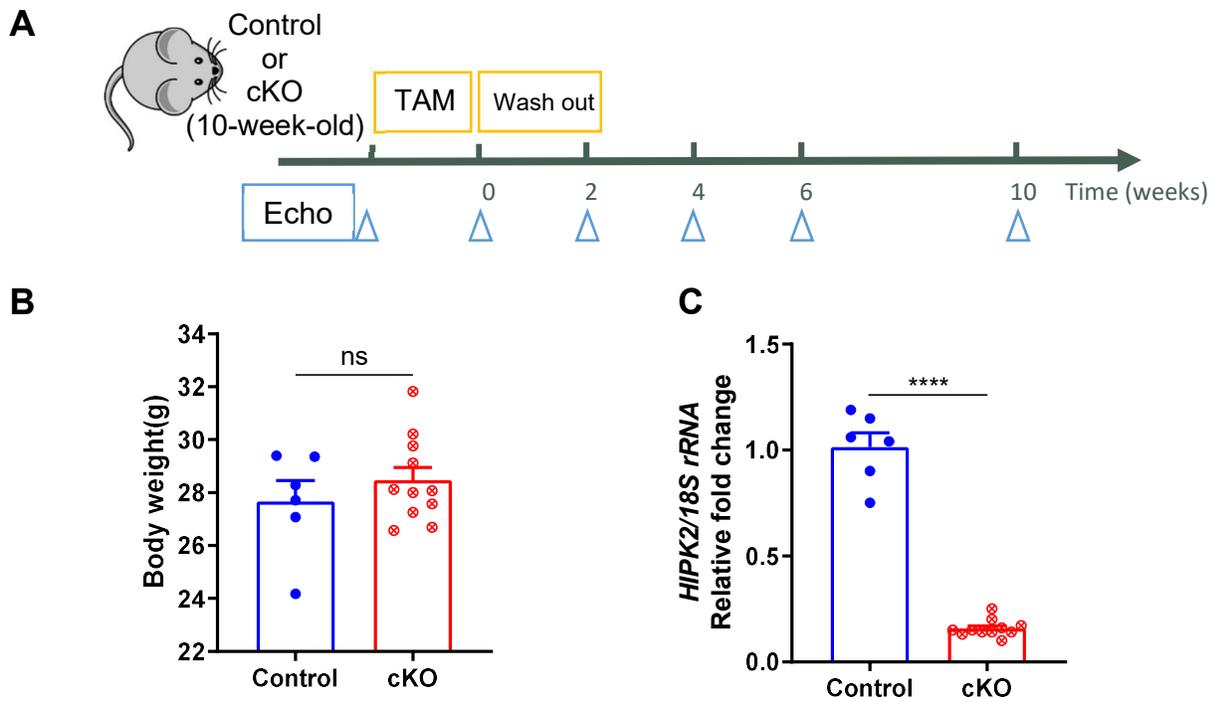
Figure 5.1 Experimental design and characterization of HIPK2 conditional KO mice. A. 10-week-old cKO or Control male mice were fed with Tamoxifen chow (TAM) for 2 weeks, and then switched on regular chow to the end of the experiment. Echocardiography was performed before the TAM treatment and every two weeks after the treatment. **B**. Body weight of cKO and Control at 4-week post-TAM. **C.** Quantification of mRNA expression of HIPK2 in cKO versus Control. Control: n=6, cKO: n=11. ****$P<0.0001$, Mann Whitney test.

Characterization of Heart Function in cKOs

The body weight was comparable between cKO and Control mice after TAM-induced deletion (Figure 5.1B). The HIPK2 expression in cKO LV was decreased by about 85% compared with Control (Figure 5.1C), suggesting a reliable deletion efficiency in the TAM-induced KO model. The heart function was examined by TTE at baseline (before on tamoxifen chow), 2-week, 4-week, 6-week, and 10-week after TAM treatment. Notably, the heart function was significantly decreased in the cKO from 2 weeks after TAM-induced deletion of HIPK2 as reflected by significantly reduced EF and FS (Figure 5.2). The cardiac dysfunction was maintained in cKOs till the end of study i.e. 10-week post-TAM. The LV also exhibited a compensated change with significant dilation of LVID at systole, as well as the thickening of the posterior wall at diastole. The heart weight was also increased in the cKO (Figure 5.3A), indicating the organ level hypertrophy. At 4-week post-TAM, the heart function slightly improved but was still worse than the Control and this condition continued to 10-week post-TAM. Consistently, the heart failure marker *NPPA* was significantly elevated in the cKO LV (Figure 5.3B). There was no significant change of pro-fibrotic gene *COL1A1* or excess fibrosis deposition in the cKO LV (Figure 5.3C).

As it is widely known that tamoxifen (TAM) and Cre have a certain amount of cardiotoxicity,[81] we also generated MerCreMer control mice (MerCreMer[+/], MCM-Control) by crossing C57BL/6J and αMHC-MerCreMer^{+/+} mice. The MCM-Control mice were also on tamoxifen chow following the same protocol as the cKO mice. The heart function was examined by TTE at indicated ages. The heart function of MCM-Control was comparable to the Control (HIPK2[flox/flox]) mice (Figure 5.4). This data suggests a minimal effect of MerCreMer on cardiac function. Overall, the above data indicated that induced deletion of HIPK2 in the adult mouse heart is detrimental to the cardiac function.
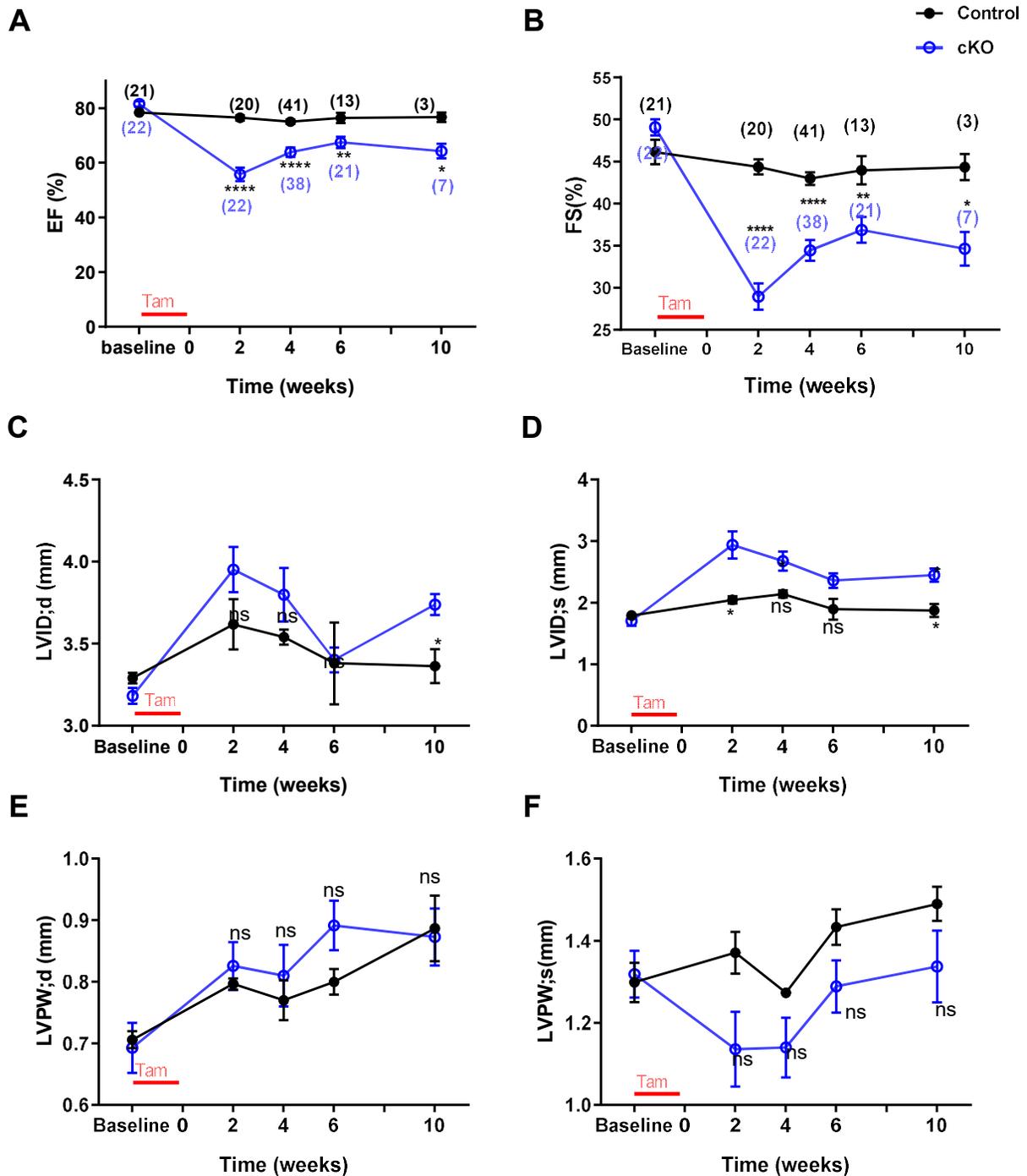
Figure 5.2 Cardiac function of HIPK2 cKO mice. Heart function of cKO and Controls was measured by transthoracic echocardiogram at 3 months and 6 months of age. **A.** Ejection fraction (EF). **B.** Fractional shortening (FS). **C.** Left ventricle internal dimension at end-diastole (LVID; d). **D.** Left ventricle internal dimension at end-systole (LVID; s). **E.** Left ventricle posterior wall thickness at end-diastole (LVPW; d). **F.** Left ventricle posterior wall thickness at end-systole (LVPW; s). *$P<0.05$, **$P<0.01$, ****$P<0.001$, Mann-Whitney test.
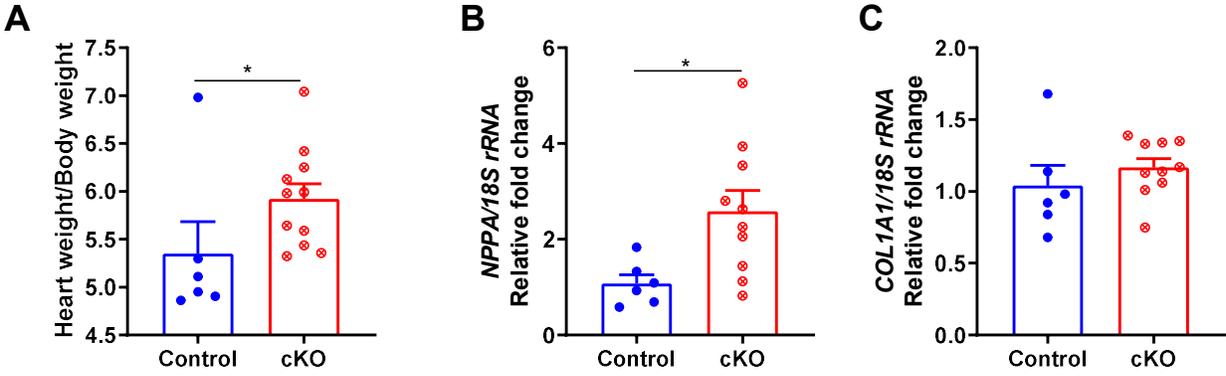
Figure 5.3 Characterization of the remodeling process in cKO mice heart. A. Heart weight normalized by body weight. **B.** Quantification of mRNA expression of *NPPA* in cKO and Control LV at 4-week post-TAM. **C.** Quantification of mRNA expression of *COL1A1* in cKO and Control LV at 4-week post-TAM. *P<0.05. Mann-Whitney test.
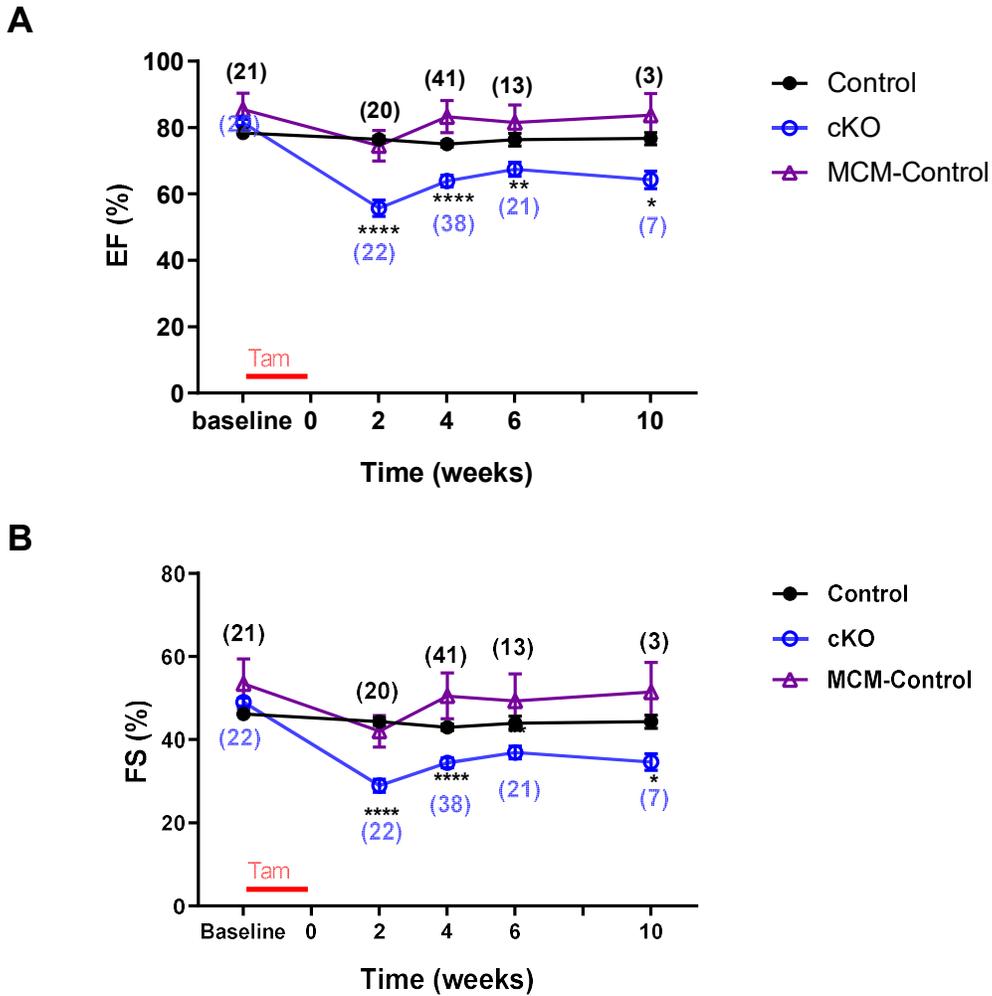
Figure 5.4 Echocardiographic assessment of MCM-Control mice and comparison with cKO. 2.5-week-old male MCM-Control mice were fed with TAM for 2 weeks and the heart function was assessed by echocardiography at indicated time points. **A.** EF. **B.** FS. n=10 in MCM-Control group.

The Expression of HIPK2 by Ages

As discussed above, the cardiac dysfunction in 3 different KO models, the global KO, the CM-KO as well as the cKO, all developed in adulthood (after 2 months of age). This is despite that αMHC-driven deletion occurs as early as at birth and the global KO mice lack gene activity throughout embryogenesis. Strikingly, HIPK2 deletion in fully mature hearts rapidly leads to decreased heart function. This suggests that HIPK2 is essential in maintaining adult heart function. Considering that HIPK2 expression level is correlated with the heart function (Chapter IV), we hypothesized that HIPK2 expression is age-related and may dominate in the fully mature heart. To examine the HIPK2 expression at different ages, we harvested hearts from C57BL/6J mice at embryonic day 12.5 (E12.5), day 1, and 4 months of age, representing embryonal, neonatal and adult stages respectively. Analysis of HIPK2 expression reveals a higher HIPK2 expression level in adults than in embryonic or neonatal hearts (Figure 5.5). This expression pattern may partially explain the time course of the cardiac phenotype we observed in all KO models.
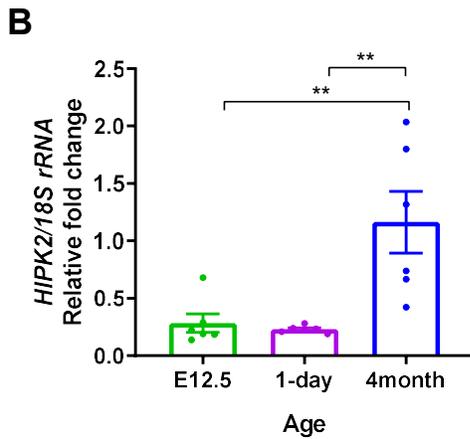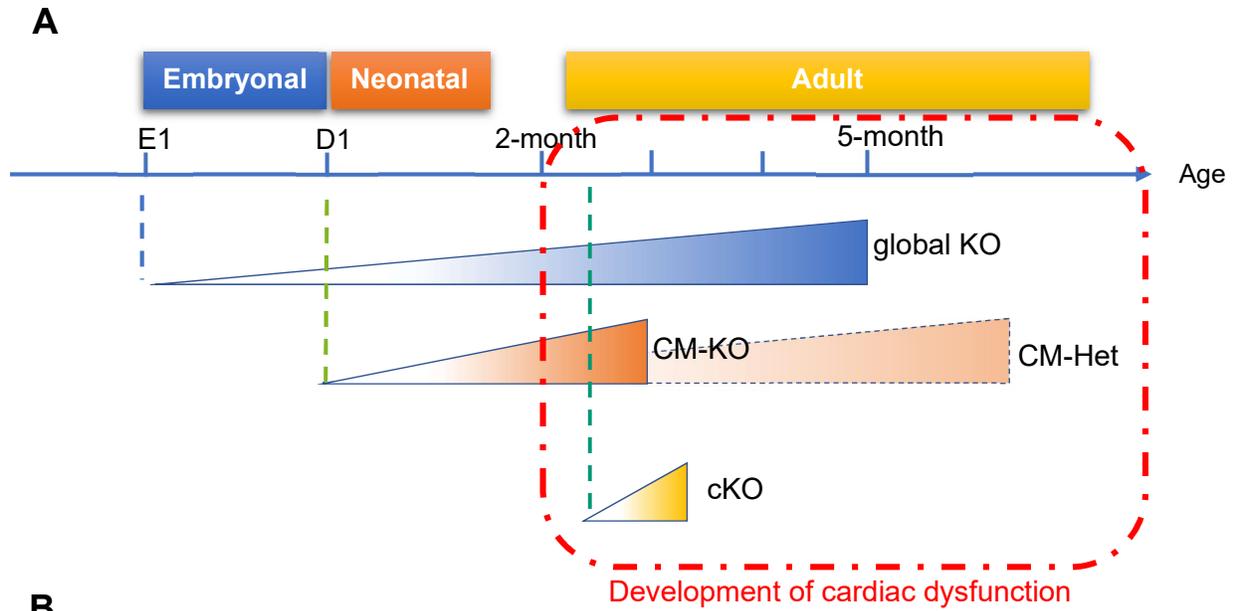
Figure 5.5 HIPK2 expresion in the heart with age. A. Schematic representation of HF progression in different HIPK2 genetic ablation models with age. Triangle indicates the development of HF. The dash line indicates the estimated start age of HIPK2 deletion. **B.** Quantification of mRNA expression of *HIPK2* in the heart with ages. Mouse heart was harvested from C57BL/6J mice at E12.5, 1 day and 4 months of age. n=6 per group. **$P<0.01$, one-way ANOVA with Tukey post hoc test.

5.4 Discussion

Using tamoxifen-induced HIPK2 conditional KO mice, we identified that deletion of HIPK2 is detrimental to the adult heart function. This finding is consistent with the finding in CM-KO and strongly supports that HIPK2 is essential for adult heart homeostasis and its deletion leads to cardiac dysfunction. The deletion in the αMHC-Cre KO hearts is as early as the neonatal stage, but they display significant phenotype only in adulthood (starting from 2 months of age). And the onset of cardiac dysfunction (3 months of age) is at similar time frame as the cKO (2-week post-TAM ≈ 3 months of age). Although this expression pattern is quite different from what observed in the nervous system, yet it reflects that HIPK2, as a transcription regulator, precisely controls gene expression in the right place and right time. The underlying regulating mechanism is still unknown, but it will be interesting to examine how and why HIPK2 is tightly regulated in the heart with age.

Regarding the potential cardiotoxicity caused by tamoxifen and Cre, our tamoxifen chow protocol ensures sufficient and stable plasma tamoxifen level to induce deletion as well as minimize the tamoxifen toxicity to the mouse. Our laboratory has compared the different protocols of tamoxifen-induced gene excision, specifically, chow diet vs IP injection and as well as the duration of the treatment. The protocol employed here is optimized to achieve the best deletion efficiency with minimal adverse effects. The minimum change of the heart function in the MCM control group also strongly supports this and indicates that the change of heart function in cKO is mainly due to the deletion of HIPK2.

Chapter 6

Identifying the Role of HIPK2 in Cardiac Fibroblasts

Part of the experimental data in this chapter was generated and provided by Dr. Prachi Umbarkar in the Lab. (marked with *)

6.1 Introduction

Virtually every form of heart disease is associated with FB activation and fibrosis. Since cardiomyocytes are notoriously known for their poor regenerative capabilities, the major way for the rest of cardiomyocytes to handle the stress is hypertrophy. Meanwhile, loss of cardiomyocytes activates fibroblasts to proliferate and increase extracellular matrix deposition which eventually replaces injured myocardium with the scar tissue. The fibroblasts are the main cell types in the cardiac interstitium, but their effects on cardiac function were underestimated for a very long time. Recent studies have demonstrated that FB-specific genetic manipulation can lead to robust cardiac phenotype. Since HIPK2 is known as a profibrotic factor in kidney fibrosis,[60] we aimed to examine the role of HIPK2 in cardiac fibroblasts and fibrosis. Our hypothesis is that deletion of HIPK2 may decrease fibrosis in the heart.

6.2 Methods

Neonatal rat cardiac fibroblasts culture

Neonatal rat cardiac fibroblasts (NRVFs) were isolated from 1-day-old neonatal rat pups and were cultured in DMEM with 10% FBS and 1% antibiotics. Only the 1st passage of the fibroblasts was used in the experiments. Fibroblasts were starved in serum-free medium for overnight and infected with adenovirus for 24 hours. Then cells were treated with TGF-β1 (10ng/mL) for 1hour.

6.3 Results

TGFβ1 is a potent profibrotic cytokine. It regulates fibrosis by activating SMAD3 via the classical TGFβ pathway. To investigate if HIPK2 can affect TGFβ1-SMAD3 pathway, NRVFs were infected with Ad-HIPK2 or Ad-LacZ (300MOI) for 24 hrs. Thereafter, cells were treated with TGFβ1 (10mg/mL) for 1 hour. The cell lysates were analyzed for the phosphorylation of SMAD3. Overexpression of HIPK2 significantly decreased the TGFβ-induced SMAD3 phosphorylation (Figure 6.1). Thus, HIPK2 can negatively regulate TGFβ1-SMAD3 pathways, which suggests a potential anti-fibrotic effect of HIPK2 in cardiac fibroblasts.

To further study the role of HIPK2 in cardiac fibroblasts and fibrosis after injury, we generated the fibroblast-specific knockout mice driven by periostin-Cre (HIPK2$^{flox/flox\ Cre/}$, cFB-KO). To achieve the FB-specific HIPK2 KO mice, we crossed the HIPK2$^{flox/flox}$ mice with periostin-Cre mice. At 4 months of age, the heart function was examined by TTE. The heart function was comparable between the cFB-KO and Control mice at baseline. We then challenged the cFB-KO and littermate controls with MI surgery. At 4 weeks post-MI, the cFB-KO displayed a marked cardiac dysfunction as reflected by significantly decreased EF and FS compared to littermate controls (Figure 6.2*). Taken together, cFB-specific deletion of HIPK2 leads to a robust detrimental cardiac phenotype.
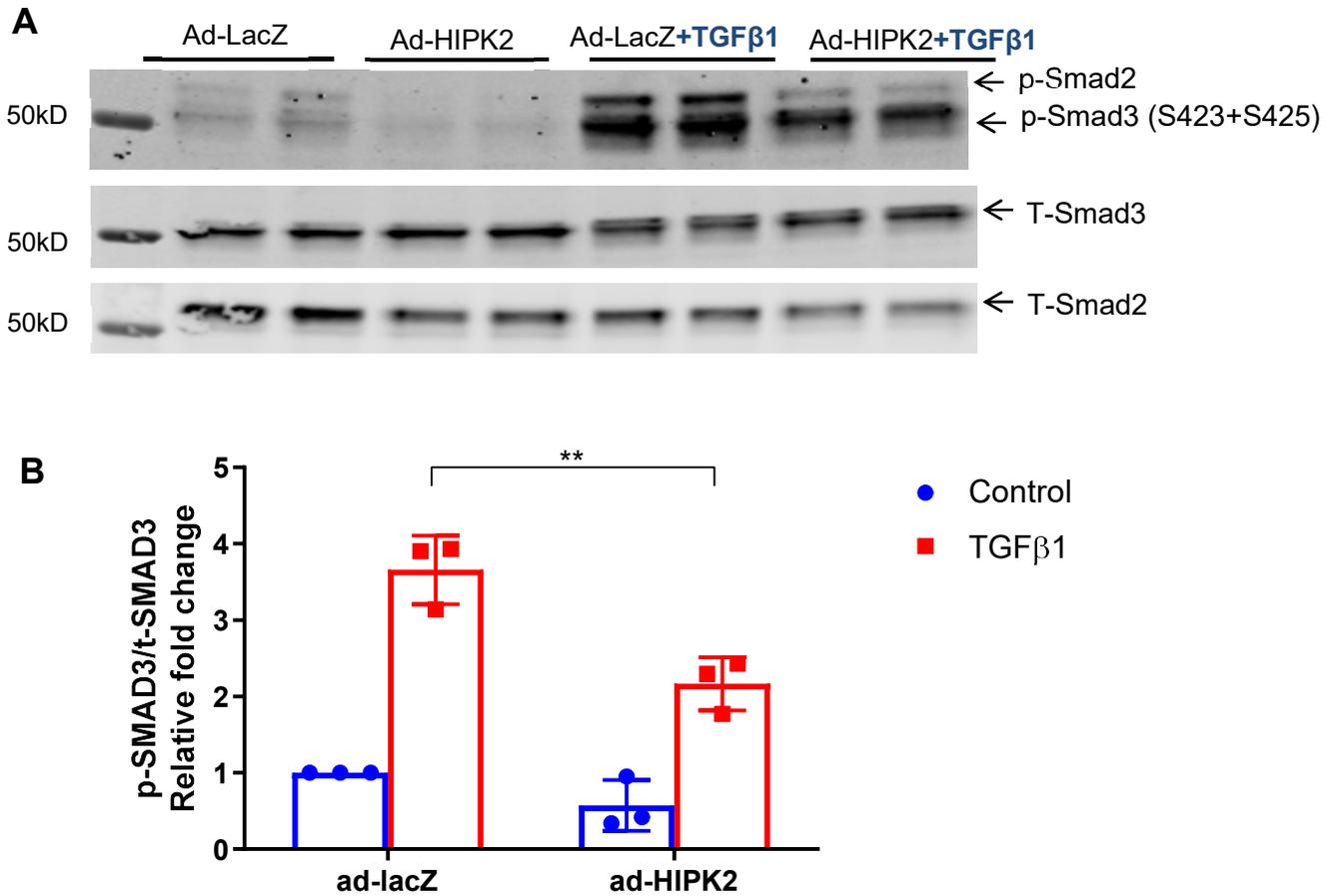
Figure 6.1 The effects of HIPK2 on TGFβ-Smad signaling in cFBs. NRVFs were infected with adenovirus expressing LacZ (Ad-LacZ) and HIPK2 (Ad-HIPK2) virus for 24 hrs and then treated with TGFβ1(10mg/mL) for 1 hour. Protein lysates were then harvested for western blot analysis to determine the phosphorylation of SMAD3. **A.** Representative immunoblot showing significantly decreased phosphorylation of SMAD3. **B.** Quantification of SMAD3 phosphorylation in Ad-HIPK2 group versus control group. n=3 independent replicates. ** $p<0.01$, two-way ANOVA with post-hoc Turkey's test.
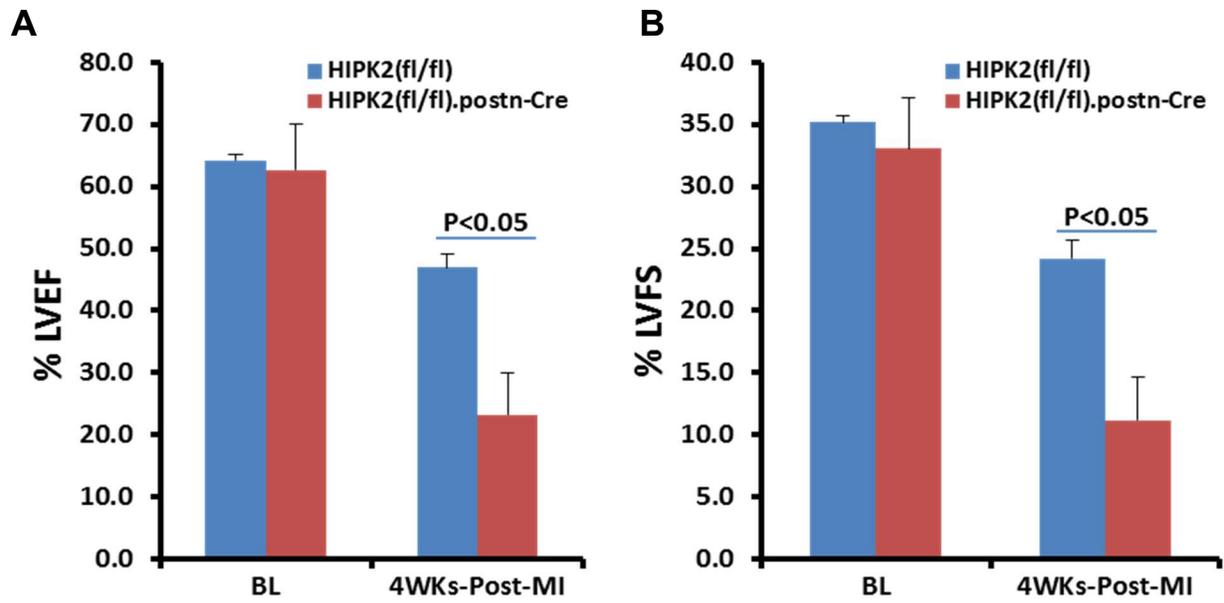
Figure 6.2* CF-HIPK2 KO leads to cardiac dysfunction post-MI. WT and CF-HIPK2 KO mice were subjected to MI surgery and followed with TTE. **A.** Left ventricular ejection fraction (LVEF). **B.** LV fractional shortening (LVFS).

6.4 Discussion

Jin et al have reported that knockout of HIPK2 can significantly decrease kidney fibrosis via inhibiting the TGFβ1-SMAD pathway. However, our results are in stark contrast with this finding and support an anti-fibrotic role of HIPK2 in cardiac fibroblasts and myocardial fibrosis. Consistent with the in vivo findings, overexpression of HIPK2 in NRCFs suppressed the TGFβ1-SMAD3 pathway. The disagreement with Jin et al[60] indicates another tissue-specific role of HIPK2 in cardiac fibroblasts versus kidney tubular cells. It would be informative to study how HIPK2 regulates TGFβ1-SMAD3 pathway and myofibroblast transformation in cFBs.

Our preliminary data indicated that deletion of HIPK2 specifically in the cardiac fibroblast can aggravate MI-induced cardiac dysfunction. It will be informative to further investigate how this loss of HIPK2 in cFBs affect fibrosis and remodeling process in ischemic hearts. Further studies are needed to elucidate the mechanism of fibrotic remodeling and healing process in the FB-specific HIPK2 KOs. Altogether, the role of HIPK2 in both cardiomyocytes, and cardiac fibroblasts are protective. Therefore, increasing expression of HIPK2 may be a promising method to preserve the cardiac function in the failing heart.

Chapter 7

Conclusion and Future Directions

7.1 Conclusion

Protein kinases are important regulators of cardiac physiology and pathophysiology. In this project, we aimed to identify novel kinase targets of heart failure by using Expression2Kinase approach (Chapter II). Herein, we identified HIPK2, a previously less studied kinase in the context of cardiac biology. We then examined the heart function by using global KO mice (Chapter III), cardiomyocyte-specific KO and heterozygous null mice (CM-KO and CM-Het, Chapter IV), and inducible cardiomyocyte-specific KO mice (cKO, Chapter V). With all these models, we observed decreased heart function occurred in adulthood, which strongly supported our key finding that 1) deletion of HIPK2 is detrimental to adult heart function. Data from both CM-KO and CM-Het mice also indicate the 2) haplo-insufficiency of HIPK2's cardiac effect and the function of HIPK2 is dependent on its gene level. Based on these findings, we hypothesized that HIPK2 expression may change with age (Chapter V). We examined the HIPK2 expression at different ages and found another character of CM HIPK2 that 3) HIPK2 expression in the heart is elevated in adulthood in comparison with embryonal and neonatal stages.

As global KO mice displayed defects in multiple organs, we mainly employed the CM-KO and CM-Het models for mechanistic studies (Chapter IV). We examined the major signaling pathways involved in cardiac remodeling and identified impaired ERK signaling as a key driver of the pathogenesis. We further validated our findings with in vitro NRVMs models using adenovirus delivered gain-of-function and loss-of-function approaches. Notably, overexpression of HIPK2 could elevate ERK phosphorylation and vice versa. Besides, this regulation is also dependent on HIPK2's kinase function. To further evaluate if HIPK2 exerts its cardiac effect via ERK signaling, we did a rescue experiment using AAV9 TnT-MEK1-CA in CM-KO mice. Intriguingly, the MEK1-CA construct successfully rescued the cardiac dysfunction in CM-KO mice by maintaining the apoptosis pathway. Overall, another key finding of this project is that 4)

deletion of HIPK2 in the heart leads to cardiac dysfunction through dysregulated ERK signaling mediated apoptosis. In addition, overexpression of HIPK2 could protect cardiomyocytes from PE-induced hypertrophy and MEK1 inhibitor-induced cell death. Since HIPK2 expression was down-regulated in ischemic cardiomyopathy (Chapter II), it is possible that 5) overexpression of HIPK2 is cardioprotective.

The last but not the least, we also examined the role of HIPK2 in cardiac fibroblasts and fibrosis (Chapter VI). 6) HIPK2 negatively regulates the TGFβ1-Smad3 pathway in cardiac fibroblasts. Consistently, CF-specific HIPK2 deletion worsens the post-MI cardiac function.

Overall, HIPK2 exhibits a protective role in both cardiomyocytes and cardiac fibroblasts. To translate it into a potential therapeutic target, more studies are needed to fully understand its function and underlying mechanisms.

7.2 Future Directions

Develop reliable HIPK2 antibodies

Antibodies are important tools to study protein function. Lack of a validated antibody is a huge caveat in the HIPK2 study field. Unfortunately, most of the published data showing HIPK2 protein expression in the cardiomyocyte,[75] brain,[39] or kidney[60] are unlikely to be reproduced in our lab. Although the tagged-protein is one common method to use, the transfection limitation in the cardiomyocyte and potentially different characteristics of endogenous and exogenous proteins are all possible concerns. It is important to generate a validated antibody with high specificity and sensitivity for better understanding the protein level changes, post-translation modifications, protein-protein interactions, and protein-chromatin interactions, etc.

Identify the mechanism of HIPK2 regulation in the heart

As this is the first study to examine the role of HIPK2 in the heart, the discovery of dysregulated ERK signaling is just a beginning, a lot of new questions are arising from the current finding.

1) Our findings showed that HIPK2 regulates heart function via ERK-mediated apoptosis. However, we still do not know i) how HIPK2 regulates ERK, ii) how ERK regulates apoptosis, iii) if there are ERK-independent apoptosis pathways, and also iv) other potential signaling pathways and cellular processes regulated by HIPK2 in the heart (will discuss in detail below).

2) HIPK2 is dynamically regulated in different tissues, ages, and disease contexts. Thus, one important question to address is how HIPK2 is regulated in cardiomyocytes—the upstream regulators or stimuli of HIPK2.

    i)   One direction is to study the stress factors that can activate or suppress HIPK2. As discussed above, hypoxia is one relevant stimulus to examine in the cardiomyocyte. Other stimuli such as mechanical stress, reaction oxygen species, inflammation factors, chemotherapies, catecholamines, and natriuretic peptides, are also reasonable to examine. Besides, how HIPK2 level is maintained at rest in CMs is also important to learn.

    ii)   The other aspect is to examine molecules that regulate HIPK2 activity. This could be achieved by employing mass spectrometry genome-wide CRISPR knockout screening in the cardiac iPSC cell lines.

3) What molecules/cellular processes are regulated by HIPK2—the downstream effectors of HIPK2. To better understand the role of HIPK2 in the heart, it is important to learn the downstream effectors of HIPK2, including i) transcription profile regulated by HIPK2, ii) proteins directly interacting with HIPK2, iii) post-translational targets of HIPK2, iv) promoters efficiency affected by HIPK2. These aims can be achieved using RNAseq, mass spectrometry, phosphoproteomics, ChIP-seq, and kinome analysis.

4) Localization of HIPK2

    With a high-quality antibody, it is also essential to learn the localization of HIPK2 and more importantly, the translocation mechanism and its relationship with its function. As an extension of the current study, this can help to understand how HIPK2, as a nuclear kinase, regulates ERK and SMAD3 phosphorylation. We also speculate that there might be some other intermediate factors

regulated by HIPK2. This study would be facilitated with a high-quality antibody and the information learned from RNAseq.

Identify the role of HIPK2 in cardiac stress

By using multiple HIPK2 KO mice, we discovered that HIPK2 is essential in maintaining normal cardiac homeostasis. However, the role of HIPK2 in response to different cardiac stress is still unknown. It will be interesting to study HIPK2 in those most commonly used cardiac injury and heart failure models:

1) TAC model: TAC model is the classical pressure-overload model to induce heart failure, and it was also the model we used to identify targets at the beginning. Considering that the cardiac dysfunction in HIPK2 KO mice is mainly due to dysregulated ERK signaling, we hypothesized that CM-KO or CM-Het null mice may have a worse cardiac function than the control group. However, it could also be possible that HIPK2-deficient hearts may have a better heart function in response to TAC since a moderate resistant to hypertrophy could be beneficial in TAC.

2) AngII/PE: AngII/PE infusion is a commonly used pharmacological-induced heart failure model. This model primarily works by activating the RAAS and the sympathetic nervous system. We hypothesize that the phenotype in this model could be similar to that of TAC model. In addition, this model may be useful to study the role of HIPK2 and GPCR mediated signaling.

3) Myocardial infarction (MI) model: MI model mimics the myocardial infarction patients with occlusion of the coronary artery. We expect to see a decreased cardiac function in the HIPK2 KO hearts which will be consistent with the finding that decreased HIPK2 in the ischemic cardiomyopathy heart tissue.

4) Ischemia/Reperfusion(I/R): I/R is an appropriate model to study acute ischemic injury and reperfusion in the heart. Since previous studies showed that HIPK2 is suppressed by hypoxia, it will be interesting to learn if HIPK2 can rescue the ischemic injury. It is also an appropriate model to study if hypoxia is a stimulus of HIPK2 expression and activity in cardiomyocytes.

Identify the protective role of HIPK2 in cardiac injury

We identified the protective effect of HIPK2 overexpression in the in vitro study. This indicates that overexpression or activation of HIPK2 is a promising therapy in the cardiac stress or injury context. I hypothesize that overexpression of HIPK2 can rescue cardiac dysfunction in TAC or MI-induced heart failure. This hypothesis can be tested by using AAV9 carried HIPK2, an arising tool applied in the clinical trial, or HIPK2 transgenic mouse models. We expect that overexpression of HIPK2 will protect the heart from cardiac injury and remodeling. It will also be useful to screen and develop potentiators/activators of HIPK2 for the treatment purpose of HF.

Identify the role of HIPK2 in cardiac fibroblasts and fibrosis

We discovered that overexpression of HIPK2 can significantly decrease the TGFβ-Smad3 pathway suggesting an anti-fibrotic role of HIPK2 in cardiac fibroblasts. Our preliminary data indicated that there is no change of heart function of periostin-Cre KO mice at baseline. However, the heart function was significantly decreased in the HIPK2 KO mice at 4-week post-MI. This strongly indicated that deletion of HIPK2 specifically in cardiac fibroblasts leads to increased susceptibility to the MI injury. It would be interesting to further investigate how HIPK2 affects cardiac fibroblasts and fibrosis. For the mechanistic studies, besides studying the underlying signaling mechanism, it will be interesting to determine how HIPK2 regulates Smad3 phosphorylation.

Since our preliminary data showed that deletion of HIPK2 only in cardiac fibroblasts was sufficient to drive a detrimental phenotype after MI, it would be of interest to see how cFB-specific deletion leads to a global cardiac phenotype. Specifically, whether this is directly caused by cFB mediated mechanism or the CM function is also affected.

Clinical Perspectives and Cardiotoxicity

HIPK2 is arising as a potential target in cancer and kidney treatment. However, based on our findings here, the systemic delivery of HIPK2 inhibitors may increase the risk of drug-induced

cardiotoxicity. 1) It is important to assess if these HIPK2 inhibitors affect the cardiac function 2) Considering the protective role of HIPK2 in the MEK1 inhibitor-induced cardiotoxicity, it will be of interest to study the underlying mechanism and if HIPK2 can protect the heart from another chemotherapy-induced cardiotoxicity.

References

1.   Benjamin EJ, Muntner P, Alonso A, Bittencourt MS, Callaway CW, Carson AP, Chamberlain AM, Chang AR, Cheng S, Das SR, Delling FN, Djousse L, Elkind MS V, Ferguson JF, Fornage M, et al. Heart Disease and Stroke Statistics-2019 Update: A Report From the American Heart Association. *Circulation*. 2019;139(10):e56–e528.

2.   Coronel R, De Groot JR, Van Lieshout JJ. Defining heart failure. *Cardiovascular Research*. 2001;50(3):419–422.

3.   Johnson MR, McBride PE, Tsai EJ, Sam F, Fonarow GC, Mitchell JE, Wilkoff BL, Januzzi JL, Kasper EK, Casey DE, Horwich T, Butler J, Geraci SA, Drazner MH, Bozkurt B, et al. 2013 ACCF/AHA Guideline for the Management of Heart Failure: Executive Summary. *Circulation*. 2013;128(16):1810–1852.

4.   Hill J a, Olson EN. Cardiac plasticity. *The New England journal of medicine*. 2008;358(13):1370–80.

5.   Cohn JN, Ferrari R, Sharpe N. Cardiac remodeling-concepts and clinical implications: A consensus paper from an International Forum on Cardiac Remodeling. *Journal of the American College of Cardiology*. 2000;35(3):569–582.

6.   Gjesdal O, Bluemke DA, Lima JA. Cardiac remodeling at the population level-risk factors, screening, and outcomes. *Nature Reviews Cardiology*. 2011;8(12):673–685.

7.   Nakamura M, Sadoshima J. Mechanisms of physiological and pathological cardiac hypertrophy. *Nature Reviews Cardiology*. 2018;15(7):387–407.

8.   Burchfield JS, Xie M, Hill J a. Pathological ventricular remodeling: mechanisms: part 1 of 2. *Circulation*. 2013;128(4):388–400.

9. Lal H, Ahmad F, Zhou J, Yu JE, Vagnozzi RJ, Guo Y, Yu D, Tsai EJ, Woodgett J, Gao E, Force T. Cardiac Fibroblast Glycogen Synthase Kinase-3β Regulates Ventricular Remodeling and Dysfunction in Ischemic Heart. *Circulation*. 2014;130(5):419–430.

10. Dhanasekaran N, Reddy EP. Signaling by dual specificity kinases. *Oncogene*. 2002;17(11):1447–1455.

11. Manning G, Whyte DB, Martinez R, Hunter T, Sudarsanam S. The Protein Kinase Complement of the Human Genome. *Science*. 2002;298(5600):1912 LP – 1934.

12. Caenepeel S, Charydczak G, Sudarsanam S, Hunter T, Manning G. The mouse kinome: Discovery and comparative genomics of all mouse protein kinases. *Proceedings of the National Academy of Sciences*. 2004;101(32):11707–11712.

13. Van Berlo JH, Maillet M, Molkentin JD. Signaling effectors underlying pathologic growth and remodeling of the heart. *Journal of Clinical Investigation*. 2013;123(1):37–45.

14. Vlahos CJ, McDowell SA, Clerk A. Kinases as therapeutic targets for heart failure. *Nature Reviews Drug Discovery*. 2003;2(2):99–113.

15. Fuller SJ, Osborne SA, Leonard SJ, Hardyman MA, Vaniotis G, Allen BG, Sugden PH, Clerk A. Cardiac protein kinases: the cardiomyocyte kinome and differential kinase expression in human failing hearts. *Cardiovascular Research*. 2015;108(1):87–98.

16. Shahin R, Habash M, Shaheen O, El-Dahiyat F, Saffour S. Research advances in kinase enzymes and inhibitors for cardiovascular disease treatment. *Future Science OA*. 2017;3(4):FSO204.

17. Murga C, Arcones AC, Cruces-Sande M, Briones AM, Salaices M, Mayor Jr. F. G Protein-Coupled Receptor Kinase 2 (GRK2) as a Potential Therapeutic Target in Cardiovascular and Metabolic Diseases. *Frontiers in Pharmacology*. 2019;10:112.

18.   Kim YYH, Choi CY, Lee SJ, Conti MA, Kim YYH. Homeodomain-interacting protein kinases, a novel family of co-repressors for homeodomain transcription factors. *Journal of Biological Chemistry*. 1998;273(40):25875–25879.

19.   Arai S, Matsushita A, Du K, Yagi K, Okazaki Y, Kurokawa R. Novel homeodomain-interacting protein kinase family member, HIPK4, phosphorylates human p53 at serine 9. *FEBS Letters*. 2007;581(29):5649–5657.

20.   Puca R, Nardinocchi L, Givol D, D'Orazi G. Regulation of p53 activity by HIPK2: Molecular mechanisms and therapeutical implications in human cancer cells. *Oncogene*. 2010;29(31):4378–4387.

21.   Kim YH, Choi CY, Kim YH. Covalent modification of the homeodomain-interacting protein kinase 2 (HIPK2) by the ubiquitin-like protein SUMO-1. *Proceedings of the National Academy of Sciences of the United States of America*. 1999;96(22):12350–5.

22.   Bon G, Di Carlo SE, Folgiero V, Avetrani P, Lazzari C, D'Orazi G, Brizzi MF, Sacchi A, Soddu S, Blandino G, Mottolese M, Falcioni R. Negative regulation of β4 integrin transcription by homeodomain-interacting protein kinase 2 and p53 impairs tumor progression. *Cancer Research*. 2009;69(14):5978–5986.

23.   Hofmann TG, Glas C, Bitomsky N. HIPK2: A tumour suppressor that controls DNA damage-induced cell fate and cytokinesis. *BioEssays*. 2013;35(1):55–64.

24.   Saul V V., Schmitz ML. Posttranslational modifications regulate HIPK2, a driver of proliferative diseases. *Journal of Molecular Medicine*. 2013;91(9):1051–1058.

25.   Wook Choi D, Yong Choi C. HIPK2 modification code for cell death and survival. *Molecular & cellular oncology*. 2014;1(2):e955999.

26. Hofmann TG, Möller A, Sirma H, Zentgraf H, Taya Y, Dröge W, Will H, Lienhard Schmitz M. Regulation of p53 activity by its interaction with homeodomain-interacting protein kinase-2. *Nature Cell Biology*. 2002;4(1):1–10.

27. D'Orazi G, Cecchinelli B, Bruno T, Manni I, Higashimoto Y, Saito S, Gostissa M, Coen S, Marchetti A, Del Sal G, Piaggio G, Fanciulli M, Appella E, Soddu S. Homeodomain-interacting protein kinase-2 phosphorylates p53 at Ser 46 and mediates apoptosis. *Nature Cell Biology*. 2002;4(1):11–20.

28. Feng Y, Zhou L, Sun X, Li Q. Homeodomain-interacting protein kinase 2 (HIPK2): a promising target for anti-cancer therapies. *Oncotarget*. 2017;8(12):20452–20461.

29. Bürglin TR, Affolter M. Homeodomain proteins: an update. *Chromosoma*. 2016;125(3):497–521.

30. Isono K, Nemoto K, Li Y, Takada Y, Suzuki R, Katsuki M, Nakagawara A, Koseki H. Overlapping Roles for Homeodomain-Interacting Protein Kinases Hipk1 and Hipk2 in the Mediation of Cell Growth in Response to Morphogenetic and Genotoxic Signals. *Molecular and Cellular Biology*. 2006;26(7):2758–2771.

31. Aikawa Y, Nguyen LA, Isono K, Takakura N, Tagata Y, Schmitz ML, Koseki H, Kitabayashi I. Roles of HIPK1 and HIPK2 in AML1- and p300-dependent transcription, hematopoiesis and blood vessel formation. *The EMBO journal*. 2006;25(17):3955–3965.

32. Shang Y, Doan CN, Arnold TD, Lee S, Tang AA, Reichardt LF, Huang EJ. Transcriptional corepressors HIPK1 and HIPK2 control angiogenesis via TGF-β-TAK1-dependent mechanism. Hogan BLM, ed. *PLoS biology*. 2013;11(4):e1001527.

33. Inoue T, Kagawa T, Inoue-Mochita M, Isono K, Ohtsu N, Nobuhisa I, Fukushima M, Tanihara H, Taga T. Involvement of the Hipk family in regulation of eyeball size, lens formation and retinal morphogenesis. *FEBS Letters*. 2010;584(14):3233–3238.

34.   Anzilotti S, Tornincasa M, Gerlini R, Conte A, Brancaccio P, Cuomo O, Bianco G, Fusco A, Annunziato L, Pignataro G, Pierantoni GM. Genetic ablation of homeodomain-interacting protein kinase 2 selectively induces apoptosis of cerebellar Purkinje cells during adulthood and generates an ataxic-like phenotype. *Cell Death and Disease*. 2015;6(12):e2004.

35.   Zhang J, Pho V, Bonasera SJ, Holzmann J, Tang AT, Hellmuth J, Tang S, Janak PH, Tecott LH, Huang EJ. Essential function of HIPK2 in TGFβ-dependent survival of midbrain dopamine neurons. *Nature Neuroscience*. 2007;10(1):77–86.

36.   Chalazonitis A, Tang AA, Shang Y, Pham TD, Hsieh I, Setlik W, Gershon MD, Huang EJ. Homeodomain interacting protein kinase 2 regulates postnatal development of enteric dopaminergic neurons and glia via BMP signaling. *The Journal of neuroscience : the official journal of the Society for Neuroscience*. 2011;31(39):13746–57.

37.   Wiggins AK, Wei G, Doxakis E, Wong C, Tang AA, Zang K, Luo EJ, Neve RL, Reichardt LF, Huang EJ. Interaction of Brn3a and HIPK2 mediates transcriptional repression of sensory neuron survival. *Journal of Cell Biology*. 2004;167(2):257–267.

38.   Doxakis E, Huang EJ, Davies AM. Homeodomain-interacting protein kinase-2 regulates apoptosis in developing sensory and sympathetic neurons. *Current biology : CB*. 2004;14(19):1761–1765.

39.   Lee S, Shang Y, Redmond SA, Urisman A, Tang AA, Li KH, Burlingame AL, Pak RA, Jovičić A, Gitler AD, Wang J, Gray NS, Seeley WW, Siddique T, Bigio EH, et al. Activation of HIPK2 Promotes ER Stress-Mediated Neurodegeneration in Amyotrophic Lateral Sclerosis. *Neuron*. 2016;91(1):41–55.

40.   Lanni C, Nardinocchi L, Puca R, Stanga S, Uberti D, Memo M, Govoni S, D'Orazi G, Racchi M. Homeodomain interacting protein kinase 2: A target for Alzheimer's beta amyloid leading to misfolded p53 and inappropriate cell survival. Bush AI, ed. *PLoS ONE*. 2010;5(4):e10171.

41.   Hattangadi SM, Burke KA, Lodish HF. Homeodomain-interacting protein kinase 2 plays an important role in normal terminal erythroid differentiation. *Blood*. 2010;115(23):4853–4861.

42.   Sjolund J, Pelorosso FG, Quigley DA, DelRosario R, Balmain A, Sjölund J, Pelorosso FG, Quigley DA, DelRosario R, Balmain A. Identification of Hipk2 as an essential regulator of white fat development. *Proceedings of the National Academy of Sciences of the United States of America*. 2014;111(20):7373–7378.

43.   Möller A, Sirma H, Hofmann TG, Rueffer S, Klimczak E, Dröge W, Will H, Schmitz ML. PML is required for homeodomain-interacting protein kinase 2 (HIPK2)-mediated p53 phosphorylation and cell cycle arrest but is dispensable for the formation of HIPK domains. *Cancer Research*. 2003;63(15):4310–4314.

44.   Di Stefano V, Blandino G, Sacchi A, Soddu S, D'Orazi G. HIPK2 neutralizes MDM2 inhibition rescuing p53 transcriptional activity and apoptotic function. *Oncogene*. 2004;23(30):5185–5192.

45.   Gresko E, Roscic A, Ritterhoff S, Vichalkovski A, Del Sal G, Schmitz ML. Autoregulatory control of the p53 response by caspase-mediated processing of HIPK2. *EMBO Journal*. 2006;25(9):1883–1894.

46.   Hofmann TG, Stollberg N, Schmitz ML, Will H. HIPK2 regulates transforming growth factor-beta-induced c-Jun NH(2)-terminal kinase activation and apoptosis in human hepatoma cells. *Cancer research*. 2003;63(23):8271–8277.

47.   Zhang Q, Yoshimatsu Y, Hildebrand J, Frisch SM, Goodman RH. Homeodomain interacting protein kinase 2 promotes apoptosis by downregulating the transcriptional corepressor CtBP. *Cell*. 2003;115(2):177–186.

48.   Lazzari C, Prodosmo A, Siepi F, Rinaldo C, Galli F, Gentileschi M, Bartolazzi A, Costanzo A, Sacchi A, Guerrini L, Soddu S. HIPK2 phosphorylates Δnp63α and promotes its degradation in

response to DNA damage. *Oncogene*. 2011;30(48):4802–4813.

49. Tan M, Gong H, Zeng Y, Tao L, Wang J, Jiang J, Xu D, Bao E, Qiu J, Liu Z. Downregulation of homeodomain-interacting protein kinase-2 contributes to bladder cancer metastasis by regulating Wnt signaling. *Journal of Cellular Biochemistry*. 2014;115(10):1762–1767.

50. Lin J, Zhang Q, Lu Y, Xue W, Xu Y, Zhu Y, Hu X. Downregulation of HIPK2 increases resistance of bladder cancer cell to cisplatin by regulating Wip1. Hofmann TG, ed. *PLoS ONE*. 2014;9(5):e98418.

51. Zhang Z, Wen P, Li F, Yao C, Wang T, Liang B, Yang Q, Ma LEI, He L. HIPK2 inhibits cell metastasis and improves chemosensitivity in esophageal squamous cell carcinoma. 2018:1113–1118.

52. Wei G, Ku S, Ma GK, Saito S, Tang A a, Zhang J, Mao J-H, Appella E, Balmain A, Huang EJ. HIPK2 represses beta-catenin-mediated transcription, epidermal stem cell expansion, and skin tumorigenesis. *Proceedings of the National Academy of Sciences of the United States of America*. 2007;104(32):13040–13045.

53. Nardinocchi L, Puca R, Sacchi A, Rechavi G, Givol D, D'Orazi G. Targeting hypoxia in cancer cells by restoring homeodomain interacting protein-kinase 2 and p53 activity and suppressing HIF-1α. Blagosklonny M V., ed. *PLoS ONE*. 2009;4(8):e6819.

54. Nardinocchi L, Puca R, Givol D, D'Orazi G. HIPK2 - A therapeutical target to be (re)activated for tumor suppression: Role in p53 activation and HIF-1α inhibition. *Cell Cycle*. 2010;9(7):1270–1275.

55. Cheng Y, Al-Beiti MAM, Wang J, Wei G, Li J, Liang S, Lu X. Correlation between homeodomain-interacting protein kinase 2 and apoptosis in cervical cancer. *Molecular Medicine Reports*. 2012;5(5):1251–1255.

56.   D'Orazi G, Sciulli MG, Di Stefano V, Riccioni S, Frattini M, Falcioni R, Bertario L, Sacchi A, Patrignani P. Homeodomain-interacting protein kinase-2 restrains cytosolic phospholipase A2-dependent prostaglandin E2 generation in human colorectal cancer cells. *Clinical Cancer Research*. 2006;12(3 I):735–741.

57.   Deshmukh H, Yeh TH, Yu J, Sharma MK, Perry A, Leonard JR, Watson MA, Gutmann DH, Nagarajan R. High-resolution, dual-platform aCGH analysis reveals frequent HIPK2 amplification and increased expression in pilocytic astrocytomas. *Oncogene*. 2008;27(34):4745–4751.

58.   Krieghoff-Henning E, Hofmann TG. *HIPK2 and cancer cell resistance to therapy.* England; 2008:751–4.

59.   Agnew C, Liu L, Liu S, Xu W, You L, Yeung W, Kannan N, Jablons D, Jura N. The crystal structure of the protein kinase HIPK2 reveals a unique architecture of its CMGC-insert region. *Journal of Biological Chemistry* . 2019.

60.   Jin Y, Ratnam K, Chuang PY, Fan Y, Zhong Y, Dai Y, Mazloom AR, Chen EY, D'Agati V, Xiong H, Ross MJ, Chen N, Ma'ayan A, He JC. A systems approach identifies HIPK2 as a key regulator of kidney fibrosis. *Nature Medicine*. 2012;18(4):580–588.

61.   Ricci A, Cherubini E, Ulivieri A, Lavra L, Sciacchitano S, Scozzi D, Mancini R, Ciliberto G, Bartolazzi A, Bruno P, Graziano P, Mariotta S. Homeodomain-interacting protein kinase2 in human idiopathic pulmonary fibrosis. *Journal of cellular physiology*. 2013;228(1):235–41.

62.   Liu R, Das B, Xiao W, Li Z, Li H, Lee K, He JC. A Novel Inhibitor of Homeodomain Interacting Protein Kinase 2 Mitigates Kidney Fibrosis through Inhibition of the TGF-β1/Smad3 Pathway. *Journal of the American Society of Nephrology : JASN*. 2017;28(7):2133–2143.

63.   Guo Y, Sui JY, Kim K, Zhang Z, Qu XA, Nam Y-J, Willette RN, Barnett J V., Knollmann BC, Force T, Lal H. Cardiomyocyte HIPK2 Maintains Basal Cardiac Function via ERK Signaling.

Circulation. 2019:CIRCULATIONAHA.119.040740.

64. Chen EY, Xu H, Gordonov S, Lim MP, Perkins MH, Ma'ayan A. Expression2Kinases: mRNA profiling linked to multiple upstream regulatory layers. *Bioinformatics*. 2012;28(1):105–111.

65. Berger SI, Posner JM, Ma'ayan A. Genes2Networks: connecting lists of gene symbols using mammalian protein interactions databases. *BMC Bioinformatics*. 2007;8(1):372.

66. Lachmann A, Ma'ayan A. KEA: Kinase enrichment analysis. *Bioinformatics*. 2009;25(5):684–686.

67. De Minicis S, Seki E, Uchinami H, Kluwe J, Zhang Y, Brenner DA, Schwabe RF. Gene Expression Profiles During Hepatic Stellate Cell Activation in Culture and In Vivo. *Gastroenterology*. 2007;132(5):1937–1946.

68. Haq S, Choukroun G, Kang ZB, Ranu H, Matsui T, Rosenzweig A, Molkentin JD, Alessandrini A, Woodgett J, Hajjar R, Michael A, Force T. Glycogen synthase kinase-3beta is a negative regulator of cardiomyocyte hypertrophy. *The Journal of cell biology*. 2000;151(1):117–130.

69. Knollmann BC, Chopra N, Hlaing T, Akin B, Yang T, Ettensohn K, Knollmann BEC, Horton KD, Weissman NJ, Holinstat I, Zhang W, Roden DM, Jones LR, Franzini-Armstrong C, Pfeifer K. Casq2 deletion causes sarcoplasmic reticulum volume increase, premature Ca2+ release, and catecholaminergic polymorphic ventricular tachycardia. *Journal of Clinical Investigation*. 2006;116(9):2510–2520.

70. Hwang HS, Kryshtal DO, Feaster TKK, Sánchez-Freire V, Zhang J, Kamp TJ, Hong CC, Wu JC, Knollmann BC. Comparable calcium handling of human iPSC-derived cardiomyocytes generated by multiple laboratories. *Journal of Molecular and Cellular Cardiology*. 2015;85:79–88.

71. Farley FW, Soriano P, Steffen LS, Dymecki SM. Widespread recombinase expression using

FLPeR (flipper) mice. *Genesis*. 2000;28:106–110.

72.   Agah R, Frenkel PA, French BA, Michael LH, Overbeek PA, Schneider MD. Gene recombination in postmitotic cells: Targeted expression of Cre recombinase provokes cardiac-restricted, site-specific rearrangement in adult ventricular muscle in vivo. *Journal of Clinical Investigation*. 1997;100(1):169–179.

73.   Dufour BD, Smith CA, Clark RL, Walker TR, Mcbride JL. Intrajugular vein delivery of AAV9-RNAi prevents neuropathological changes and weight loss in huntington's disease mice. *Molecular Therapy*. 2014;22(4):797–810.

74.   Skarnes WC, Rosen B, West AP, Koutsourakis M, Bushell W, Iyer V, Mujica AO, Thomas M, Harrow J, Cox T, Jackson D, Severin J, Biggs P, Fu J, Nefedov M, et al. A conditional knockout resource for the genome-wide study of mouse gene function. *Nature*. 2011;474(7351):337.

75.   Liu X, Xiao J, Zhu H, Wei X, Platt C, Damilano F, Xiao C, Bezzerides V, Boström P, Che L, Zhang C, Spiegelman BM, Rosenzweig A. MiR-222 is necessary for exercise-induced cardiac growth and protects against pathological cardiac remodeling. *Cell Metabolism*. 2015;21(4):584–595.

76.   Kehat I, Davis J, Tiburcy M, Accornero F, Saba-El-Leil MK, Maillet M, York AJ, Lorenz JN, Zimmermann WH, Meloche S, Molkentin JD. Extracellular signal-regulated kinases 1 and 2 regulate the balance between eccentric and concentric cardiac growth. *Circulation Research*. 2011;108(2):176–83.

77.   Bueno OF, De Windt LJ, Tymitz KM, Witt S a, Kimball TR, Klevitsky R, Hewett TE, Jones SP, Lefer DJ, Peng CF, Kitsis RN, Molkentin JD. The MEK1-ERK1/2 signaling pathway promotes compensated cardiac hypertrophy in transgenic mice. *The EMBO journal*. 2000;19(23):6341–50.

78.   Mansour SJ, Matten WT, Hermann AS, Candia JM, Rong S, Fukasawa K, Vande Woude GF, Ahn

NG. Transformation of mammalian cells by constitutively active MAP kinase kinase. *Science*. 1994;265(5174):966-970.

79.   Banks M, Crowell K, Proctor A, Jensen BC. Cardiovascular Effects of the MEK Inhibitor, Trametinib: A Case Report, Literature Review, and Consideration of Mechanism. *Cardiovascular Toxicology*. 2017;17(4):487–493.

80.   Pugach EK, Richmond PA, Azofeifa JG, Dowell RD, Leinwand LA. Prolonged Cre expression driven by the α-myosin heavy chain promoter can be cardiotoxic. *Journal of Molecular and Cellular Cardiology*. 2015;86:54–61.

81.   Davis J, Maillet M, Miano JM, Molkentin JD. Lost in Transgenesis. *Circulation Research*. 2012;111(6):761–777.

82.   Blaquiere JA, Verheyen EM. Homeodomain-Interacting Protein Kinases: Diverse and Complex Roles in Development and Disease. Biology AJBT-CT in D, ed. *Current Topics in Developmental Biology*. 2017;123:73–103.

83.   Yndestad A, Damås JK, Eiken HG, Holm T, Haug T, Simonsen S, Frøland SS, Gullestad L, Aukrust P. Enhanced myocyte contractility and Ca2+ handling in a calcineurin transgenic model of heart failure. *Cardiovascular Research*. 2002;54(1):105–116.

84.   Umbarkar P, Singh AP, Gupte M, Verma VK, Galindo CL, Guo Y, Zhang Q, McNamara JW, Force T, Lal H. Cardiomyocyte SMAD4-dependent TGF-β signaling is essential to maintain adult heart homeostasis. *JACC Basic Transl Sci*. 2019;4:41–53.

85.   Baines CP, Zhang J, Wang GW, Zheng YT, Xiu JX, Cardwell EM, Bolli R, Ping P. Mitochondrial PKCε and MAPK form signaling modules in the murine heart: Enhanced mitochondrial PKCε-MAPK interactions and differential MAPK activation in PKCε-induced cardioprotection. *Circulation Research*. 2002;90(4):390–397.

86.   Nugent MM, Lee K, He JC. HIPK2 is a new drug target for anti-fibrosis therapy in kidney disease.

Frontiers in Physiology. 2015;6(April):132.